

Julius-Maximilians-Universität Würzburg

**The role of the Rho GTPases Rac1
and Cdc42 for platelet function and formation**

**Die Rolle der Rho GTPasen Rac1 und Cdc42 in
Thrombozytenfunktion und -bildung**



**Doctoral thesis for a doctoral degree
at the Graduate School of Life Sciences,
Section Biomedicine**

submitted by

Irina Pleines

from

Göttingen

Würzburg, 2009

Submitted on:

Members of the *Promotionskomitee*:

Chairperson: Prof. Dr. Michael Sendtner

Primary Supervisor: Prof. Dr. Bernhard Nieswandt

Supervisor (Second): Prof. Dr. Georg Krohne

Supervisor (Third): Prof. Dr. Ulrich Walter

Date of Public Defence:

Date of Receipt of Certificate:

TABLE OF CONTENTS

1 INTRODUCTION	1
1.1 Platelet activation and thrombus formation	1
1.2 Integration of signaling events during platelet activation	3
1.3 Platelet elaboration from megakaryocytes	5
1.4 Small GTPases of the Rho family	8
1.4.1 Rho GTPases in platelets and the hematopoietic system.....	9
1.4.2 Rac1	10
1.4.3 Cdc42	12
1.4.4 Rho GTPases in megakaryopoiesis and platelet biogenesis	12
1.5 Aim of the study	13
2 MATERIALS AND METHODS	14
2.1 Materials	14
2.1.1 Kits and reagents.....	14
2.1.2 Cell culture materials	16
2.1.3 Antibodies.....	17
2.1.3.1 Purchased primary and secondary antibodies	17
2.1.3.2 Monoclonal Antibodies (mAbs).....	18
2.1.4 Animals.....	18
2.1.5 Buffers and media	19
2.2 Methods	22
2.2.1 Mouse genotyping	22
2.2.1.1 Isolation of genomic DNA from mouse ears	22
2.2.1.2 Sample preparation for PCR.....	22
2.2.1.3 Detection of the <i>Cdc42</i> floxed allele by PCR.....	23
2.2.1.4 Detection of the <i>Rac1</i> floxed allele by PCR.....	23
2.2.1.5 Detection of the Mx-Cre transgene by PCR	24
2.2.1.6 Detection of the PF4-Cre transgene by PCR	24
2.2.2 <i>In vitro</i> analysis of platelet function	25
2.2.2.1 Platelet preparation and washing	25
2.2.2.2 Platelet counting	25
2.2.2.3 Immunoblotting	26
2.2.2.4 Flow cytometry.....	26
2.2.2.5 Aggregometry and agglutination.....	27
2.2.2.6 Static adhesion assays	27
2.2.2.7 Intracellular calcium measurements	28
2.2.2.8 Adhesion under flow conditions.....	28
2.2.2.9 Measurement of platelet nucleotide content and ATP release.....	29
2.2.2.10 Measurement of platelet P-selectin, vWF and serotonin content and	29

serotonin release	29
2.2.2.11 Measurement of IP ₁	30
2.2.2.12 Tyrosine phosphorylation and immunoprecipitation	30
2.2.2.13 Determination of platelet filamentous (F)-actin content	31
2.2.3 <i>In vivo</i> analysis of platelet function	31
2.2.3.1 Determination of platelet life span	31
2.2.3.2 Bleeding time assay	32
2.2.3.3 Intravital microscopy of thrombus formation in FeCl ₃ -injured mesenteric arterioles ...	32
2.2.3.4 Monitoring of platelet adhesion to the injured carotid artery by intravital microscopy.	32
2.2.4 Megakaryocyte (MK) analysis	33
2.2.4.1 Isolation of MKs from fetal liver, purification by BSA gradient and study of proplatelet formation	33
2.2.4.2 Isolation and culture of MKs from bone marrow of adult mice	33
2.2.4.3 Determination of MK ploidy by flow cytometry	34
2.2.5 Electron microscopy	34
2.2.5.1 Transmission electron microscopy (TEM) of MKs <i>in situ</i>	34
2.2.5.2 TEM of platelets in suspension	35
2.2.5.3 Scanning electron microscopy (SEM) of platelets	36
2.2.5.4 Visualization of the platelet cytoskeleton by SEM	36
2.2.6 Histology	37
2.2.6.1 Preparation of paraffin sections	37
2.2.6.2 Hematoxylin/eosin staining of paraffin sections	37
2.2.7 Data analysis	37
3 RESULTS	38
3.1 Rac1 is essential for phospholipase C-γ2 activation in platelets	38
3.1.1 Rac1 is dispensable for platelet production but essential for lamellipodia formation	38
3.1.2 Scanning electron microscopy studies of <i>Rac1</i> ^{-/-} platelets	39
3.1.3 <i>Rac1</i> ^{-/-} platelets show diminished responses to GPVI and CLEC-2 stimulation	40
3.1.4 Defective PLC γ 2 activation and Ca ²⁺ mobilization in <i>Rac1</i> ^{-/-} platelets	44
3.1.5 Defective adhesion and aggregation of <i>Rac1</i> ^{-/-} platelets on collagen under flow	46
3.1.6 Defective arterial thrombus formation in <i>Rac1</i> ^{-/-} mice <i>in vivo</i>	48
3.2 <i>Cdc42</i>^{-/-} platelets display increased secretion but largely unaltered filopodia formation	50
3.2.1 <i>Cdc42</i> ^{-/-} mice display mild thrombocytopenia	50
3.2.2 <i>Cdc42</i> ^{-/-} platelets form filopodia and fully spread on fibrinogen	51
3.2.3 <i>Cdc42</i> ^{-/-} platelets exhibit reduced filopodia extension following adhesion on immobilized vWF	54
3.2.4 Increased secretion in <i>Cdc42</i> ^{-/-} platelets	55
3.2.5 Enhanced aggregation of <i>Cdc42</i> ^{-/-} platelets at low agonist concentrations	57
3.2.6 <i>Cdc42</i> ^{-/-} platelets form aggregates of increased size on collagen under flow	58
3.2.7 <i>Cdc42</i> ^{-/-} platelets display a decreased life span <i>in vivo</i>	59

3.2.8	Prolonged bleeding times in <i>Cdc42</i> ^{-/-} mice.....	60
3.2.9	Accelerated occlusive arterial thrombus formation in <i>Cdc42</i> ^{-/-} mice	61
3.2.10	Increased amounts of phosphorylated cofilin in <i>Cdc42</i> ^{-/-} platelets.....	62
3.3	Double deficiency of Rac1 and Cdc42 severely affects platelet function and production	63
3.3.1	Study of <i>Rac1/Cdc42</i> ^{-/-} platelets.....	64
3.3.1.1	<i>Rac1/Cdc42</i> double deficiency leads to macrothrombocytopenia and formation of abnormal platelets	64
3.3.1.2	<i>Rac1/Cdc42</i> ^{-/-} platelets are unable to spread on fibrinogen upon activation.....	66
3.3.1.3	Defective integrin activation and degranulation in <i>Rac1/Cdc42</i> ^{-/-} platelets.....	68
3.3.1.4	<i>Rac1/Cdc42</i> ^{-/-} platelets are rapidly cleared from the circulation.....	69
3.3.1.5	<i>Rac1/Cdc42</i> ^{-/-} mice display defective hemostasis and defective thrombus formation <i>in vivo</i>	71
3.3.2	Megakaryocyte studies.....	72
3.3.2.1	Megakaryocytes are present in spleen and bone marrow of <i>Cdc42</i> ^{-/-} and <i>Rac1/Cdc42</i> ^{-/-} mice.....	72
3.3.2.2	Proplatelet formation is decreased in <i>Cdc42</i> ^{-/-} MKs and nearly abrogated in <i>Rac1/Cdc42</i> ^{-/-} MKs.....	73
3.3.2.3	Intact endomitosis in MKs derived from <i>Rac1</i> ^{-/-} , <i>Cdc42</i> ^{-/-} and <i>Rac1/Cdc42</i> ^{-/-} mice	74
3.3.2.4	Reduced presence of demarcation membranes in bone marrow MKs from <i>Cdc42</i> ^{-/-} and <i>Rac1/Cdc42</i> ^{-/-} mice	75
4	DISCUSSION	79
4.1	Rac1 mediates phospholipase C-γ2 activation in platelets independently of tyrosine phosphorylation.....	80
4.2	A complex phenotype dominated by increased secretion in mice lacking Cdc42 in platelets	82
4.3	Rac1 and Cdc42 play redundant roles in megakaryocyte maturation and platelet formation	87
4.4	Concluding remarks and outlook.....	89
5	REFERENCES.....	91
6	APPENDIX	100
	Abbreviations	100
	Curriculum Vitae	103
	Acknowledgements	104
	Publications	105
	Affidavit.....	107

SUMMARY

Platelet activation induces cytoskeletal rearrangements involving a change from discoid to spheric shape, secretion, and eventually adhesion and spreading on immobilized ligands. Small GTPases of the Rho family, such as Rac1 and Cdc42, are known to be involved in these processes by facilitating the formation of lamellipodia and filopodia, respectively. This thesis focuses on the role Rac1 and Cdc42 for platelet function and formation from their precursor cells, the megakaryocytes (MKs), using conditional knock-out mice.

In the first part of the work, the involvement of Rac1 in the activation of the enzyme phospholipase (PL) C γ 2 in the signaling pathway of the major platelet collagen receptor glycoprotein (GP) VI was investigated. It was found that Rac1 is essential for PLC γ 2 activation independently of tyrosine phosphorylation of the enzyme, resulting in a specific platelet activation defect downstream of GPVI, whereas signaling of other activating receptors remains unaffected. Since Rac1-deficient mice were protected from arterial thrombosis in two different *in vivo* models, the GTPase might serve as a potential target for the development of new drugs for the treatment and prophylaxis of cardio- and cerebrovascular diseases.

The second part of the thesis deals with the first characterization of MK- and platelet-specific Cdc42 knock-out mice. Cdc42-deficient mice displayed mild thrombocytopenia and platelet production from mutant MKs was markedly reduced. Unexpectedly, Cdc42-deficient platelets showed increased granule content and release upon activation, leading to accelerated thrombus formation *in vitro* and *in vivo*. Furthermore, Cdc42 was not generally required for filopodia formation upon platelet activation. Thus, these results indicate that Cdc42, unlike Rac1, is involved in multiple signaling pathways essential for proper platelet formation and function.

Finally, the outcome of combined deletion of Rac1 and Cdc42 was studied. In contrast to single deficiency of either GTPase, platelet production from double-deficient MKs was virtually abrogated, resulting in dramatic macrothrombocytopenia in the animals. Formed platelets were largely non-functional leading to a severe hemostatic defect and defective thrombus formation in double-deficient mice *in vivo*. These results demonstrate for the first time a functional redundancy of Rac1 and Cdc42 in the hematopoietic system.

ZUSAMMENFASSUNG

Umstrukturierungen des Zytoskeletts spielen eine bedeutende Rolle bei der Aktivierung von Thrombozyten und sind in diesem Zusammenhang unerlässlich für Formänderung, Sekretion, sowie für Adhäsion und Ausbreitung auf immobilisierten Adhäsionsproteinen. Es wird vermutet, dass kleine GTPasen der Rho-Proteinfamilie, wie z.B. Rac1 und Cdc42, maßgeblich an diesen Prozessen beteiligt sind, indem sie die Bildung von Lamellipodien bzw. Filopodien bewirken. Die hier vorliegende Dissertation beschäftigt sich mit der Funktion von Rac1 und Cdc42 sowohl für die Aktivierung von Thrombozyten, als auch für deren Neubildung aus ihren Vorläuferzellen, den Megakaryozyten (MKs). Zu diesem Zweck wurden konditionale Knock-out-Mäuse generiert und *in vitro* und *in vivo* analysiert.

Der erste Teil der Arbeit beinhaltete die Untersuchung der Rolle von Rac1 im Signalweg des wichtigsten Thrombozyten-Kollagen-Rezeptors, Glykoprotein (GP) VI, dessen Stimulation zur Aktivierung des Enzyms Phospholipase $\gamma 2$ (PLC $\gamma 2$) führt. Es konnte gezeigt werden, dass Rac1 notwendig für PLC $\gamma 2$ -Aktivierung ist, und zwar unabhängig von der simultan stattfindenden Tyrosin-Phosphorylierung des Enzyms. Dies führte dazu, dass in Rac1-defizienten Thrombozyten spezifisch der GPVI-Signalweg blockiert war, während die Aktivierung durch andere Rezeptoren unverändert funktionierte. Da Rac1-defiziente Mäuse vor arteriellem Gefäßverschluss (Thrombose) in zwei verschiedenen *in vivo* Modellen geschützt waren, könnte Rac1 einen potenziellen Angriffspunkt für die Entwicklung neuer antithrombotisch wirksamer Medikamente darstellen.

Im zweiten Teil der Dissertation wurden erstmals die Auswirkungen eines MK- und Thrombozyten-spezifischen Cdc42-Knock-outs charakterisiert. Cdc42-defiziente Mäuse zeigten eine leichte Thrombozytopenie und die Neubildung von Thrombozyten aus defizienten MKs war merklich beeinträchtigt. Entgegen aller Erwartungen waren sowohl Inhalt, als auch Freisetzung von Granula aus Cdc42-defizienten Thrombozyten stark erhöht, was zu beschleunigter Thrombusbildung *in vitro* und Gefäßverschluss *in vivo* führte. Überdies war Cdc42 generell nicht essentiell für die Ausbildung von Filopodien nach Thrombozytenaktivierung. Diese Ergebnisse deuten darauf hin, dass Cdc42 an einer Vielzahl von Signalwegen beteiligt ist, welche für die korrekte Bildung und Funktion von Thrombozyten unabdingbar sind.

Der letzte Teil der Arbeit beschäftigte sich mit den Auswirkungen einer Doppeldefizienz von Rac1 und Cdc42. Im Gegensatz zur jeweiligen Einfachdefizienz war die Bildung von Thrombozyten aus doppeldefizienten MKs fast komplett blockiert, was eine stark ausgeprägte Makrothrombozytopenie in den betroffenen Tieren zur Folge hatte. Die wenigen gebildeten Thrombozyten waren in ihrer Funktion stark beeinträchtigt. Dies führte zusammen mit den extrem niedrigen Thrombozytenzahlen dazu, dass in doppeldefizienten Mäusen sowohl Hämostase als auch Thrombusbildung defekt waren. Diese Resultate zeigen erstmals eine funktionelle Redundanz von Rac1 und Cdc42 im hämatopoetischen System.

1 INTRODUCTION

Platelets are small anuclear discoid-shaped cells which are produced by fragmentation of megakaryocytes in the bone marrow and subsequently released into the blood stream. They evolved relatively late and are only found in mammals. The number of platelets in the blood is astonishingly high, in the range of 250,000/ μl in humans and 1,000,000/ μl in mice. Human platelets circulate in the blood for up to 10 days, whereas the life span of murine platelets is restricted to approximately 5 days. Aged platelets are constantly cleared by the reticulo-endothelial system in spleen and liver and most of the produced platelets encounter this fate. However, upon damage of the endothelial cell layer in blood vessels, exposed components of the extracellular matrix (ECM) trigger rapid platelet adhesion and activation. Activated platelets release substances which lead, together with locally produced thrombin, to recruitment and activation of further platelets resulting in platelet aggregation and thrombus formation. The formation of a platelet plug by these processes is essential to seal vascular damages and to prevent blood loss. On the downside, thrombus formation under pathological conditions, such as upon rupture of an atherosclerotic plaque in stenosed vessels, can lead to irreversible occlusion and thereby to myocardial infarction or, if occurring in the brain, to stroke. Since these events represent leading causes of death in western societies, platelet inhibition is one major strategy to prevent or treat ischemic cardio- and cerebrovascular diseases.

Platelet activation has to be tightly regulated to ensure efficient plug formation and wound healing on the one hand while, on the other hand, uncontrolled adhesion and activation has to be avoided. Therefore, platelets possess various adhesion receptors and ingenious regulation mechanisms in order to ensure controlled spatial and temporal activation.

1.1 Platelet activation and thrombus formation

Platelet activation and thrombus formation at sites of vascular injury involve multiple signaling processes, which can be divided into three major steps (Fig. 1). In the first step, platelets come into contact with the exposed ECM. Under conditions of high shear this contact, called “tethering”, is mediated by interaction between platelet glycoprotein (GP) Ib and von Willebrand Factor (vWF) immobilized on collagen of the ECM¹. However, the GPIb-vWF interaction is not stable enough to allow firm

adhesion but rather serves to slow the platelets down, resulting in platelet “rolling” on the vessel wall.

Enabled by the tethering process, in the second step of thrombus formation platelets bind to the ECM protein collagen via the platelet-specific immunoglobulin superfamily receptor glycoprotein (GP) VI^{2;3}. This interaction triggers activation of platelet integrins and induces the release of secondary mediators, namely thromboxane A₂ (TXA₂) and adenosine diphosphate (ADP). Together with thrombin produced at the site of injury, these mediators contribute to platelet activation by binding to G protein-coupled receptors (G_q, G_{12/13}, G_i), subsequently inducing full platelet activation⁴.

In the third step, firm platelet adhesion on the ECM is mediated by active, high-affinity $\beta 1$ integrins, which bind to collagen ($\alpha 2\beta 1$), fibronectin ($\alpha 5\beta 1$) and laminin ($\alpha 6\beta 1$), as well as by the major platelet integrin, $\alpha_{IIb}\beta_3$, which binds to fibronectin and vWF on the ECM. Finally, thrombus growth is induced by recruitment and activation of further platelets from the blood stream via released ADP and TXA₂ and subsequent bridging of platelets via fibrinogen and vWF bound to integrin $\alpha_{IIb}\beta_3$.

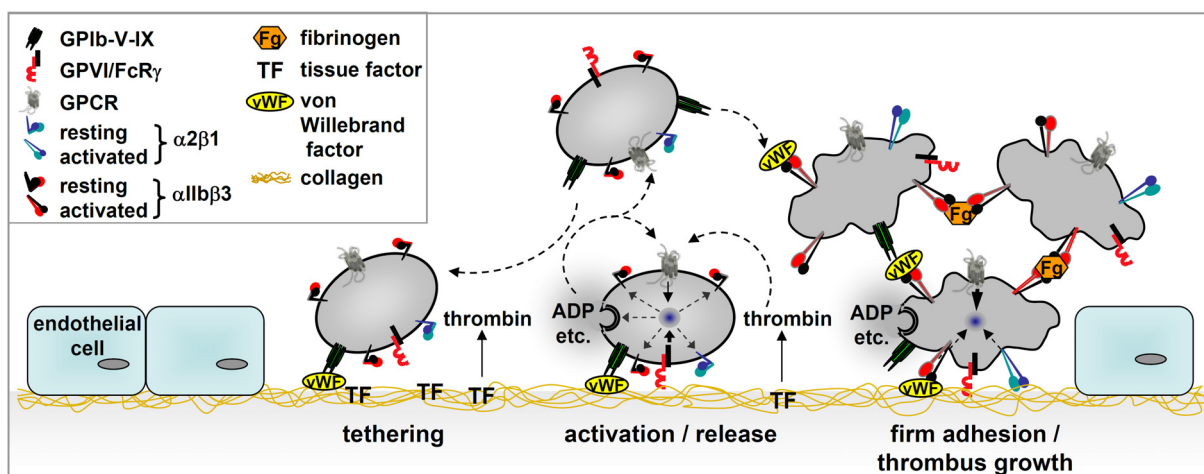


Figure 1. Platelet activation and aggregation on the ECM. Interaction of GPIb with vWF immobilized on the ECM mediates platelet tethering and thereby enables GPVI to bind to exposed collagen. The GPVI-collagen interaction results in release of the secondary mediators ADP and TXA₂, and the shift of platelet integrins to the activated high-affinity state, thereby mediating full platelet activation. In parallel, tissue factor (TF) locally induces thrombin formation which contributes to platelet activation. Activated platelet integrins mediate firm adhesion of platelets and thrombus growth by binding to ligands on the ECM ($\alpha 2\beta 1$, $\alpha_{IIb}\beta_3$), as well as by bridging platelets via fibrinogen and vWF bound to $\alpha_{IIb}\beta_3$. Taken from: Varga-Szabo D, Pleines I and Nieswandt B, *Arterioscler Thromb Vasc Biol*, 2008⁵.

1.2 Integration of signaling events during platelet activation

Platelets express a variety of receptors on the plasma membrane which, during the activation process, induce two major signaling pathways both leading to the activation of phospholipase (PL) C isoforms⁵.

Soluble agonists such as thrombin, ADP and TXA₂ stimulate receptors that couple to heterotrimeric G proteins (Gq) and lead to activation of phospholipase (PL) C β (Fig. 2)⁶. Furthermore, G protein-coupled signaling stimulates activation of Rho GTPases which induce signaling pathways leading to cytoskeletal rearrangements and subsequent shape change and cell spreading⁴.

The other pathway involves platelet adhesion receptors and culminates in activation of PLC γ 2. In the initial phase of platelet activation, this pathway is triggered by activation of the collagen receptor GPVI⁷ or the C-type lectin-like receptor 2 (CLEC-2), the receptor for the snake venom toxin rhodocytin (RC)⁸. Signaling induced by these receptors is similar to that used by immunoreceptors and involves tyrosine phosphorylation cascades downstream of the receptor-associated *immunoreceptor tyrosine activation motif* (ITAM) (GPVI) or YXXL motif (CLEC-2) culminating in the activation of effector enzymes, most notably PLC γ 2 (Fig. 2,8)⁹.

In both cases, activated PLCs produce inositol 1,4,5-trisphosphate (IP₃) and diacylglycerol (DAG) by cleavage of phosphatidylinositol-4,5-bisphosphate (PIP₂). IP₃ then triggers Ca²⁺ mobilization from intracellular stores and subsequent opening of Ca²⁺ channels in the plasma membrane, leading to *store operated Ca²⁺ entry* (SOCE)^{5;10}. DAG activates protein kinase C (PKC) and may contribute to Ca²⁺ entry by non-SOCE mechanisms¹¹. Elevations in intracellular calcium concentration [Ca²⁺]_i are a central step during platelet activation and a prerequisite for proper cellular responses including firm adhesion, as well as granule secretion and aggregation.

Secretion of intracellular granules is crucial for the recruitment and activation of further platelets from the blood stream. Two different types of releasable granules exist in platelets: α granules contain various proteins including growth factors and thrombogenic proteins, such as thrombospondin, fibronectin and vWF. P-selectin expression on the platelet surface upon α granule release is one major degranulation marker and therefore widely used to assess the activation state of platelets *in vitro*. Dense granules contain small molecules, notably ADP and adenosine triphosphate (ATP), as well as histamine and serotonin¹². Upon platelet activation with strong

agonists and a subsequent increase in $[Ca^{2+}]_i$, these granules are first centralized and then secreted^{13;14}, thereby promoting platelet aggregation and thrombus growth.

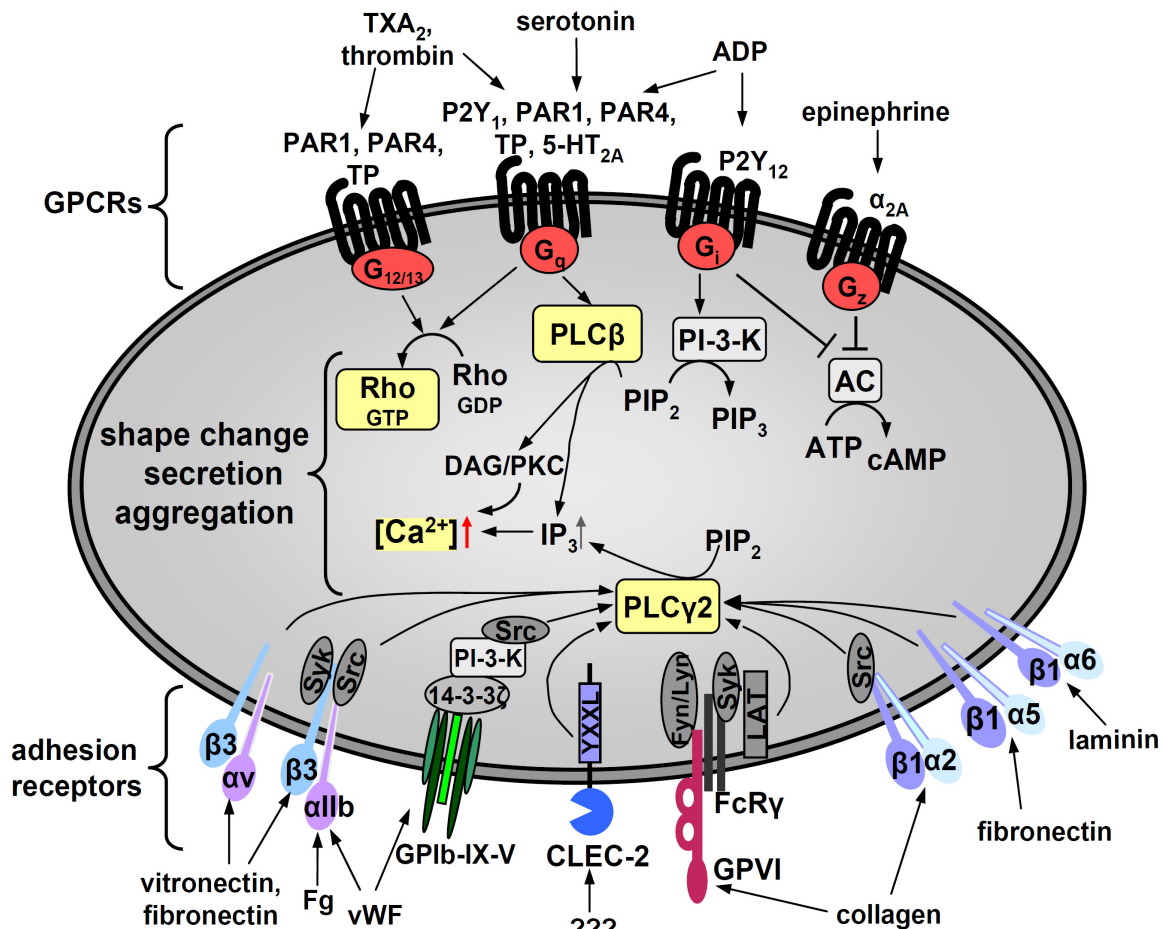


Figure 2. Major signaling pathways in platelets. Two major signaling pathways exist in platelets. Soluble agonists activate G protein-coupled receptors (GPCRs). These agonists comprise secondary mediators released from activated platelets, such as TXA_2 , ADP, epinephrine and serotonin, as well as locally produced thrombin and induce various signaling pathways involving $G_{12/13}$, G_q and $G_{i/z}$. Signaling downstream of G_q leads to activation of $PLC\beta$. Furthermore, GPCRs induce activation of Rho GTPases leading to cytoskeletal rearrangements upon platelet activation. Adhesion receptors, such as the major platelet activating receptor GPVI, CLEC-2, active integrins and probably GPIb induce $PLC\gamma_2$ activation upon ligand binding. PLCs cleave phosphatidylinositol-4,5-bisphosphate (PIP_2) in DAG and IP_3 . IP_3 and DAG induce and increase in cytosolic calcium, which is crucial for the platelet activating response. Abbreviations: PI-3-K, phosphoinositide-3-kinase; Fg, fibrinogen; PIP_3 , phosphatidylinositol-3,4,5-trisphosphate; AC, adenylate cyclase; LAT, linker for activation of T cells. Modified from: Varga-Szabo D, Pleines I and Nieswandt B, *Arterioscler Thromb Vasc Biol* 2008⁵.

1.3 Platelet elaboration from megakaryocytes

Platelets are synthesized by precursor cells called megakaryocytes (MKs). MKs are myeloid cells which reside primarily in the bone marrow but are also found in spleen and lung.

MKs differentiate from pluripotent hematopoietic stem cells (HSCs) that develop into two types of precursors: burst-forming cells (BFU) and colony-forming cells (CFU) (Fig. 3)^{15;16}. Further development culminates in the formation of direct megakaryocyte precursors (CFU-Meg) which differentiate into megakaryocytes. Currently, thrombopoietin (TPO) is thought to be the primary regulator of thrombopoiesis, since it is the only cytokine required for MKs to constantly produce platelets¹⁷. TPO acts in concert with other cytokines, including interleukin (IL)-3, IL-6, IL-11, granulocyte macrophage colony-stimulating factor (GM-CSF) and stromal cell-derived factor-1 (SDF-1), although these factors are not essential for MK maturation. Platelet factor 4 (PF4) is a cytokine which is produced very late during megakaryopoiesis, predominantly in mature MKs. In addition to chemokines and cytokines, MK formation is tightly regulated by various transcription factors, most importantly NF-E2 and GATA-1¹⁸.

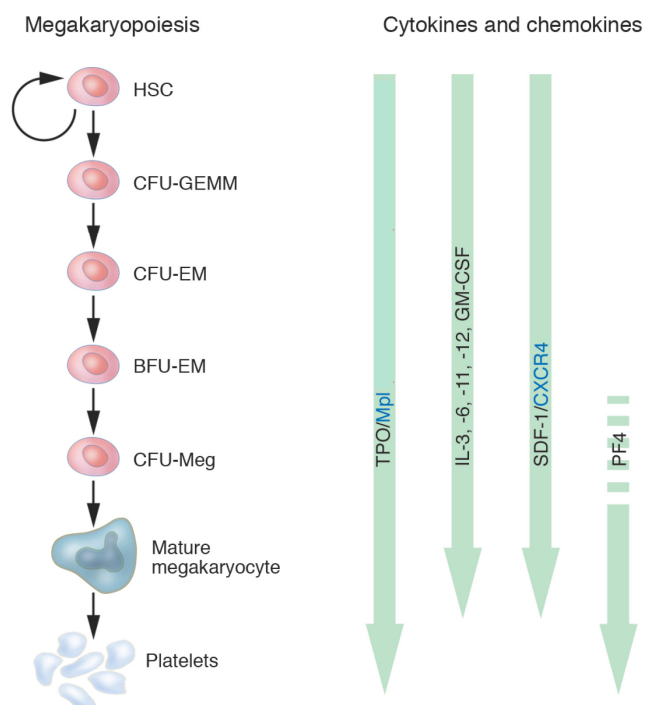


Figure 3: Regulation of megakaryopoiesis by cytokines and chemokines. Left: A scheme based on the classical pathway of megakaryopoiesis is shown. Cytokines and chemokines that influence that process are depicted on the right side as green arrows to indicate the approximate level of development at which they have their influence. Open white areas in arrows indicate levels at which the cytokine is not known to act. Blue text refers to cytokine receptors of significance in megakaryopoiesis. Abbreviations: CFU, colony-forming unit; CFU-GEMM, CFU, granulocyte, erythrocyte, macrophage, megakaryocyte; CFU-EM, CFU, erythrocyte, megakaryocyte; BFU-EM, burst-forming unit, erythrocyte, megakaryocyte; CFU-Meg, CFU, megakaryocyte. Modified from: Pang L *et al.*, *JCI* 2005¹⁵.

MKs are highly specialized for platelet biogenesis and their maturation is characterized by sequential steps¹⁹. First, MKs undergo multiple rounds of

endomitosis that amplifies the DNA up to 64-fold (modal ploidy: 16N in human and mice) and results in a polyploid, multi-lobed nucleus.

In the next step, cytoplasmic maturation is initiated, including synthesis of platelet-specific granules and organelles, as well as formation of a characteristic demarcation membrane system (DMS) that has continuity with the plasma membrane (Fig. 4b)¹⁸. At the end of this process, human MKs enlarge up to 100 μm in diameter (mice: 30-50 μm) and are fully equipped with the elements necessary for platelet production.

The exact mechanism of platelet biogenesis has been controversially discussed over the last decades. Some investigators supported the idea of a defragmentation model according to which mature MKs “burst” into thousands of platelets in the bone marrow. On the other hand, the flow model of platelet formation implies that mature MKs form pseudopodial extensions, so-called proplatelets, along which platelets are assembled (Fig. 4a). However, all recent studies using *in vitro* or *in vivo* imaging consistently report pseudopodia (proplatelet) formation from MKs as a common feature of platelet biogenesis, wherein the DMS seems to function as membrane reservoir for newly formed proplatelets²⁰. *In vitro*, proplatelets are clearly visible structures, whereas *in vivo*, MKs display demarcation membrane invaginations resulting in so-called proplatelet territories (Fig. 4a,b). Very recent studies *in vivo* demonstrated that, under physiological conditions, mature MKs shed proplatelet-like structures into sinusoids of the bone marrow which are then further fragmented to platelets by the shear forces present in blood vessels (Fig. 4b)^{21;22}.

Proplatelet formation from mature MKs involves multiple morphological changes. The importance of tubulin polymerization in this context is well established. Microtubule sliding does not only enable proplatelet elongation, but also mediates organelle trafficking into later platelets^{23;24}.

In contrast, little is known about the role of the actin cytoskeleton during megakaryocyte maturation and platelet biogenesis, although actin polymerization was shown to be involved in branching of proplatelets²⁵. However, there is increasing evidence that signaling by small GTPases of the Rho family might play an important role in these processes.

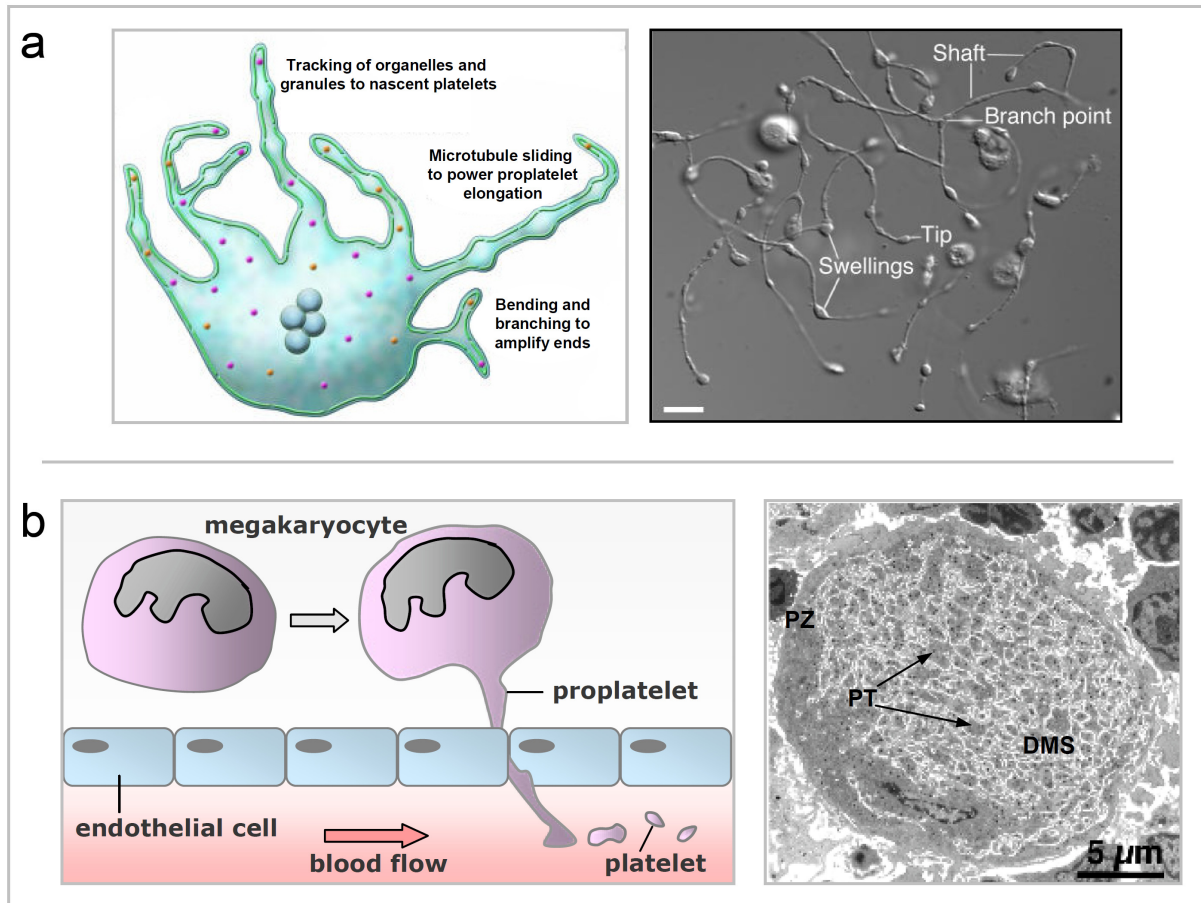


Figure 4. Proplatelet formation from megakaryocytes. (a) Proplatelet formation *in vitro*. Left: After endomitosis and cytoplasmic maturation, the megakaryocyte forms pseudopodia which elongate into proplatelets. Sliding of overlapping microtubules drives proplatelet elongation and organelle trafficking into proplatelets. Bending and branching of the proplatelets serves to amplify ends. In the end of the process, the whole megakaryocyte is converted into a mass of proplatelets. Right: Differential interference contrast image of mouse proplatelets originated from one megakaryocyte. Bar, 5 μm . Modified from: Patel SR, Hartwig JH, Italiano JE, *JCI* 2005²⁵. (b) Proplatelet formation in bone marrow *in vivo*. Left: Mature megakaryocytes are situated in the vascular niche where molecules such as vWF induce proplatelet formation. Proplatelets cross the endothelial barrier and shear forces induce release of proplatelet fragments or individual platelets into the circulation. Right: Electron microscopy image of a mature megakaryocyte in the bone marrow. Note the presence of proplatelet territories (PTs) generated by the demarcation membrane system (DMS). Membrane invaginations and organelles are absent in the peripheral zone (PZ) of mature megakaryocytes. Bar, 5 μm . Modified from: Bluteau D *et al.*, *JTH* 2009²⁶ and Eckly A *et al.*, *Blood* 2009²⁷.

1.4 Small GTPases of the Rho family

Rho GTPases are small (20-25 kDa) members of the superfamily of Ras-related proteins which are found in all eukaryotic cells²⁸ and are best known for their functions in regulation of the actin cytoskeleton.

The family of mammalian Rho GTPases comprises 20 members in total, the most widely known being RhoA, Rac1 and Cdc42. Most Rho GTPases cycle between a guanosine triphosphate (GTP)-bound, active, and a guanosine diphosphate (GDP)-bound, inactive form (Fig. 5). Cycling between the two activation states is regulated by guanine nucleotide exchange factors (GEFs), GTPase-activating proteins (GAPs) and guanine nucleotide-dissociation inhibitors (GDIs). In the active, GTP-bound form, Rho GTPases bind to their effector molecules, thereby inducing multiple processes, including cell adhesion, division and migration, as well as vesicle transport and microtubule dynamics. Furthermore, they participate in the regulation of morphogenesis, cell cycle progression and gene expression²⁸.

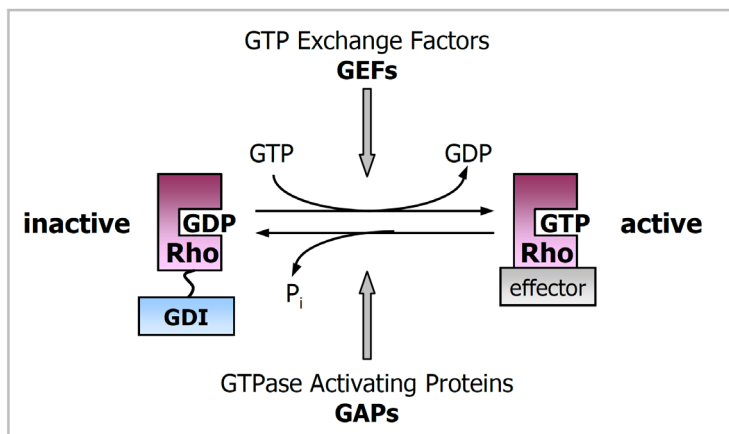


Figure 5. **Activation cycle of Rho GTPases.** Rho GTPases cycle between an inactive, GDP-bound and an active, GTP-bound state which allows binding of effector molecules. Exchange from GDP to GTP is mediated by GEFs, whereas GAPs mediate inactivation of Rho GTPases by increasing their intrinsic GTPase activity. GDIs bind to C-terminal prenyl groups of some GTPases, sequestering them away from their regulators.

Much knowledge about the roles of Rho GTPases has been gained by overexpression studies in cell lines using dominant negative or constitutively active Rho proteins to either inhibit or overstimulate the respective signaling pathways. However, many of those studies yielded conflicting results often caused by unspecific side effects of the used reagents.

Therefore, the recent generation of (conditional) knock-out mice for several GTPases has provided new tools to reliably study the effect of GTPase deficiency with a minimal risk of secondary effects²⁹.

1.4.1 Rho GTPases in platelets and the hematopoietic system

Platelet activation at sites of vascular injury induces multiple cytoskeletal rearrangements including a change from discoid to spheric shape (the so-called “shape change”), and eventually adhesion to and spreading on immobilized ligands or matrices, such as fibrinogen or collagens. Whereas RhoA activation in platelets has been shown to be essential for stress fiber formation and platelet shape change^{30;31}, Cdc42 and Rac1 have been suggested to induce the formation of filopodia and lamellipodia, respectively^{32;33}.

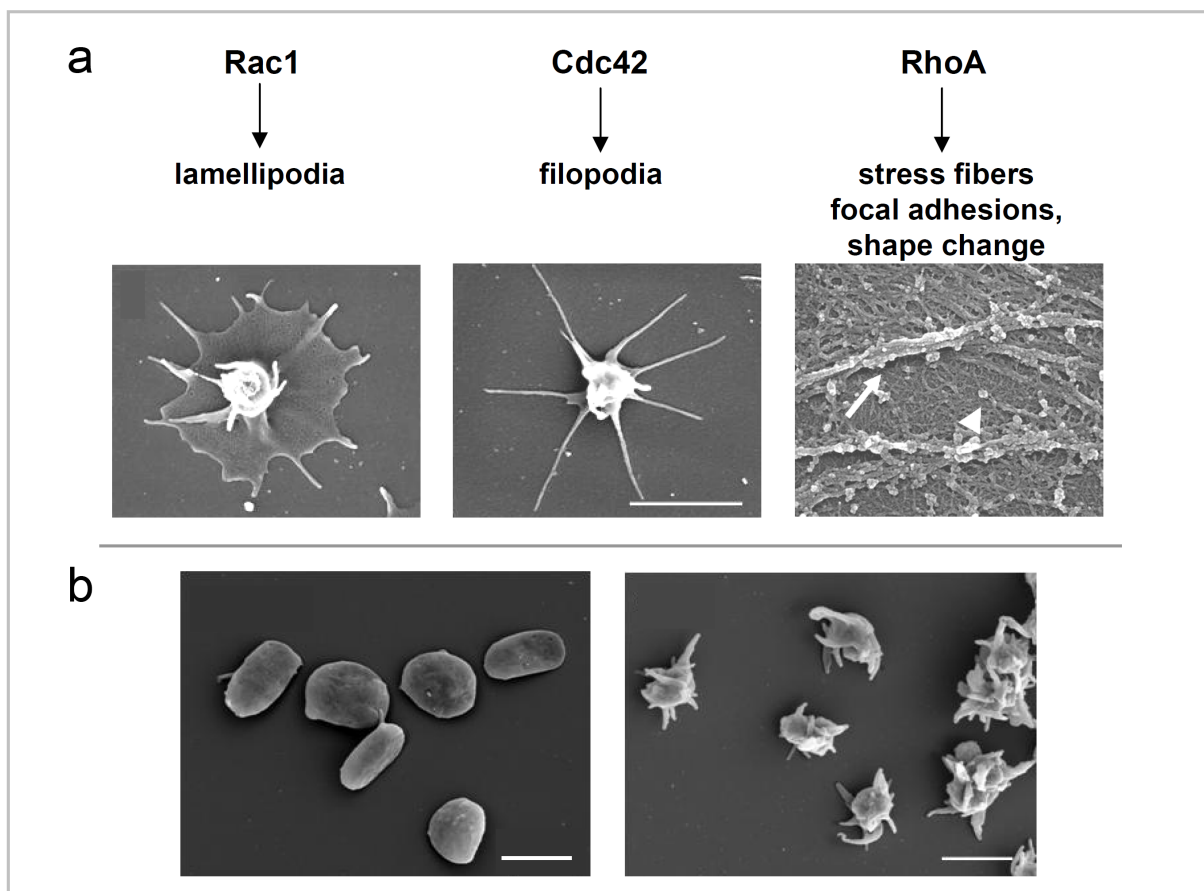


Figure 6. Rho GTPases mediate cytoskeletal rearrangements in activated platelets. (a) Characteristic scanning electron microscopy images of activated platelets forming lamellipodia and filopodia, as well as visualization of stress fibers. Bar, 1 μm (Nieswandt and Gachet, personal results). The role of Cdc42 for filopodia formation in platelets is questioned in this study. (b) Scanning electron microscopy images of resting platelets (left) or activated platelets in suspension (right). Resting platelets have a discoid shape whereas activated platelets in suspension are of spheric shape and form numerous filopodia. Bar, 2 μm (Nieswandt and Gachet, personal results).

Platelet filopodia and lamellipodia formation can be nicely visualized by static adhesion assays e.g. spreading on matrices, such as collagen or fibrinogen (Fig. 6a). Platelets activated in suspension exhibit profound shape change and the formation of

numerous filopodia (Fig. 6b). An overview of signaling events leading to lamellipodia and filopodia formation by Rac1 and Cdc42 is shown in Fig. 7²⁹.

Although the crucial role of Rho GTPases for the regulation of actin rearrangements in platelets is well established, more recent studies indicate that the GTPases participate in many additional signaling pathways during the process of platelet activation. Furthermore, their function in megakaryocyte and platelet formation is largely unclear. This thesis focuses on the role of the Rho GTPases Rac1 and Cdc42 for platelet function and production using conditional knock-out mice.

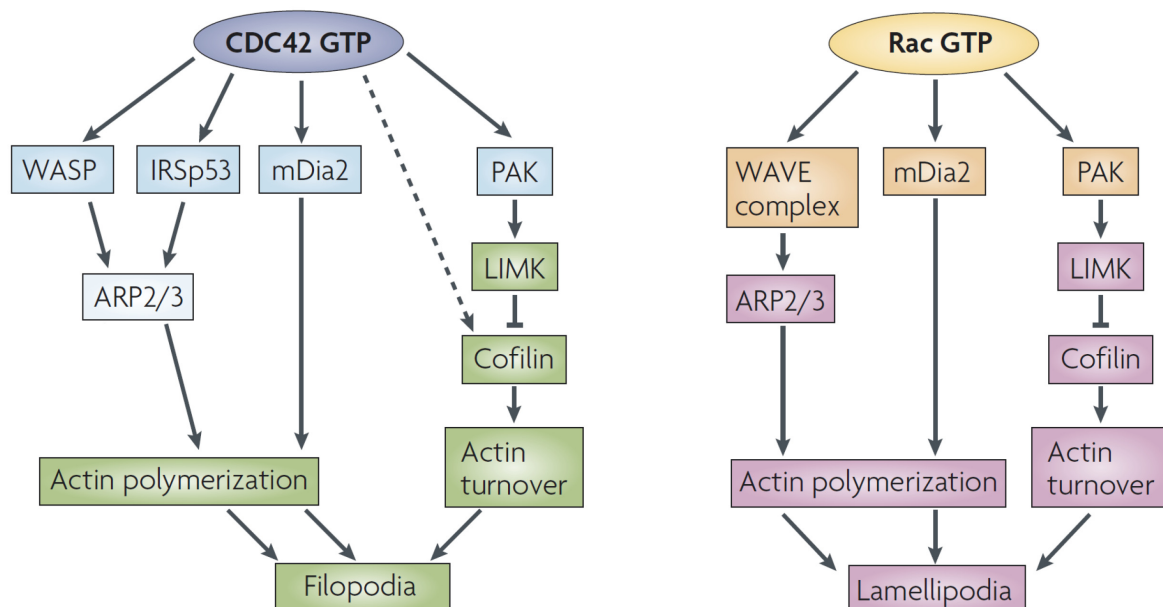


Figure 7. Formation of filopodia and lamellipodia by Cdc42 and Rac1. Cdc42 can bind and activate Wiscott-Aldrich syndrome protein (WASP) or the insulin-receptor substrate p53 (IRSp53) Tyr Kinase which results in activation of the actin-related protein (ARP)2/3 complex, thereby inducing actin polymerization and filopodia formation. Rac1 activates the ARP2/3 complex through the WASP-family verprolin-homologous protein (WAVE) complex. Both Rac1 and Cdc42 can also induce actin polymerization by activation of the formin mammalian diaphanous-2 (mDia2). Activation of Ser/Thr p21-activated kinase (PAK) by Rac1 or Cdc42 leads to phosphorylation of LIM kinase (LIMK) which phosphorylates and inhibits cofilin, thereby decreasing actin turnover. Modified from: Heasman SJ and Ridley AJ, *Nature Reviews* 2008²⁹.

1.4.2 Rac1

The subfamily of Rac GTPases comprises three isoforms (Rac1, 2, 3). Rac1 and 3 are widely expressed, whereas Rac2 expression is restricted to hematopoietic cells. Constitutive deletion of Rac1 in mice leads to embryonic lethality before embryonic day (E) 9.5³⁴. Rac1 is best known for its ability to induce lamellipodia formation in various cell types. In the hematopoietic system, knock-out studies showed that Rac1 was not required for the maintenance of steady-state hematopoiesis, however, it was essential for engraftment of hematopoietic stem cells (HSCs) after bone marrow

transplantation in mice *in vivo*³⁵. Further studies demonstrated an important and redundant role for Rac1 and Rac2 during early B and T cell development, so that deficiency of Rac1 alone had no effect on maturation of these cells³⁶⁻³⁸.

Of the three Rac isoforms, only Rac1 has been found to be expressed in detectable amounts in platelets³³. Rac1 activation in platelets downstream of G-protein coupled receptor (GPCR) stimulation, e.g. by thrombin, is well established³⁹⁻⁴² (Fig. 2) and previous studies have indicated that Rac1 may become activated downstream of integrin α IIb β 3, thereby regulating lamellipodia formation⁴³. This was recently confirmed by McCarty *et al.* in Rac1-deficient murine platelets who in addition observed an unexplained selective impairment of GPVI-, but not GPCR-induced aggregation (Fig. 8)³³. In contrast to that study, Akbar *et al.* reported a general secretion defect in Rac1-deficient murine platelets and in human platelets treated with a selective Rac1 inhibitor⁴⁴.

Several studies demonstrated Rac1 activation after GPVI/ITAM stimulation. However, Rac1 activation in this context was mostly suggested to occur not directly but as a second step after release of secondary mediators and subsequent induction of G protein-coupled signaling^{42;45}. Interestingly, using heterologous cell systems and cell-free assays, Piechulek *et al.* have shown that Rac1 may be involved in the activation of PLC γ 2 by a mechanism independent of tyrosine phosphorylation of the enzyme, thereby providing a possible direct link between GPVI signaling and Rac1 activity⁴⁶. However, the role of Rac1 downstream of ITAM-coupled receptor activation in platelets has not been analyzed in detail.

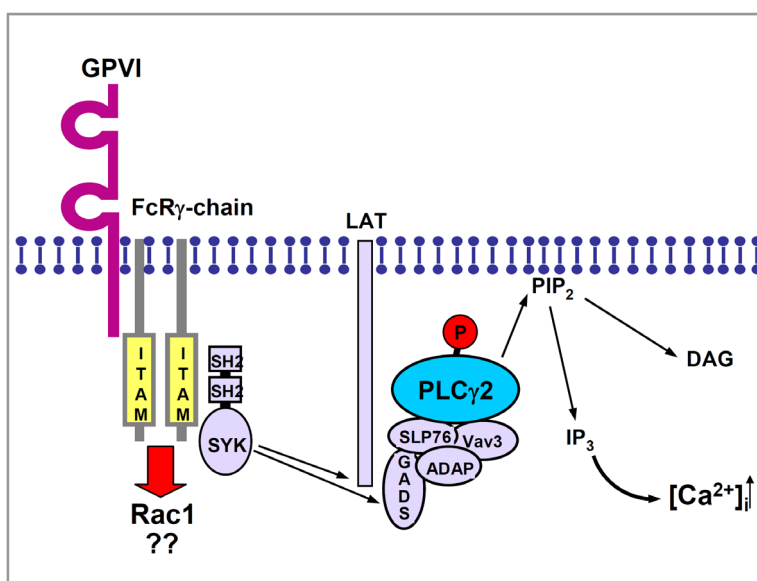


Figure 8. The GPVI signaling pathway. GPVI is non-covalently associated with the Fc receptor- γ (FcR γ) chain which bears an immunoreceptor tyrosine activation motif (ITAM). Activation of GPVI by collagen-binding induces tyrosine phosphorylation of the ITAM and SYK. Subsequently a phosphorylation cascade is initiated which involves several adaptor proteins, including LAT and SLP-76, and results in activation of the effector protein PLC γ . PLC γ induces the generation of DAG and IP₃ resulting in Ca²⁺ mobilization. The role of Rac1 downstream of GPVI activation is unclear.

1.4.3 Cdc42

Cdc42 is ubiquitously expressed and was first identified in yeast as a cell cycle-regulating protein. In mammalian cells, however, the GTPase has been shown to be involved in a variety of signaling processes including actin cytoskeletal reorganization, gene transcription, cell proliferation and differentiation⁴⁷. Constitutive deletion of Cdc42 in mice leads to death of the embryos before E 7.5⁴⁸.

In the hematopoietic system, recent reports using conditional knock-out mice revealed a crucial role for Cdc42 in regulating the balance between myelopoiesis and erythropoiesis, as well as for B cell development and activation and regulation of neutrophil polarity⁴⁹⁻⁵¹. Further studies reported a role for the GTPase in macrophage chemotaxis and phagocytosis^{52;53} and migration of monocytes⁵⁴.

Cdc42 has been demonstrated to be an important mediator of filopodia formation in various cell types. However, recent studies suggest that filopodia formation can also occur independently of Cdc42, involving most notably the novel Rho GTPase Rho-in filopodia (Rif) and the lipid-phosphatase-related protein-1 (LPR1)^{55;56}. Importantly, genetic targeting demonstrated that Cdc42 is not required for filopodia formation in embryonic fibroblastoid cells⁵⁷.

In addition to filopodia formation, Cdc42 has also been shown in several studies to be crucially involved in exocytosis in different cell types, such as neuroendocrine^{58;59} and MIN6 beta cells⁶⁰⁻⁶², as well as endothelial cells^{63;64}. Furthermore, in the hematopoietic system, Cdc42 activation was postulated to be essential for mediation of antigen-stimulated degranulation in RBL mast cells^{65;66}.

Despite a number of previous studies on the function of Cdc42 in platelets, its role in platelet activation and cytoskeletal reorganization, as well as its impact on degranulation and thrombus formation is currently unclear.

1.4.4 Rho GTPases in megakaryopoiesis and platelet biogenesis

As already mentioned, there is still little known about the impact of actin cytoskeletal rearrangements during megakaryocyte maturation and platelet production in general and the importance of Rho GTPases in particular.

Inhibition of the Rab GTPase Rab27b in primary MKs resulted in abrogated proplatelet formation while MK differentiation and ploidy remained unaltered⁶⁷.

Recently, overexpression studies revealed a negative regulation of proplatelet formation by RhoA *in vitro*⁶⁸. In line with this, modification of RhoA downstream effector pathways by inhibition of myosin light chain (MLC) phosphorylation or MLC II, as well as megakaryocyte-specific deletion of MYH9, the main myosin heavy chain, resulted in increased proplatelet formation^{27;69}. Although the function of Rac1 in megakaryocyte maturation and platelet production has not been studied in detail, it is assumed that the GTPase is dispensable for these processes since platelet count and size were normal in Rac1 conditional knock-out mice. In contrast, the role of Cdc42 during megakaryocyte maturation and platelet biogenesis is largely unknown.

1.5 Aim of the study

Cytoskeletal rearrangements play a crucial role during platelet shape change, secretion and spreading and small GTPases of the Rho family have been reported to be importantly involved in these processes. However, although a large number of studies address the function of Rho GTPases in various cell types, their role for platelet function is still largely unclear.

The aim of this thesis was (I) to investigate the function of the Rho GTPases Rac1 and Cdc42 for platelet function and signaling and (II) to gain new insights into their role for platelet production from megakaryocytes. For this purpose, conditional knock-out mice were generated using the Cre/loxP system with two different promoter strategies and analysis of single-, as well as double-deficient mice was performed.

2 MATERIALS AND METHODS

2.1 Materials

2.1.1 Kits and reagents

acetic acid	Roth (Karlsruhe, Germany)
ADP	Sigma (Deisenhofen, Germany)
agarose	Roth (Karlsruhe, Germany)
agarose, low melting	Euromedex (France)
ammonium peroxodisulphat (APS)	Roth (Karlsruhe, Germany)
apyrase (grade III)	Sigma (Deisenhofen, Germany)
atipamezol	Pfizer (Karlsruhe, Germany)
ATP release kit	Roche Diagnostics (Mannheim)
avertin (2,2,2-tribromoethanol and 2-methyl-2-butanol)	Sigma(Deisenhofen, Germany)
beta-mercaptoethanol	Roth (Karlsruhe, Germany)
bovine serum albumin (BSA)	AppliChem (Darmstadt, Germany)
calcium chloride	Roth (Karlsruhe, Germany)
Complete mini protease inhibitors (+EDTA)	Roche Diagnostics (Mannheim)
convulxin	Alexis Biochemicals (San Diego, USA)
Dylight-488	Pierce (Rockford, IL, USA)
Dynal Mouse T cell negative isolation kit	Invitrogen (Karlsruhe, Germany)
EDTA	AppliChem (Darmstadt, Germany)
enhanced chemoluminescence (ECL) detection substrate	PerkinElmer LAS (Boston, USA)
dNTP mix	Fermentas (St. Leon-Rot, Germany)
eosin	Roth (Karlsruhe, Germany)
epinephrine	Sigma (Deisenhofen, Germany)
epon 812	Roth (Karlsruhe, Germany)
ethanol	Roth (Karlsruhe, Germany)
ethidium bromide	Roth (Karlsruhe, Germany)
Eukitt mounting medium	Sigma (Deisenhofen, Germany)
fat-free dry milk	AppliChem (Darmstadt, Germany)
fentanyl	Janssen-Cilag GmbH (Neuss, Germany)

fibrillar type I collagen (Horm)	Nycomed (Munich, Germany)
flumazenil	Delta Select GmbH (Dreieich, Germany)
fluorescein-isothiocyanate (FITC)	Molecular Probes (Oregon, USA)
Fura-2 acetoxymethyl ester (AM)	Molecular Probes (Oregon, USA)
gelatine capsules	Agar scientific (Stansted, England)
GeneRuler 1kb DNA Ladder	Fermentas (St. Leon-Rot, Germany)
glucose	Roth (Karlsruhe, Germany)
glutaraldehyde	Roth (Karlsruhe, Germany)
hematoxylin	Sigma (Deisenhofen, Germany)
HEPES	Roth (Karlsruhe, Germany)
Hexomethyldizilasin (HMDS)	Merck (Darmstadt, Germany)
high molecular weight heparin	Sigma (Deisenhofen, Germany)
human fibrinogen	Sigma (Deisenhofen, Germany)
human vWF	CSL Behring (Hattersheim, Germany)
igepal CA-630	Sigma (Deisenhofen, Germany)
indomethacin	Sigma (Deisenhofen, Germany)
Integrilin	GlaxoSmithKline (Germany)
IP ₁ ELISA kit	Cisbio (Paris, France)
isopropanol	Roth (Karlsruhe, Germany)
6x Loading Dye Solution	Fermentas (St. Leon-Rot, Germany)
magnesium chloride	Roth (Karlsruhe, Germany)
medetomidine	Pfizer (Karlsruhe, Germany)
midazolam	Roche Pharma AG (Grenzach- Wyhlen, Germany)
mouse PF4 ELISA kit	RayBiotech (Georgia, USA)
mouse P-selectin ELISA kit	RayBiotech (Georgia, USA)
naloxon	Delta Select GmbH (Dreieich, Germany)
osmic acid solution 2% for electron microscopy	Merck (Darmstadt, Germany)
PageRuler Prestained Protein Ladder	Fermentas (St. Leon-Rot, Germany)
paraformaldehyde	Roth (Karlsruhe, Germany)
phalloidin-FITC	Sigma (Deisenhofen, Germany)

phenol/chloroform/isoamylalcohol	AppliChem (Darmstadt, Germany)
phorbol 12-myristate 13-acetate (PMA)	Sigma (Deisenhofen, Germany)
pI-pC	GE Healthcare (Buckinghamshire, England)
Pluronic F-127	Invitrogen (Karlsruhe, Germany)
Poly-L-lysine	Sigma (Deisenhofen, Germany)
potassium acetate	Roth (Karlsruhe, Germany)
prostacyclin	Calbiochem (Bad Soden, Germany)
R-phycoerythrin (PE)	EUROPA (Cambridge, UK)
Rotiphorese Gel 30 (PAA)	Roth (Karlsruhe, Germany)
Serotonin ELISA kit	IBL (Hamburg, Germany)
sodium chloride	AppliChem (Darmstadt, Germany)
sodium cacodylate	Roth (Karlsruhe, Germany)
tannic acid	Merck (Darmstadt, Germany)
Taq polymerase	Fermentas (St. Leon-Rot, Germany)
Taq polymerase buffer (10x)	Fermentas (St. Leon-Rot, Germany)
TEMED	Roth (Karlsruhe, Germany)
3,3',5,5'-tetramethylbenzidine (TMB)	EUROPA (Cambridge, UK)
thapsigargin	Molecular Probes (Oregon, USA)
thrombin	Roche Diagnostics (Mannheim)
triton X-100	AppliChem (Darmstadt, Germany)
uranyl acetate	Ladd Research Industries (USA)
U46619	Alexis Biochemicals (San Diego, USA)

Collagen-related peptide (CRP) was kindly provided by S.P. Watson (University of Birmingham, UK). Rhodocytin was a generous gift from Johannes Eble (University Hospital Frankfurt, Germany). Botrocetin was kindly provided by Francois Lanza (EFS Alsace, Strasbourg, France). All other chemicals were obtained from Sigma (Deisenhofen, Germany) or Roth (Karlsruhe, Germany).

2.1.2 Cell culture materials

BSA, low endotoxin	PAA Laboratories (Cölbe, Germany)
DMEM + GlutaMAX-I	Gibco (Karlsruhe, Germany)
D-PBS	Gibco (Karlsruhe, Germany)

Foetal Bovine Serum (FCS)	Gibco (Karlsruhe, Germany)
IMDM + GlutaMAX-I	Gibco (Karlsruhe, Germany)
Penicillin-Streptomycin	Gibco (Karlsruhe, Germany)
Steritop Bottle Top Filter 0.22 µm	Millipore (Massachusetts, USA)
thrombopoietin	Invitrogen (Karlsruhe, Germany)
tissue culture dishes (100x20 mm)	BD Falcon (Bedford, USA)
well plates (6-well, 24-well or 96-well)	BD Falcon (Bedford, USA)

2.1.3 Antibodies

2.1.3.1 Purchased primary and secondary antibodies

CD3 antibody	BD Biosciences (Heidelberg, Germany)
CD11b antibody	BD Biosciences
CD45R/B220 antibody	BD Biosciences
Cdc42 antibody	BD Biosciences
cofilin antibody	Cell Signaling Technologies (USA)
hFibrinogen antibody	DAKO (Hamburg, Germany)
hvwf antibody	DAKO (Hamburg, Germany)
Ly-6G and Ly-6C antibody	BD Biosciences
PLC γ 2 antibody clone Q20	Santa Cruz Biotechnologies (USA)
phosphocofilin antibody	Cell Signaling Technologies (USA)
phosphotyrosine antibody clone 4G10	Upstate (CA, USA)
Rac1 antibody	BD Biosciences
RFc (CD16/CD32/Fc γ III/II) antibody	DAKO (Hamburg, Germany)
Ter119 antibody	BD Biosciences
hvwf-HRP antibody	DAKO (Hamburg, Germany)
hFibrinogen-FITC antibody	DAKO (Hamburg, Germany)
rabbit anti-FITC-HRP antibody	DAKO (Hamburg, Germany)
rat anti-mouse IgG-HRP	DAKO (Hamburg, Germany)

2.1.3.2 Monoclonal Antibodies (mAbs)

mAbs generated and modified in our laboratory:

antibody	isotype	antigen	described in
JAQ1	IgG2a	GPVI	⁷⁰
DOM2	IgG1	GPV	⁷¹
JON/A	IgG2b	GPIIb/IIIa	⁷²
JON1	IgG2a	GPIIb/IIIa	⁷¹
ULF1	IgG2a	CD9	⁷¹
p0p4	IgG2b	GPIb α	⁷¹
p0p6	IgG2b	GPIX	⁷¹
MWReg 30	IgG1	α 2 integrin	Unpublished
12C6	IgG2b	α 2 integrin	Unpublished
WUG1.9	IgG1	P-selectin	Unpublished

2.1.4 Animals

Mice with floxed *Rac1*⁷³ or *Cdc42* genes⁷⁴ were kindly provided by Cord Brakebusch (Copenhagen, Denmark). Transgenic mice carrying either the Mx-Cre transgene (Mx-cre+)⁷⁵ or the PF4-Cre transgene (PF4-Cre+)⁷⁶ were from Cord Brakebusch and Radek Skoda (Basel, Switzerland), respectively.

For the Mx-Cre strategy, gene deletion was induced in 5 to 6 week-old ((fl/fl)/Mx-cre+) mice (25-30 g body weight) by two intraperitoneal injections of 200 μ g polyinosinic-polycytidylic acid (pI-pC) in a two-day interval. Control mice ((fl/fl)/Mx-cre-) received the same treatment and were derived from the same litters. Ten days after the last injection, the mice were tested for successful knock-out by western blot analysis of platelet lysates. For experiments, mice were used at least 2 weeks after pI-pC injection. In case of the PF4-Cre strategy, gene deletion occurred intrinsically upon activation of the PF4 promoter during megakaryopoiesis.

All used mice were maintained on a mixed SV/129/C57/Bl-6 background. Animal studies were approved by the district government of Lower Franconia (Bezirksregierung Unterfranken).

2.1.5 Buffers and media

All buffers were prepared and diluted using aqua ad iniectabilia (DeltaSelect Pfullingen, Germany) or double-distilled water (ddH₂O).

Acid-citrate-dextrose (ACD) buffer, pH 4.5	
trisodium citrate dehydrate	85 mM
citric acid anhydrous	65 mM
glucose anhydrous	110 mM
Blocking solution for immunoblotting	
BSA or fat-free dry milk in PBS or washing buffer	5%
Blotting buffer A for immunoblotting	
TRIS, pH 10.4	0.3 M
methanol	20%
Blotting buffer B for immunoblotting	
TRIS, pH 10.4	25 mM
methanol	20%
Blotting buffer C for immunoblotting	
ε-amino-n-caproic acid, pH 7.6	4 mM
methanol	20%
Cacodylate buffer (electron microscopy), pH 7.2	
sodium cacodylate	50 mM
CATCH buffer (modified)	
HEPES	25 mM
EDTA	3 mM
BSA	3.5%
in PBS, pH 7.2	
Coating buffer (ELISA), pH 9.0	
NaHCO ₃	50 mM
Coomassie staining solution	
acetic acid	10%
methanol	40%
Coomassie Brilliant blue	0.01%
Coomassie destaining solution	
acetic acid	10%
methanol	40%
Decalcification buffer	
EDTA	10%
in PBS, pH 7.2	

Fixation buffer I (electron microscopy)	
sodium cacodylate, pH 7.2	0.1 M
glutaraldehyde	2.5%
formaldehyde	2%
Fixation buffer II (electron microscopy)	
sodium cacodylate, pH 7.2	50 mM
osmium tetroxid	2%
IP buffer	
TRIS/HCl, pH 8.0	15 mM
NaCl	155 mM
EDTA	1 mM
NaN ₃	0.005%
Laemmli buffer for SDS-PAGE	
TRIS	40 mM
glycine	0.95 M
SDS	0.5%
Lysis buffer (DNA isolation), pH 7.2	
TRIS base	100 mM
EDTA	5 mM
NaCl	200 mM
SDS	0.2%
add Proteinase K (20 mg/ ml)	100 µg/ml
Lysis buffer (tyrosine phosphorylation), pH 7.5	
NaCl	300 mM
TRIS	20 mM
EGTA	2 mM
EDTA	2 mM
Na ₃ VO ₄	2 mM
Igepal CA-630	2%
add complete mini protease inhibitors	
MK Medium	
IMDM	
FCS	10%
Penicillin-Streptomycin	1%
TPO	50 ng/ml
Permeabilization buffer (electron microscopy)	
Taxol	10 ⁻⁵ M
Triton X-100	0.75%
Phalloidin	10 ⁻⁶ M
PFA	0.1%
add PHEM (pH 7.2) and complete mini protease inhibitors	

PHEM, pH 7.2	
PIPES	60 mM
HEPES	25 mM
EGTA	10 mM
MgSO ₄	2 mM
Phosphate buffered saline (PBS), pH 7.14	
NaCl	137 mM
KCl	2.7 mM
KH ₂ PO ₄	1.5 mM
Na ₂ HPO ₄	8 mM
Propidium iodide staining solution	
propidium iodide	25 µg/ml
RNase	100 µg/ml
in PBS, pH 7.2	
SDS sample buffer, 2x	
β-mercaptoethanol (for reduced conditions)	10%
TRIS buffer (1.25 M), pH 6.8	10%
glycerine	20%
SDS	4%
bromophenolblue	0.02%
Separating gel buffer, pH 8.8	
TRIS/HCl	1.5 M
Stacking gel buffer, pH 6.8	
TRIS/HCl	0.5 M
Stripping buffer, pH 6.8	
TRIS/HCl	62.5 mM
SDS	2%
β-mercaptoethanol	100 mM
50x TAE	
TRIS	0.2 M
acetic acid	5.7%
EDTA (0.5 M, pH 8)	10%
TE buffer, pH 8	
TRIS base	10 mM
EDTA	1 mM
Tris-buffered saline (TBS), pH 7.3	
NaCl	137 mM
TRIS/HCl	20 mM

Tyrode's buffer, pH 7.3

NaCl	137 mM
KCl	2.7 mM
NaHCO ₃	12 mM
NaH ₂ PO ₄	0.43 mM
CaCl ₂	1 mM
MgCl ₂	1 mM
HEPES	5 mM
BSA	0.35%
glucose	0.1%

Washing buffer (western blot)

Tween 20 in PBS, pH 7.2	0.1%
----------------------------	------

2.2 Methods**2.2.1 Mouse genotyping****2.2.1.1 Isolation of genomic DNA from mouse ears**

An approximately 5 mm² part of one ear was dissolved in 500 µl DNA lysis buffer by overnight incubation at 56°C under shaking conditions (900 rpm). 500 µl phenol/chloroform were added and, after vigorous shaking, samples were centrifuged at 14000 rpm for 10 min at room temperature (RT). Approximately 450 µl supernatant were taken and transferred into a new tube containing 500 µl isopropanol. After vigorous shaking, samples were centrifuged at 14000 rpm for 10 min at 4°C. The resulting DNA pellet was washed with 500 µl of 70% ethanol and centrifuged at 14000 rpm for 10 min at 4°C. After a second washing step, the DNA pellet was left to dry and finally resuspended in 100 µl TE buffer. Genotyping by PCR was performed using 2 µl DNA solution and 20 µl PCR reaction were separated on agarose gels for analysis.

2.2.1.2 Sample preparation for PCR

The pipeting scheme shown is representative for 1 sample (final volume: 50 µl) for the below described genotyping PCRs.

2 μ l	DNA solution
5 μ l	10x Taq buffer
5 μ l	MgCl ₂ (25 mM)
2 μ l	dNTPs (10 μ M)
2 μ l	primer 1 1:10 (stock: 1 μ g/ μ l)
2 μ l	primer 2 1:10 (stock: 1 μ g/ μ l)
0.5 μ l	Taq polymerase
31.5 μ l	H ₂ O

2.2.1.3 Detection of the *Cdc42* floxed allele by PCR

- **Primers**

Cdc42_for 5' ATG TAG TGT CTG TCC ATT GG 3'

Cdc42_rev 5' TCT GCC ATC TAC ACA TAC AC 3'

- **PCR program**

95°C 2:00 min

95°C	0:30 min	10x
63°C	0:30 min	
(-1 °C each cycle)		
72°C	0:45 min	

95°C	0:30 min	35x
53°C	0:30 min	
72°C	0:45 min	

72°C 4:00 min
4°C ∞

- **Resulting band sizes**

wt allele : 200 bp

floxed allele : 300 bp

2.2.1.4 Detection of the *Rac1* floxed allele by PCR

- **Primers**

Rac1_for 5' GTC TTG AGT TAC ATC TCT GG 3'

Rac1_rev 5' CTG ACG CCA ACA ACT ATG C 3'

- **PCR program**

95°C 5:00 min

95°C	0:30 min	10x
63°C	0:30 min	
(-1 °C each cycle)		
72°C	0:30 min	

95°C	0:30 min	35x
53°C	0:30 min	
72°C	0:30 min	

72°C	7:00 min
4°C	∞

- **Resulting band sizes**

wt allele	: 236 bp
floxed allele	: 318 bp

2.2.1.5 Detection of the Mx-Cre transgene by PCR

- **Primers**

Mx-Cre_for	5' AAC ATG CTT CAT CGT CGG 3'
Mx-Cre_rev	5' TTC GGA TCA TCA GCT ACA CC 3'

- **PCR program**

95°C	3:00 min
------	----------

95°C	0:30 min	10x
63°C	0:30 min	
(-1 °C each cycle)		
72°C	0:30 min	

95°C	0:30 min	35x
53°C	0:30 min	
72°C	0:30 min	

72°C	7:00 min
4°C	∞

- **Resulting band sizes**

wt	: no PCR product
Mx-Cre+	: 400 bp

2.2.1.6 Detection of the PF4-Cre transgene by PCR

- **Primers**

PF4-Cre_for	5' CCC ATA CAG CAC ACC TTT G 3'
PF4-Cre_rev	5' TGC ACA GTC AGC AGG TT 3'

- **PCR program**

96°C	3:00 min
------	----------

94°C	0:30 min	35x
58°C	0:30 min	
72°C	0:45 min	
72°C	3:00 min	
4°C	∞	

- **Resulting band sizes**

wt : no PCR product
PF4-Cre+ : 450 bp

2.2.2 *In vitro* analysis of platelet function

2.2.2.1 Platelet preparation and washing

Mice were bled under isofluran anesthesia from the retroorbital plexus. 700 µl blood were collected into an Eppendorf tube containing either 300 µl heparin in TBS (20 U/ml, pH 7.3) or 300 µl acid citrate dextrose (ACD). Blood was centrifuged at 1800 rpm for 5 min at RT. Supernatant and buffy coat were transferred into a new tube and centrifuged at 800 rpm for 6 min at RT to obtain platelet rich plasma (prp). To prepare washed platelets, prp was centrifuged at 2500 rpm for 5 min at RT in the presence of prostacyclin (PGI₂) (0.1 µg/ml) and the pellet was resuspended in 1 ml Ca²⁺-free Tyrode's buffer containing PGI₂ (0.1 µg/ml) and apyrase (0.02 U/ml). After 10 min incubation at 37°C the sample was centrifuged at 2500 rpm for 5 min. After a second washing step, the platelet pellet was resuspended in 500 µl Tyrode's buffer containing apyrase (0.02 U/ml) and left to incubate for at least 30 min at 37°C before analysis.

2.2.2.2 Platelet counting

For determination of platelet count and size, 50 µl blood were drawn from the retroorbital plexus of anesthetized mice using heparinized microcapillaries and collected into an Eppendorf tube containing 300 µl heparin in TBS (20 U/ml, pH 7.3). Platelet counts and size were determined using a Sysmex KX-21N automated hematology analyzer (Sysmex Corp., Kobe, Japan).

2.2.2.3 Immunoblotting

For western blot analysis, prp was prepared as described in section 2.2.2.1. Prp was centrifuged at 2500 rpm for 5 min and platelets were washed twice in PBS + 5 mM EDTA. The final platelet pellet was resuspended in IP buffer containing protease inhibitors to a final concentration of at least 0.5×10^6 platelets/ μ l and Igepal was added to a final concentration of 1%. After incubation for 20 min at 4°C and centrifugation at 14000 rpm for 5 min, the supernatant was mixed with an equal amount of 2x SDS sample buffer and boiled at 95°C for 5 min. Samples were separated by 12 or 15% SDS-PAGE and transferred onto a polyvinylidene difluoride (PVDF) membrane. To prevent non-specific antibody binding, membranes were blocked in 5% fat-free milk or 5% BSA dissolved in washing buffer for 2 h at RT or over night (o/n) at 4°C. Membranes were incubated with the required primary antibody (5 μ g/ml) o/n at 4°C with gentle shaking. Afterwards membranes were washed three times with washing buffer for 15 min at RT under shaking conditions. Next, membranes were incubated with appropriated HRP-labeled secondary antibodies for 1 h at RT. After three washing steps, proteins were visualized by ECL.

2.2.2.4 Flow cytometry

For determination of glycoprotein expression levels, platelets (1×10^6) were stained for 10 min at RT with saturating amounts of fluorophore-conjugated antibodies described in section 2.1.3.2, and analyzed directly after addition of 500 μ l PBS. For activation studies, platelets were activated with appropriate agonists or reagents for 15 min at RT in the presence of saturating amounts of phycoerythrin (PE)-coupled JON/A and fluorescein isothiocyanate (FITC)-coupled P-selectin antibodies. The reaction was stopped by addition of 500 μ l PBS and samples were analyzed on a FACSCalibur (Becton Dickinson, Heidelberg, Germany). For a two-colour staining, the following settings were used:

Detectors/Amps:

Parameter	Detector	Voltage
P1	FSC	E01
P2	SSC	380
P3	FI1	650
P4	FI2	580
P5	FI3	150

Threshold:

Value	Parameter
253	FSC-H
52	SSC-H
52	FI1-H
52	FI2-H
52	FI3-H

Compensation:

FI1	2.4% of FI2
FI2	7.0% of FI1
FI2	0% of FI3
FI3	0% of FI2

2.2.2.5 Aggregometry and agglutination

Washed platelets were adjusted to a concentration of 0.3×10^6 platelets/ml with Tyrode's buffer. Alternatively, heparinized prp was used and diluted 1:3 in Tyrode's buffer. For determination of aggregation, agonists or reagents (100-fold concentrated) were added and light transmission was recorded over 10 min on an Apact 4-channel optical aggregation system (APACT, Hamburg, Germany). Agglutination was induced in washed platelets by addition of 5 $\mu\text{g/ml}$ botrocetin and 10 $\mu\text{g/ml}$ human vWF in the presence of 40 $\mu\text{g/ml}$ Integrilin. For calibration of each measurement before agonist addition, Tyrode's buffer (for washed platelets) or 1:3-diluted plasma (for prp) was set as 100% aggregation and washed platelet suspension or prp was set as 0% aggregation.

2.2.2.6 Static adhesion assays**2.2.2.6.1 Adhesion on human fibrinogen or collagen-related peptide**

Glass coverslips were coated with 100 μg human fibrinogen or 100 $\mu\text{g/ml}$ collagen-related peptide (CRP) (diluted in PBS) overnight at 4°C under humid conditions and blocked for 2 h at RT with PBS 2% BSA. The coverslips were rinsed with Tyrode's buffer and washed platelets (100 μl with 0.03×10^6 platelets/ μl) were added and incubated at RT for the indicated time periods. The coverslips were rinsed again with Tyrode's buffer and platelets were visualized with a Zeiss Axiovert 200 inverted microscope (x100) using differential interference contrast (DIC) microscopy.

Representative images were taken and evaluated according to different platelet spreading stages.

2.2.2.6.2 Adhesion on murine vWF

Glass cover slips were coated with a polyclonal rabbit anti-human von Willebrand Factor (vWF) antibody (6.2 µg/ml, DAKO) for 2 h at 37°C under humid conditions and incubated with 10 µg/ml of mouse recombinant vWF for 2 h at RT. The coverslips were blocked for 1 h at RT with PBS 1% BSA. 300 µl of washed platelets at 0.03×10^6 platelets/µl were incubated with Integrilin (40 µg/ml) and botrocetin (2 µg/ml) and were allowed to adhere on the prepared coverslips for 20 min at 37°C. Samples were rinsed with PBS, fixed with 2.5% glutaraldehyde and processed for scanning electron microscopy (SEM).

2.2.2.7 Intracellular calcium measurements

Washed platelets at a concentration of approximately 0.4×10^6 platelets/µl in Ca^{2+} -free Tyrode's buffer were loaded with fura-2 AM (5 µM) in the presence of Pluronic F-127 (0.2 µg/ml) for 30 min at 37°C. After labeling, platelets were washed once and resuspended in Tyrode's buffer containing either 1 mM Ca^{2+} (for measurement of SOCE) or no Ca^{2+} (for measurement of store release). Stirred platelets were activated with appropriate agonists or reagents and fluorescence was measured with a PerkinElmer LS 55 fluorimeter. Excitation was alternated between 340 and 380 nm, and emission was measured at 509 nm. Each measurement was calibrated using 1% Triton X-100 and EGTA.

2.2.2.8 Adhesion under flow conditions

Coverslips (24 x 60 mm) were coated with 200 µg/ml fibrillar type-I collagen (Horm) o/n at 37°C and blocked for 1 h with 1% BSA. Blood (700 µl) was collected into 300 µl TBS (pH 7.3) containing 20 U/ml heparin and platelets were labeled with a Dylight-488 conjugated anti-GPIX Ig derivative (0.2 µg/ml) for 5 min at 37°C. Two parts of blood were diluted with 1 part Tyrode's buffer and filled into a 1 ml syringe. Perfusion studies were performed as follows. Transparent flow chambers with a slit depth of 50 µm, equipped with the coated coverslips, were connected to the syringe filled with diluted whole blood. Perfusion was performed using a pulse-free pump under high or

low shear stress equivalent to a wall shear rate of 1000 s^{-1} or 150 s^{-1} (4 min and 10 min). Thereafter, coverslips were washed by a 4 min perfusion with Tyrode's buffer at the same shear stress and phase-contrast and fluorescent images were recorded from at least five different microscope fields (40x objective). Image analysis was performed off-line using MetaVue[®] software. Thrombus formation was expressed as the mean percentage of total area covered by thrombi, and as the mean integrated fluorescence intensity per mm^2 .

2.2.2.9 Measurement of platelet nucleotide content and ATP release

For determination of platelet nucleotide contents, washed platelets were resuspended in Ca^{2+} -free Tyrode's buffer and proteins were precipitated with ice-cold 6.6 N perchloric acid. After centrifugation, nucleotides were isolated from supernatants with trioctylamine and freon (vol/vol) and measured by HPLC. For determination of ATP release washed platelets were adjusted to a concentration of $0.4 \times 10^6/\mu\text{l}$. Platelets were activated with the indicated agonists for 2 min at 37°C under stirring conditions (1000 rpm). Following activation, EDTA (3 mM final concentration) and formaldehyde (0.1% final concentration) were added and platelets were fixed for 2 h. The platelets were then centrifuged for 1 min at 13,000 rpm and 100 μl supernatant were added to 100 μl absolute ethanol. Samples were stored at -20°C until measuring. Levels of ATP in 12.5 μl sample were quantified using a bioluminescence assay kit according to the manufacturers' instructions and a Fluostar Optima luminometer (BMG Lab Technologies, Germany).

2.2.2.10 Measurement of platelet P-selectin, vWF and serotonin content and serotonin release

For determination of platelet P-selectin and vWF content, washed platelets at a concentration of 0.4×10^6 platelets/ μl were lysed in IP buffer containing 1% Igepal, incubated for 30 min at 4°C and centrifuged 5 min at 14000 rpm. P-selectin content was determined using a mouse P-selectin ELISA according to the manufacturers' protocol. For determination of vWF content, ELISA plates were coated with 10 $\mu\text{g}/\text{ml}$ rabbit anti-human vWF antibody in coating buffer o/n at 4°C and blocked with TBS 0.1% Tween 5% BSA. A \log^2 dilution of the samples in blocking buffer was prepared in the plate and incubated 2h at 37°C . After washing with TBS 0.1% Tween, samples were incubated with HRP-coupled rabbit anti-human antibody (1:3000 in blocking

buffer). After washing, ELISAs were developed using TMB-one substrate and plates were read at 450 nm. For determination of platelet serotonin content washed platelets were prepared as described above and lysed by two repeated freezing-thawing cycles using liquid nitrogen. After centrifugation for 5 min at 14000 rpm, the serotonin content in 10 μ l s/n was determined using a human serotonin ELISA kit according to the manufacturers' protocol. For determination of serotonin release washed platelets were activated with the indicated agonists for 2 min at 37°C, immediately centrifuged 1 min at 10000 rpm and the serotonin concentration in 10 μ l s/n was measured by ELISA.

2.2.2.11 Measurement of IP₁

Washed platelets were adjusted to a concentration of $0.7 \times 10^6/\mu$ l in a modified phosphate-free Tyrode's buffer containing 2 mM Ca²⁺ and 50 mM LiCl₂. Apyrase, indomethacin and EDTA were added to a final concentration of 2 U/ml, 10 μ M and 5 mM, respectively. Platelets were activated with the indicated agonists for 5 min at 37°C (350 rpm). After stimulation, platelets were lysed in the buffer supplied by the IP one ELISA kit (Cisbio, Paris, France). 50 μ l of lysed platelets were used for the IP₁ ELISA assay according to the manufacturers' protocol.

2.2.2.12 Tyrosine phosphorylation and immunoprecipitation

For tyrosine phosphorylation studies, equal amounts of platelets from wild-type and knock-out animals in suspension (0.7×10^6 platelets/ μ l) were stimulated with 2.5 μ g/ml convulxin under stirring conditions (1000 rpm) at 37°C. Stimulation was stopped by the addition of an equal volume ice-cold lysis buffer. For whole-cell tyrosine-phosphorylation, Laemmli's sample buffer was added; samples were incubated at 95°C for 5 min and separated by SDS-PAGE on 4-12% pre-cast NuPage Bis-Tris gradient gels (Invitrogen, Karlsruhe, Germany) under reducing conditions followed by transfer onto a PVDF membrane. For immunoprecipitation of individual proteins, following platelet lysis, samples were incubated with 2 μ g anti-PLC γ 2 antibody for 1 h at 4°C on a rotor and subsequently with Protein G-Sepharose at 4°C o/n. Immunoprecipitated proteins were washed three times in IP buffer before being boiled in Laemmli's sample buffer at 95°C for 5 min. Proteins were separated by SDS-PAGE on 4-12% pre-cast NuPage Bis-Tris gradient gels under reducing conditions followed by transfer onto a PVDF membrane. Membranes were blocked

for 1 h in 5% BSA in PBS and then incubated with the anti-phosphotyrosine antibody 4G10 for 1 h at RT. The membranes were then washed 4x 15 min in washing buffer before being incubated with secondary anti-mouse horseradish peroxidase-conjugated antibody in washing buffer. Following extensive washing, the membranes were developed using an enhanced chemiluminescence detection system. For tyrosine phosphorylation studies of individual proteins, membranes were incubated for 35 min at 50°C in stripping buffer and reprobbed with anti-PLC γ 2 antibody. Western blots were developed like described above.

2.2.2.13 Determination of platelet filamentous (F)-actin content

Washed platelets were prepared and the platelet count was adjusted to 0.2×10^6 platelets/ μ l in Ca²⁺-free Tyrode's buffer. Platelets were diluted 1:10 in Tyrode's buffer in a final volume of 50 μ l per condition, 5 μ l Dylight 649-conjugated anti-GPIX Ig derivative were added and samples were incubated 3 min at 37°C. Next, platelets were stimulated with 1 U/ml thrombin (final concentration) for 2 min at 37°C (400 rpm) and fixed for 10 min at 37°C by addition of 0.55% volume 10% PFA in PBS. Samples were centrifuged 5 min at 2500 rpm, the pellet was resuspended in 55 μ l Tyrode's buffer containing 0.1 volume % Triton-X 100 and 50 μ l were mixed with phalloidin-FITC at a final concentration of 10 μ M. Samples were incubated 30 min at RT in the dark and the reaction was stopped by addition of 500 μ l PBS. Samples were centrifuged 5 min at 2500 rpm and the pellet was resuspended in 500 μ l PBS. Samples were put on ice and immediately analyzed using a FACSCalibur (Beckton Dickinson, Heidelberg, Germany).

2.2.3 *In vivo* analysis of platelet function

2.2.3.1 Determination of platelet life span

Mice were injected intravenously with a Dylight-488 conjugated anti-GPIX Ig derivative (0.5 μ g/g body weight). At 1 h after injection (day 0), as well as at the other indicated time points, 50 μ l blood were collected and the percentage of GPIX-positive platelets was determined by flow cytometry.

2.2.3.2 Bleeding time assay

Mice were anesthetized and a 2 mm segment of the tail tip was removed with a scalpel. Tail bleeding was monitored by gently absorbing blood with filter paper at 20 second intervals, without directly contacting the wound site. When no blood was observed on the paper, bleeding was determined to have ceased. Experiments were stopped after 20 minutes.

2.2.3.3 Intravital microscopy of thrombus formation in FeCl₃-injured mesenteric arterioles

Mice (4-5 weeks of age) were anesthetized, and the mesentery was exteriorized through a midline abdominal incision. Arterioles (35-60 μm diameter) were visualized with a Zeiss Axiovert 200 inverted microscope (x10) equipped with a 100-W HBO fluorescent lamp source, and a CoolSNAP-EZ camera (Visitron, Munich, Germany). Digital images were recorded and analyzed off-line using Metavue software. Injury was induced by topical application of a 3 mm² filter paper saturated with FeCl₃ (20%). Adhesion and aggregation of fluorescently labeled platelets (Dylight-488 conjugated anti-GPIX Ig derivative) in arterioles was monitored for 40 min or until complete occlusion occurred (blood flow stopped for >1 min).

2.2.3.4 Monitoring of platelet adhesion to the injured carotid artery by intravital microscopy

Anesthetized mice were injected with carboxyfluorescein succinimidyl ester (CFSE)-labeled platelets of donor mice of the same genotype. The carotid artery was injured through ligation using a surgical filament and adhesion of platelets to the vessel wall was monitored over 10 min by fluorescence microscopy *in vivo*.

2.2.3.5 Intravital microscopy of thrombus formation in the abdominal aorta

The abdominal aorta of anesthetized mice was mechanically injured by a firm (5 sec) compression with a forceps and blood flow was monitored using an ultrasonic flow probe for 45 min or until full occlusion.

2.2.4 Megakaryocyte (MK) analysis

2.2.4.1 Isolation of MKs from fetal liver, purification by BSA gradient and study of proplatelet formation

Embryos of embryonic day (E) 13.5-14.5 were obtained from time-mated females, livers were removed, transferred into 1 ml pre-warmed DMEM and the remaining part of the body was kept in PBS and used for genotyping. Liver cells were resuspended 10x each using 19G and 22G needles and a 1 ml syringe and the cell suspension was centrifuged 5 min at 900 rpm (RT). The cells were resuspended in 2 ml MK medium, divided into 2 wells of a 12-well plate and incubated at 37°C, 5% CO₂. At day 3 of culture, MKs were purified by a BSA gradient following the protocol of Shivdasani *et al.*⁷⁷ and the isolated MKs were resuspended in 1 ml MK medium. For analysis of proplatelet formation, appr. 3000 cells/well were cultured in 96-well plates (triplicates) for one additional day and the percentage of proplatelet-forming MKs per visual field (20x objective) was determined. The remaining cells were cultured in one well of a 12-well plate for further analysis.

2.2.4.2 Isolation and culture of MKs from bone marrow of adult mice

Femur and tibiae of adult (approximately 6 week-old) mice were isolated and the bone marrow was flushed out using 2 ml modified CATCH buffer. Cells were homogenized using 23G needles and a 1 ml syringe and filtered through a cell strainer (40 µm, Falcon, Bedford, USA). The cell strainer was washed using 8 ml modified CATCH buffer and cells were counted using a Neubauer Chamber. MKs were purified by negative selection with the Dynal mouse T cell negative isolation kit according to the manufacturers' protocol using anti-B220, anti-GR-1 (Ly-6G/C), anti-CD3, anti-Ter-119 and anti-Mac1α antibodies (1:50 dilution). For this, the cells were centrifuged 10 min at 1200 rpm (RT) and the pellet was resuspended in PBS to a concentration of 100x10⁶ cells/ml. Antibodies and washed magnetic beads were added and the cells were incubated 20 min at RT with gentle shaking. Afterwards, the beads were washed with three times PBS using a magnetic rack and the washing fractions were collected. Cells were counted and centrifuged 10 min at 1200 rpm (RT). For analysis of proplatelet formation, the cells were plated on 96-well plates at a concentration of 5000 cells/well in MK medium, incubated for 4-6 days at 37°C, 5% CO₂, and proplatelet formation was analyzed as described above. The remaining

cells were cultured in 6-well plates at a concentration of 0.25×10^6 cells/well for further analysis.

2.2.4.3 Determination of MK ploidy by flow cytometry

When using fetal liver, fetal liver cells were cultured for 3 days as described 2.2.4.1 and used directly. Femur and tibia of adult mice were isolated and bone marrow was flushed out using 2 ml modified CATCH buffer. 200 μ l of the suspension were transferred into a FACS tube and centrifuged 5 min at 1200 rpm (RT). One additional sample was prepared for the isotype control. Cells were resuspended in 400 μ l 1:1 mixture CATCH/PBS 5% FCS. For saturation of unspecific binding sites, all samples were incubated with anti-RFc (CD16/CD32 Fc γ III/II) antibody (1:50 dilution) for 15 min on ice. Staining of GPIIb was directly afterwards performed using a FITC-conjugated anti- α 2 integrin (GPIIb) Ig derivative (5D7-FITC) at a 1:2.5 dilution for 20 min on ice. The isotype control was incubated with anti-rat IgG1-FITC under the same conditions. For washing, 1 ml 1:1 mixture CATCH/PBS 5% FCS were added and samples were centrifuged 5 min at 1200 rpm (RT). For fixation, cells were resuspended in 250 μ l PBS 0.1% EDTA, mixed well, an equal volume PBS 1% PFA was added and samples were incubated 10 min on ice. Cells were washed by addition of 3 ml PBS and centrifugation for 10 min at 1200 rpm (RT). For Permeabilization, cells were resuspended in 500 μ l PBS 0.1% Tween, incubated 10 min on ice and washed as described above. Cells were resuspended in 500 μ l propidium iodide (PI) staining solution, stained over night at 4°C in the dark and analyzed using a FACSCalibur (Becton Dickinson). For analysis, the GPIIb/PI-positive population was gated and the mean ploidy of the different ploidy stages was determined.

2.2.5 Electron microscopy

2.2.5.1 Transmission electron microscopy (TEM) of MKs *in situ*

For transmission electron microscopy the femura of mice were cut into approximately 1.5 mm pieces and fixed for 3 hours or over night at 4°C with fixation buffer I. The bone was removed with forceps and the bone marrow was washed with cacodylate buffer and subsequently fixed for 2 hours at 4°C with fixation buffer II. Samples were washed with distilled water and stained over night with 0.5% aqueous uranyl acetate,

dehydrated with ethanol and embedded in Epon 812. Ultrathin sections were stained with 2% uranyl acetate (in 100% ethanol) followed by lead citrate as described⁷⁸. Sections were inspected with an EM900 electron microscope (Zeiss, Oberkochen, Germany). Negatives were digitalized by scanning and processed with Adobe Photoshop.

2.2.5.2 TEM of platelets in suspension

Washed platelets were adjusted to a concentration of 0.3×10^6 platelets/ μl in Tyrode's buffer. Platelets were activated with 0.1 U/ml thrombin or 5 μM ADP (final concentration) under stirring conditions at 37°C and fixed by addition of an equal amount cacodylate buffer containing 5% glutaraldehyde for 10 min at 37°C without stirring. For complete fixation samples were incubated for 1 h at RT and afterwards at 4°C until further processing. Next, a small amount of the sample was further diluted to 1:10 in cacodylate buffer and washed three times by addition of 1 ml cacodylate buffer and subsequent centrifugation for 5 min at 1000 g (RT). Platelets were then left to adhere 1 h on poly-L-lysine-coated coverslips and processed for scanning electron microscopy (see 2.2.5.3). The remaining samples were washed three times for 5 min by addition of 1 ml cacodylate buffer and subsequent centrifugation for 5 min at 1500 g (37°C). A 2% low melting agarose solution in cacodylate buffer was prepared and kept at 45°C. After the final washing step, platelets were resuspended carefully in 1 ml agarose solution and immediately centrifuged 5 min at 14000 rpm (37°C). All except 100 μl agarose solution were discarded and samples were incubated on ice for 10 min. The hardened agarose pellets were cut out of the tubes and the platelet pellets were cut into approximately 1 mm² pieces and stored in cacodylate buffer. Samples were fixed in cacodylate buffer containing 1% OsO₄ for 45 min - 1 h at RT, washed twice with ddH₂O and incubated 60 min at 4°C in 2% uranylacetate in ddH₂O. After three washing steps with ddH₂O, samples were dehydrated in 70% (4x5 min), 95% (3x15 min) and 100% (3x15 min) ethanol. Next samples were incubated first in 100% propylenoxyde (2x10 min) and then in a 1:1 mixture propylenoxyde/epon (1x60 min) under rotating conditions. After 2 further incubations in epon at RT (first step: over night, second step: 2-3 h) samples were embedded in gelatine capsules and left to dry for 48 h at 60%. 50 nm thin sections were cut using a ultra microtom (Leica Ultracut UCT), contrasted and analyzed (Philips).

2.2.5.3 Scanning electron microscopy (SEM) of platelets

For immobilization and visualization of platelets fixed in suspension, coverslips were coated with 0.01% poly-L-lysine for 15 min at RT and left to dry over night at RT. Fixed platelets (see 2.2.5.2) were left to adhere for 20 min - 1h and further processes as described below.

For static adhesion, roundish coverslips (12 mm diameter) were coated with 100 µg/ml human fibrinogen in PBS for 2 h at RT, blocked 1 h with 1% BSA in PBS and shortly washed with PBS. Washed platelets were adjusted to a concentration of 0.03×10^6 platelets/µl, activated with 0.01 U/ml thrombin and 100 µl were immediately added to the coverslips and incubated at 37°C for the indicated time points. Samples were fixed by addition of 300 µl cacodylate buffer containing 2.5% glutaraldehyde for 1 h at 37°C and 1 h at RT and kept at 4°C until further processing. Coverslips were washed twice with 200 µl cacodylate buffer and dehydrated in 70% (4x5 min), 80% (1x5 min), 95% (1x5 min) and 100% (2x30 min) ethanol. Next, the coverslips were incubated with increasing concentrations of hexamethyldizilasin (HMDS) in 100% ethanol (25%: 1x 5 min; 50%: 1x5 min; 75%: 1x5 min, 100%: 2x5 min). Samples were left to dry, sputtered with gold using a Cressington Sputter Coater 108 Auto and a 0.2 µm thin gold foil (both from Cressington, Chalk Hill, England) and analyzed using a FEI electron microscope (Philips).

2.2.5.4 Visualization of the platelet cytoskeleton by SEM

Washed platelets were adjusted to a concentration of 0.03×10^6 platelets/µl, activated and incubated on fibrinogen-coated coverslips as described in section 2.2.5.3. Afterwards, the coverslips were immediately treated with 500 µl permeabilization buffer for 2 min at 37°C. Reactions were stopped by addition of the same volume PHEM containing 4% PFA and 0.4% glutaraldehyde and incubated 1 h at RT and afterwards over night at 4°C. Coverslips were next washed in PHEM (1x), ddH₂O (5x), 0.2% aqueous tannic acid (1x2 min), ddH₂O (5x), 0.5% OsO₄ (1x5 min) and ddH₂O (5x). Subsequently, coverslips were dehydrated and further processed for SEM as described above.

2.2.6 Histology

2.2.6.1 Preparation of paraffin sections

Spleen and femurs from adult mice were washed in PBS and fixed over night in PBS 4% PFA. Afterwards, organs were washed 3 times with PBS and spleens were directly dehydrated and embedded in paraffin. Fixed femurs were incubated for 3 further weeks in 10 ml decalcification buffer with the buffer being changed twice per week. After decalcification, femurs were also embedded in paraffin. Organs were cut using a Microm Cool Cut microtom (Thermo Scientific, Braunschweig, Germany) to prepare 5 μ m thin sections.

2.2.6.2 Hematoxylin/eosin staining of paraffin sections

Sections were deparaffinated by two incubations in Xylol (3 min each). Rehydration was carried out using decreasing ethanol concentrations (100, 96, 90, 80 and 70%) with 2 incubation time in each solution and a final 2 min incubation in deionized water. Next, sections were stained 2 min with hematoxylin, followed by a 10 min washing step using running tap water and 2 min staining with 0.05% Eosin G. The sections were washed shortly and dehydration was carried out using the same ethanol concentrations and incubation times as described above, but in reversed order. Finally sections were incubated twice in Xylol for each 3 min, dried and mounted using Eukitt mounting medium. Samples were analyzed using a Leica DHI 4000B inverse microscope equipped with a Leica digital camera.

2.2.7 Data analysis

Results are shown as mean \pm SD from at least three individual experiments per group. Statistical analysis between wild-type and knock-out groups were assessed by the Mann-Whitney U-test. *P*-values <0.05 were considered statistically significant.

3 RESULTS

3.1 Rac1 is essential for phospholipase C- γ 2 activation in platelets

3.1.1 Rac1 is dispensable for platelet production but essential for lamellipodia formation

Lack of functional Rac1 leads to embryonic lethality in mice³⁴. Since at the time of the study, PF4-Cre mice were not available, conditional knock-out mice were generated by using the Mx-Cre/loxP system^{73;75}. Deletion of the *Rac1* gene in *Rac1* (fl/fl cre+) mice was induced by repeated injections of pl-pC which induces Cre expression in the hematopoietic system and leads to efficient gene deletion in megakaryocytes and, consequently, protein deficiency in platelets^{2;79}. *Rac1* (fl/fl) mice not carrying Mx-Cre were used as wild-type controls. Ten days after the last injection, the absence of Rac1 in platelets from *Rac1* (fl/fl cre+, further referred to as *Rac1*^{-/-}) mice was confirmed by Western blot analysis of whole cell lysates (Fig. 9a) using GPIIIa levels as loading control.

	wild-type	<i>Rac1</i> ^{-/-}
GPIb	454 ± 28	403 ± 23
GPV	290 ± 6	262 ± 6
GPIX	486 ± 27	470 ± 17
GPVI	45 ± 6	40 ± 3
α2	118 ± 4	113 ± 10
β1	171 ± 2	185 ± 29
αIIbβ3	586 ± 44	545 ± 59
CD9	1260 ± 214	1080 ± 49
mean FSC	560 ± 35	455 ± 43

Table 1. Platelet membrane glycoprotein expression in *Rac1*^{-/-} platelets. Diluted whole blood was stained with fluorophore-labeled antibodies at saturating concentrations for 15 min at RT and analyzed on a FACSCalibur (Becton Dickinson, Heidelberg). Platelets were gated by FSC/SSC characteristics. Results are given as the mean fluorescence intensity ± SD of 6-12 mice per group. Mean platelet size (mean FSC) was determined by FSC characteristics. (Pleines I *et al.*, *Pflugers Arch* 2009⁸⁰.)

Deletion of Rac1 had no significant effect on peripheral platelet counts (Fig. 9b) or the expression of prominent surface receptors including integrins α IIb β 3 and α 2 β 1 as well as GPIb and GPVI (Table 1). In line with this, the life span of *Rac1*^{-/-} platelets was comparable to wild-type platelets (Fig. 9c). These results strongly indicated that Rac1 is not essential for megakaryocyte development and platelet production.

Furthermore, in accordance with the proposed function of Rac1⁴³, *Rac1*^{-/-} platelets failed to form lamellipodia and to spread on a fibrinogen coated surface upon thrombin stimulation, but retained the ability to adhere and form filopodia, confirming recent results from McCarty *et al.*³³ (Fig. 9d).

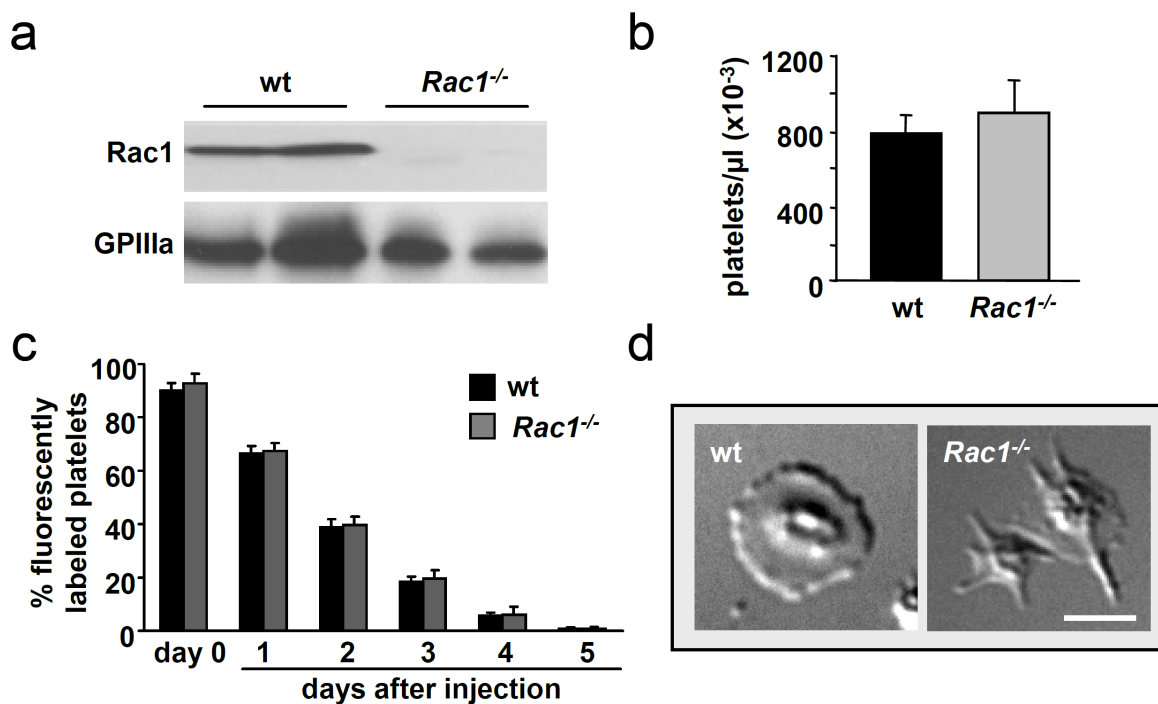


Figure 9. Rac1 is dispensable for platelet production but essential for lamellipodia formation. (a) Western blot analysis of Rac1 expression in wild-type and *Rac1*^{-/-} platelets 10 days after the first pl-pC injection. GPIIIa was used as control. (b) Peripheral platelet counts (n=6 per group). (c) *Rac1*^{-/-} platelets have a normal life span. Wild-type (black) and *Rac1*^{-/-} mice (gray) were injected intravenously with Dylight-488 conjugated anti-GPIX Ig derivative (0.5 $\mu\text{g/g}$ body weight) and the population of fluorescently labeled platelets was monitored over 5 days using flow cytometry. (d) Washed platelets from the indicated mice were allowed to adhere and spread on immobilized human fibrinogen upon thrombin activation. DIC images taken at t=45 min, representative of 6 individual experiments. Bar, 5 μm . (Pleines I *et al.*, *Pflugers Arch* 2009⁸⁰.)

3.1.2 Scanning electron microscopy studies of *Rac1*^{-/-} platelets

To study the morphology of *Rac1*^{-/-} platelets in more detail, scanning electron microscopy (SEM) was performed. The results confirmed unaltered size of resting platelets, as compared to wild-type platelets (Fig. 10a), as well as the inability of *Rac1*^{-/-} platelets to form lamellipodia on fibrinogen upon thrombin activation (Fig. 10b, upper panel). Visualization of the cytoskeleton of activated platelets by SEM demonstrated the presence of actin stress fibers in wild-type platelets, whereas *Rac1*^{-/-} platelets were only able to form filopodia (Fig. 10b, lower panel). In contrast, when activated in suspension with ADP or thrombin, *Rac1*^{-/-} and wild-type platelets exhibited similar morphology (Fig. 10c). This result indicated that lamellipodia formation may rather be of importance for platelet spreading on ligand-covered surfaces, such as the ECM, than for platelet aggregation in the flowing blood.

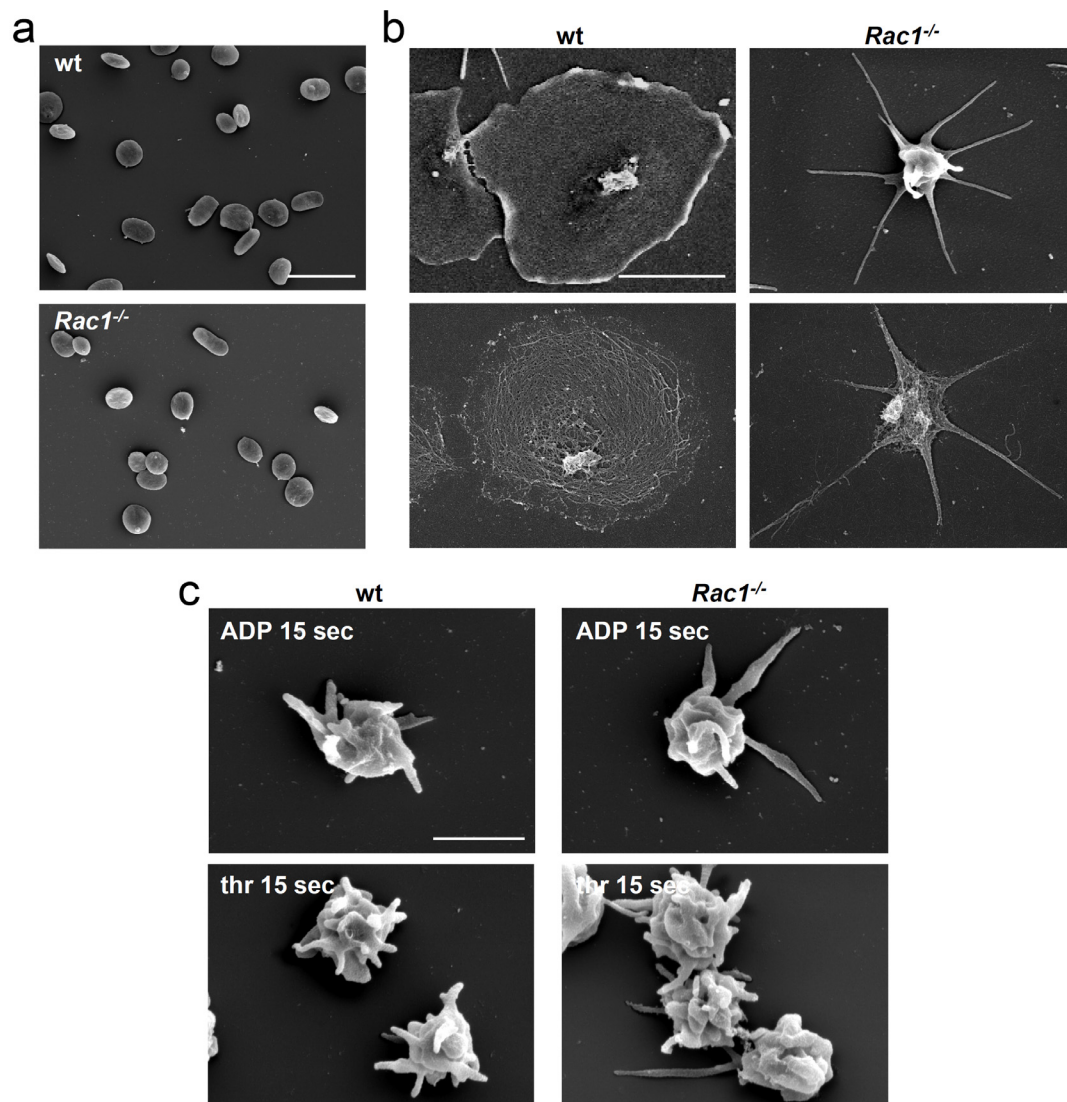


Figure 10. Scanning electron microscopy studies of *Rac1*^{-/-} platelets. (a–c) Scanning electron microscopy (SEM) of *Rac1*^{-/-} and wild-type platelets. (a) resting platelets immobilized on poly-L-lysine. Bar, 5 µm. (b) Spread *Rac1*^{-/-} and wild-type platelets upon activation with 0.01 U/ml thrombin on human fibrinogen (100 µg/ml, 30 min). Upper panel: SEM of intact platelets. Lower panel: visualization of the actin cytoskeleton after denudation of the plasma membrane. Bar, 2 µm. (c) Morphology of *Rac1*^{-/-} and wild-type platelets in suspension at 15 seconds after activation with thrombin (0.1 U/ml, upper panel) or ADP (5 µM, lower panel). Bar, 1 µm.

3.1.3 *Rac1*^{-/-} platelets show diminished responses to GPVI and CLEC-2 stimulation

The response of *Rac1*^{-/-} platelets to different agonists was tested by standard aggregometry. In response to thrombin, ADP, and the stable TXA₂ analog U46619 *Rac1*^{-/-} platelets aggregated normally at all tested concentrations (Fig. 11a,d), although a slightly faster reversion of ADP-induced aggregation was consistently observed with mutant platelets as compared to the wild-type controls. In contrast, *Rac1*^{-/-} platelets showed a clear reduction in their reactivity towards collagen which was most evident at low and intermediate concentrations of the agonist (Fig. 11b,d).

Since platelet activation by collagen is mediated by GPVI, in the next step, a possible defect in this pathway was tested by use of the GPVI-specific agonist collagen related peptide (CRP). Again, a markedly reduced response was found in *Rac1*^{-/-} platelets that was most evident at low and intermediate concentrations (Fig. 11b,d). Interestingly, rhodocytin (RC)-induced aggregation was also impaired at low and intermediate concentrations, suggesting defective signaling downstream of CLEC-2^{8;81}.

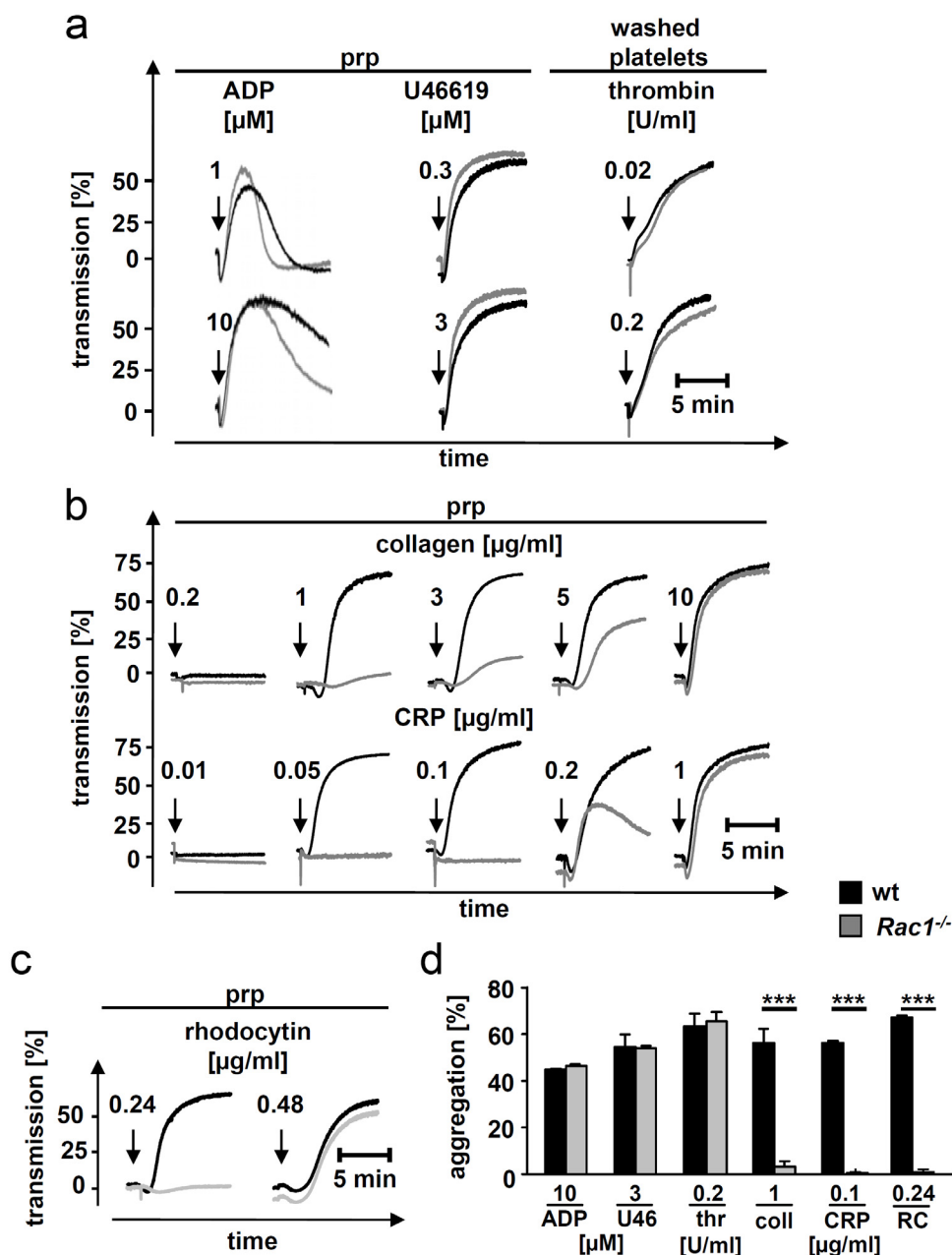


Figure 11. *Rac1*^{-/-} platelets show impaired aggregation responses to GPVI agonists. Washed platelets from wild-type (black line) and *Rac1*^{-/-} (gray line) mice were activated with the indicated concentrations of (a) ADP, U46619 and thrombin, (b) collagen and CRP or (c) rhodocytin. The experiments were performed in the presence of 70 μg/ml human fibrinogen. Thrombin stimulation was done in the absence of human fibrinogen. The results shown are representative of 9-15 individual experiments. (d) Bar graphs of results obtained by aggregometry. Results are given as the mean % of aggregation ± SD. (Pleines I *et al.*, *Pflügers Arch* 2009⁸⁰.)

It is well established that under conditions of standard aggregometry, aggregation in response to collagen, and to a lower extent also to CRP, is amplified by released mediators, such as ADP and TXA₂, making it difficult to directly assess defects in individual signaling pathways. Therefore, platelets were pre-incubated with apyrase (2 U/ml) and indomethacin (10 μM) to prevent the effects of these mediators and then stimulated with high concentrations of collagen (20 μg/ml) or CRP (10 μg/ml). Under these conditions, wild-type but not *Rac1*^{-/-} platelets were able to aggregate, strongly indicating a selective GPVI signaling defect in the absence of Rac1 (Fig. 12).

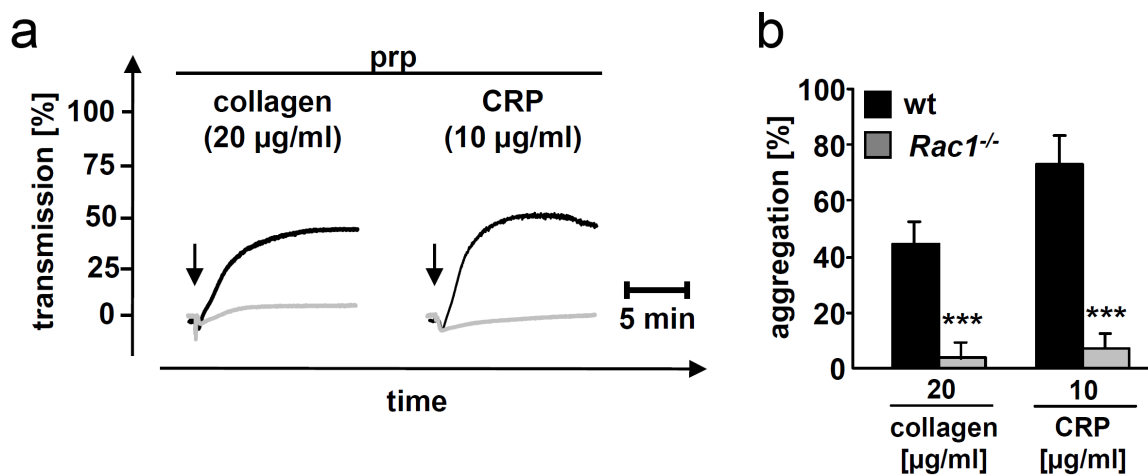


Figure 12. Aggregation of *Rac1*^{-/-} platelets upon GPVI stimulation is abolished in presence of inhibitors of secondary agonists. (a) Washed platelets from wild-type (black line) and *Rac1*^{-/-} (gray line) mice were incubated with high concentrations of apyrase (2 U/ml) and indomethacin (10 μM) and activated with the indicated concentrations of collagen and CRP. The experiments were performed in the presence of 70 μg/ml human fibrinogen. The results shown are representative of 4 individual experiments. (b) Bar graphs of results obtained by aggregometry. Results are given as the mean % of aggregation ± SD. (Pleines I *et al.*, *Pflugers Arch* 2009⁸⁰.)

The results of aggregometry were confirmed by flow cytometric analysis of single platelets in diluted suspensions, i.e. under experimental conditions that largely exclude the accumulation of released mediators^{82;83}. Washed platelets were stimulated with increasing concentrations of CRP, RC, thrombin and ADP and the activation of integrin αIIbβ3 (JON/A-PE⁷²), as well as degranulation-dependent surface exposure of P-selectin was determined. Equally strong αIIbβ3 activation was observed in control and *Rac1*^{-/-} platelets in response to thrombin and ADP (Fig. 13a,c). Likewise, thrombin-induced P-selectin expression was indistinguishable between the two groups at all tested concentrations (Fig. 13b,c), whereas ADP, as expected, failed to induce significant P-selectin expression. In contrast, the response of *Rac1*^{-/-} platelets to CRP or the GPVI-activating snake venom protein convulxin (CVX) was virtually abolished, even at very high concentrations of the agonists. Similarly, αIIbβ3 activation and P-selectin expression were dramatically impaired in

response to RC in *Rac1*^{-/-} platelets. This selective secretion defect was also confirmed when ATP release was determined. Thrombin induced comparable ATP release in control and *Rac1*^{-/-} platelets, whereas CRP- or CVX-induced ATP release was minimal in the mutant cells (Fig. 13d).

Together, these results demonstrate a pronounced defect in *Rac1*^{-/-} platelets in the ITAM and ITAM-like signaling pathways mediated by GPVI and CLEC-2, respectively, but normal responses to G protein-coupled agonists.

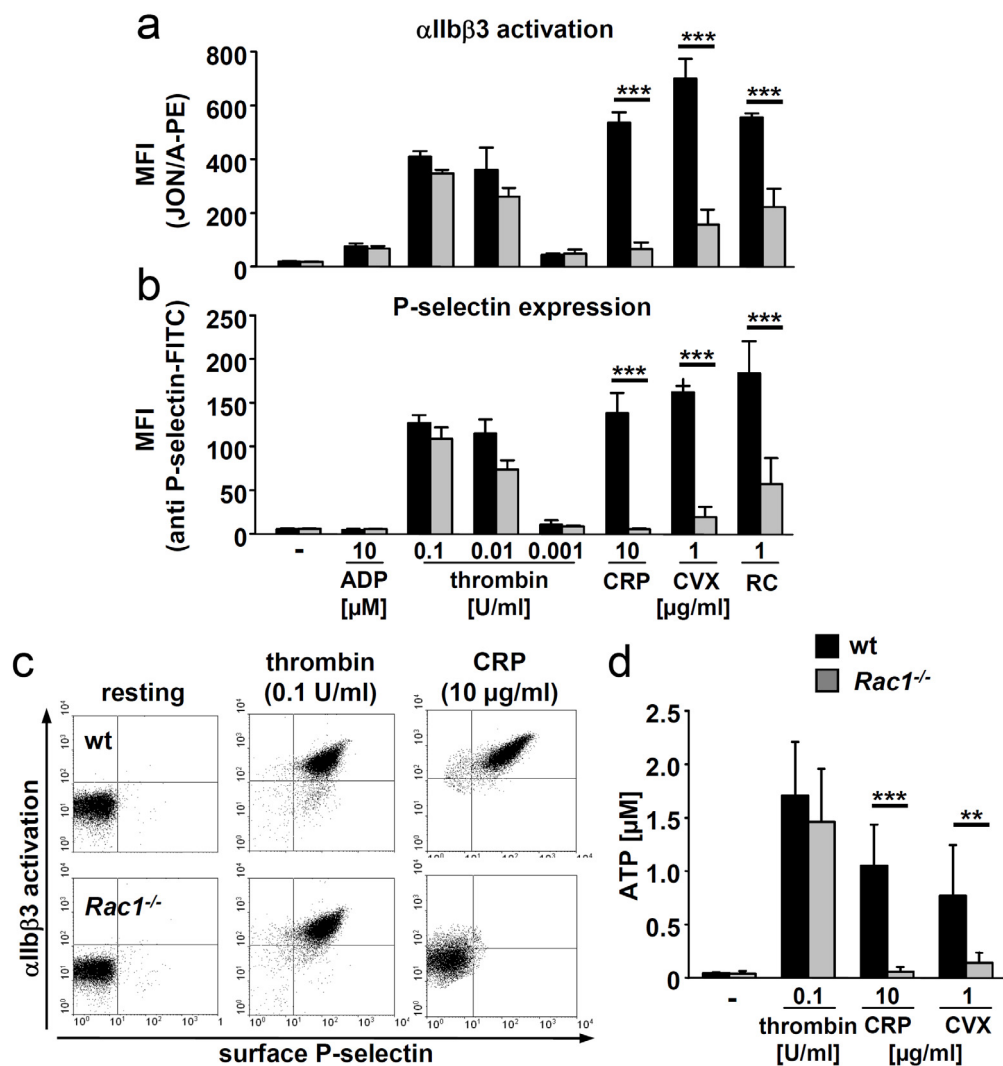


Figure 13. Defective α IIb β 3 activation and granule secretion in *Rac1*^{-/-} platelets in response to GPVI and CLEC-2 stimulation. Washed blood from wild-type and *Rac1*^{-/-} mice was incubated for 15 min with the indicated agonists in the presence of JON/A-PE directed against the activated form of mouse α IIb β 3 and a FITC-conjugated anti-mouse P-selectin antibody. Data shown are mean fluorescence intensities (MFI) \pm SD (n=6 per group) for (a) JON/A-PE and (b) anti-P-selectin-FITC. (c) Representative dot plots (F11/F12). (d) Measurement of released ATP. Washed platelets were incubated for 2 min at 37°C with the indicated agonists and fixed. ATP present in the supernatant was measured using a luminometric assay. Results are given as mean ATP concentration (μ M) \pm SD (n=6 per group). (Pleines I *et al.*, *Pflugers Arch* 2009⁸⁰.)

3.1.4 Defective PLC γ 2 activation and Ca $^{2+}$ mobilization in *Rac1* $^{-/-}$ platelets

The results shown above suggested that Rac1 might be directly involved in ITAM/ITAM-like signaling upstream of Ca $^{2+}$ mobilization and PKC activation as these processes were obviously functional downstream of Gq-coupled agonists. To test this directly, changes in [Ca $^{2+}$] $_i$ in response to thrombin and CRP were assessed. As shown in Fig. 14a and b, intracellular Ca $^{2+}$ mobilization in response to CRP was significantly reduced in *Rac1* $^{-/-}$ platelets compared to controls as determined in the absence of extracellular Ca $^{2+}$. As a direct consequence, the subsequent Ca $^{2+}$ entry was also dramatically diminished in the mutant cells. In contrast, unaltered Ca $^{2+}$ mobilization and entry was seen in response to thrombin stimulation. These results suggested that Rac1 may be required for efficient activation of PLC γ 2, but not PLC β .

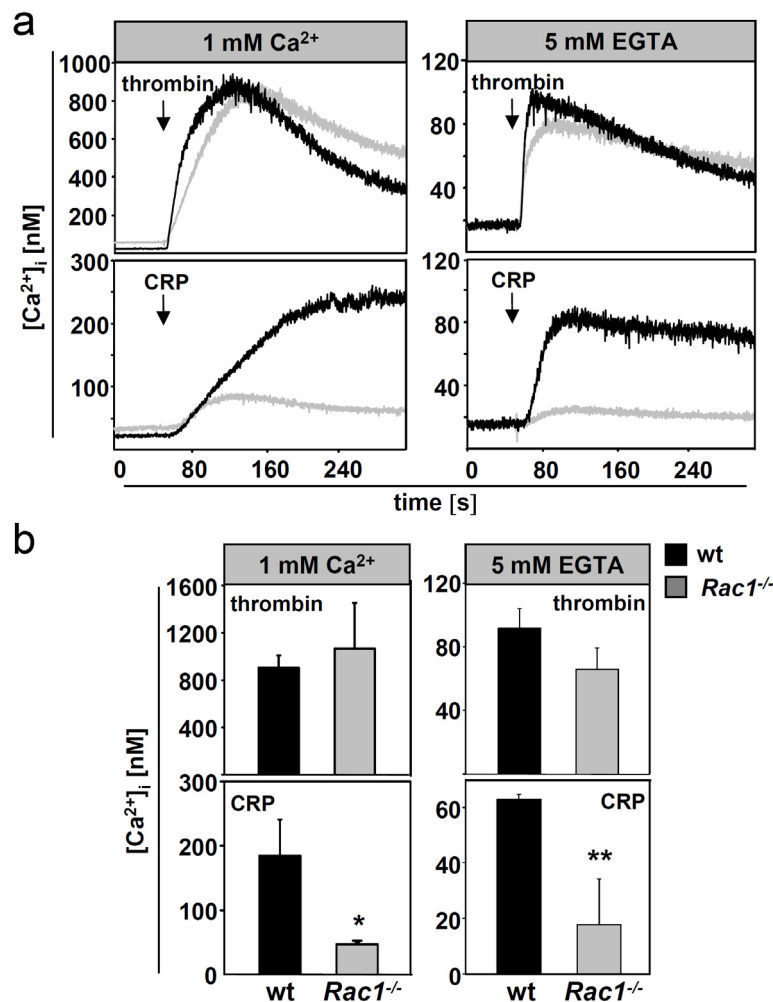


Figure 14. Defective calcium mobilization upon GPVI stimulation in *Rac1* $^{-/-}$ platelets. (a) Time course of intracellular calcium mobilization in wild-type (black curve) and *Rac1* $^{-/-}$ platelets (gray curve) in response to thrombin (0.1 U/ml) and CRP (5 μ g/ml) in the presence (1 mM Ca $^{2+}$) and absence (5 mM EGTA) of extracellular Ca $^{2+}$. Results shown are representative of 6 individual experiments. (b) Maximal increase of cytosolic Ca $^{2+}$ concentration of wild-type (black bars) and *Rac1* $^{-/-}$ platelets (gray bars) after activation with the indicated agonists. Results are given as mean [Ca $^{2+}$] $_i$ (nM) \pm SD, n=3 per group. (Pleines I *et al.*, *Pflugers Arch* 2009⁸⁰.)

To test this more directly, PLC γ 2 activity was analyzed by indirect measurement of inositol trisphosphate (IP $_3$) using an IP $_1$ ELISA (Fig. 15a). The IP $_3$ lifetime within the cell is very short (less than 30 sec) before it is transformed into IP $_2$ and IP $_1$. IP $_1$ can accumulate in the cell after addition of Li $^+$ ions which inhibits its degradation to myo-inositol. Therefore, IP $_1$ was quantified after platelet activation with thrombin (1 U/ml) or CVX (1 μ g/ml) in the presence of apyrase (2 U/ml) and indomethacin (10 μ M). While thrombin-induced IP $_1$ production was comparable in control and *Rac1* $^{-/-}$ platelets, the response to CVX was markedly reduced in the mutant cells as compared to controls (137 \pm 17 nM vs. 418 \pm 37.1 nM, n=3, P<0.001), indicating that the activity of PLC γ 2 was indeed affected in the absence of Rac1 (Fig. 15a).

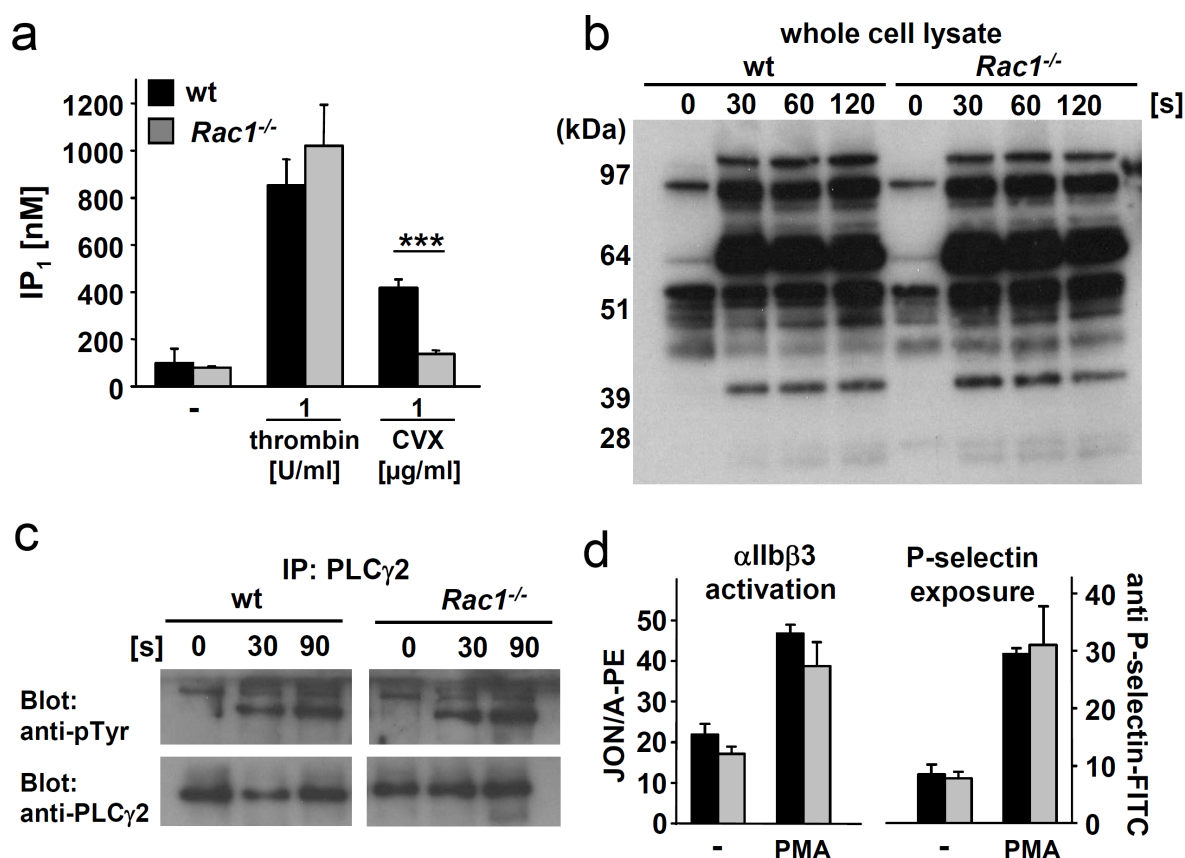


Figure 15. Defective GPVI- induced PLC γ 2 activation in *Rac1* $^{-/-}$ platelets. (a) Quantification of produced IP $_1$ upon activation. Washed platelets from wild-type and *Rac1* $^{-/-}$ mice were stimulated with the indicated agonists. Platelets were lysed and IP $_1$, a specific metabolite of IP $_3$, was quantified using an ELISA assay. Results are given as the mean IP $_1$ concentration (nM) \pm SD (n=3 per group). (b) Determination of tyrosine phosphorylation. Washed platelets from wild-type and *Rac1* $^{-/-}$ mice were stimulated with 1 μ g/ml CVX and aliquots were taken at the indicated time points. Samples were blotted and stained using an antibody against phosphorylated tyrosine. The result shown is representative for three individual experiments. (c) Immunoprecipitation using a PLC γ 2-specific antibody. Washed platelets from wild-type and *Rac1* $^{-/-}$ mice were stimulated as described under (a). Precipitates were blotted and stained using an antibody specific for phosphorylated tyrosine (upper panel) and an antibody against PLC γ 2 (lower panel). The result shown is representative for three individual experiments. (d) Washed platelets were activated with 1 μ g/ml PMA, stained with JON/A-PE and anti-P-selectin-FITC and directly analysed by flow cytometry. The results are expressed as MFI \pm SD (n=6 per group). (Pleines I *et al.*, *Pflugers Arch* 2009⁸⁰.)

The PLC γ 2 activation defect was not based on reduced tyrosine phosphorylation of the enzyme in response to GPVI stimulation as shown by whole cell tyrosine phosphorylation experiments, where the CVX-induced changes were indistinguishable between control and *Rac1*^{-/-} platelets, including strong phosphorylation of a protein that migrated at the known position of PLC γ 2 (155 kDa) (Fig. 15b). This was further confirmed by immunoprecipitation experiments, which yielded comparable increases in tyrosine phosphorylation of PLC γ 2 in control and mutant platelets (Fig. 15c).

To also test a possible involvement of Rac1 in the GPVI signaling cascade downstream of PLC γ 2 but independent of Ca²⁺ mobilization, PKC-dependent activation was assessed. For this, control and *Rac1*^{-/-} platelets were stimulated with the DAG analog PMA. No differences in aggregation (not shown), integrin α IIb β 3 activation, or P-selectin exposure were found (Fig. 15d), suggesting that Rac1 is not required for PKC-mediated activation processes in platelets.

3.1.5 Defective adhesion and aggregation of *Rac1*^{-/-} platelets on collagen under flow

To investigate the functional consequences of Rac1 deficiency under more physiological conditions, platelet adhesion and thrombus formation on a collagen-coated surface under flow in a whole blood perfusion system was analyzed⁸⁴. Under both high (1000 s⁻¹) and low (150 s⁻¹) shear conditions, wild-type platelets rapidly adhered to the collagen surface and recruited additional platelets from the blood stream resulting in the formation of stable three-dimensional aggregates (Fig. 16a, left, b). In sharp contrast, adhesion of *Rac1*^{-/-} platelets was significantly reduced as compared to the control and the formation of stable three-dimensional thrombi was virtually abrogated. As a result, the surface area covered by platelets at the end of the perfusion period was markedly reduced for *Rac1*^{-/-} blood as compared to wild-type and consisted almost exclusively of a single platelet layer (Fig. 16 a, middle, b).

These results demonstrated that Rac1 was essential for the formation of stable three-dimensional platelet thrombi on collagen under flow conditions. This is in line with a recent study by McCarty *et al.* who made similar observations but attributed this defect mainly to the important function of Rac1 in the agonist-induced reorganization of the cytoskeleton leading to lamellipodia formation and spreading³³. In contrast to

this hypothesis, the data shown here indicated that the defect in GPVI-induced activation and release of ADP and TXA₂ could also be responsible for the inability to form three-dimensional thrombi. To discriminate between these two possibilities, it was next tested whether thrombus formation of *Rac1*^{-/-} platelets could be restored by exogenously adding the ‘missing’ secondary acting agonists. For this, ADP and U46619 were co-infused into *Rac1*^{-/-} blood directly before it entered the flow chamber⁸⁵. Under these experimental conditions, large thrombi formed within 2 min under high (Fig. 16a right, b) and low (not shown) shear conditions. These thrombi were stable and did not detach from the collagen-coated surface or shed emboli, demonstrating that *Rac1*^{-/-} platelets can adhere and form shear-resistant thrombi on collagen when stimulated appropriately. These results suggest that the defect in GPVI-dependent cellular activation rather than the inability to form lamellipodia is the major cause for the markedly reduced thrombus stability observed with *Rac1*^{-/-} platelets. This hypothesis is also in line with the observed unaltered morphology of *Rac1*^{-/-} platelets activated in suspension (Fig. 10c).

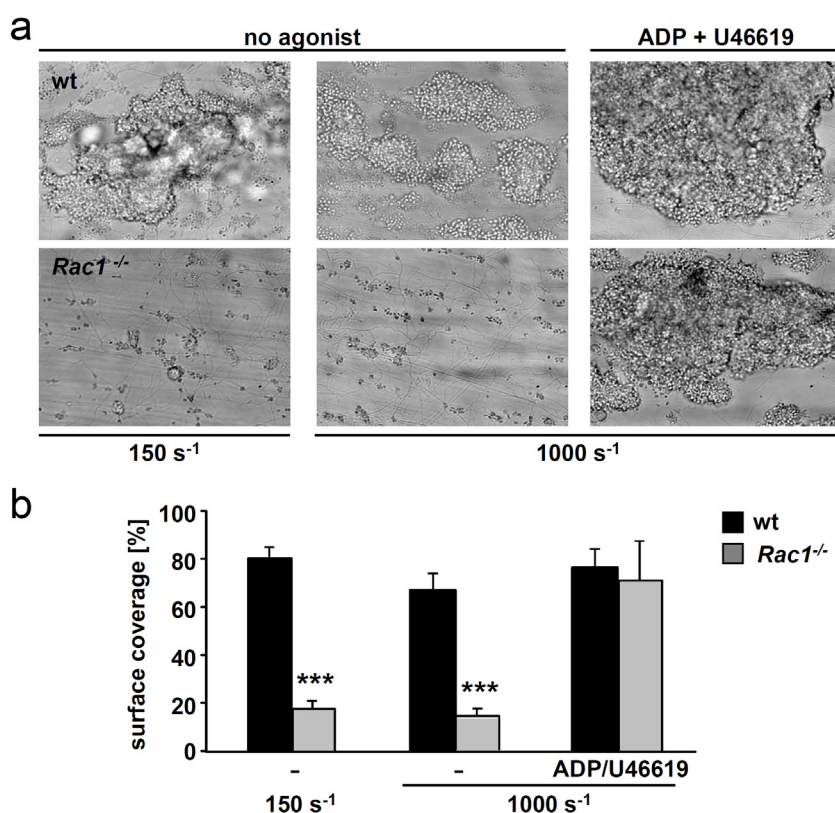


Figure 16. Impaired adhesion and defective thrombus formation of *Rac1*^{-/-} platelets on collagen under flow. Whole heparinized blood of *Rac1*^{-/-} and wild-type mice was perfused over a collagen coated cover slip for 4 min or 10 min at high (1000 s⁻¹) or low (150 s⁻¹) shear rates, respectively. Where indicated, 10 μM ADP and 1 μM U46619 were co-infused into the blood shortly before it entered the flow chamber. (a) Representative phase contrast images and (b) surface area covered by platelets (%) ± SD (n=6 per group) taken at the end of the perfusion time. (Pleines I *et al.*, *Pflugers Arch* 2009⁸⁰.)

3.1.6 Defective arterial thrombus formation in *Rac1*^{-/-} mice *in vivo*

The above described experiments indicated that *Rac1* deficiency results in a marked GPVI signaling defect and an inability of the platelets to spread on different substrates. To test the significance of this defect in arterial thrombus formation *in vivo*, two different well-established thrombosis models were used. In the first model, platelet adhesion at the injured carotid artery was analyzed by *in vivo* fluorescence microscopy (Fig. 17a,b). This model allows the visualization and quantification of platelet adhesion on the exposed subendothelial matrix which has been shown to be a largely GPVI-dependent process⁸⁶. Platelets purified from donor mice of the same genotype were fluorescently labeled and injected into recipient mice. Vascular injury was induced by vigorous ligation of the carotid artery, a process that consistently causes disruption of the endothelial layer and frequent breaching of the internal elastic lamina, followed by rapid collagen-dependent platelet adhesion and aggregate formation. In wild-type mice, numerous platelets adhered to the site of injury within the first minutes after injury and virtually all platelets establishing an initial contact with the subendothelium remained firmly adherent ($2,579 \pm 218/\text{mm}^2$, $t=5$ min) (Fig. 17a,b). In contrast, in *Rac1*^{-/-} mice, the number of adherent platelets was reduced by 57% as compared to control ($1120.7 \pm 74.6/\text{mm}^2$, $t=5$ min). An even more pronounced reduction in adhesion was observed in mice, in which GPVI had been depleted by treatment with the anti-GPVI antibody JAQ1⁷⁰ ($362.7 \pm 42/\text{mm}^2$, $t=5$ min), which served as a positive control. These results confirmed the importance of GPVI-collagen interactions for platelet recruitment in this arterial injury model and revealed a central role of *Rac1* in this process.

The significance of *Rac1* for arterial thrombus formation was demonstrated in a second model, where injury is mechanically induced in the aorta, and blood flow is monitored with an ultrasonic perivascular Doppler flow meter (Fig. 17c,d). After a transient increase directly after injury, blood flow progressively decreased for several minutes in all animals. In all wild-type mice (7/7), this decrease resulted in complete and irreversible occlusion of the vessel within maximally 7 min thereafter (mean occlusion time 3.0 ± 2.3 min). In sharp contrast, while a progressive reduction in blood flow was observed during the first minutes after injury in *Rac1*^{-/-} mice, blood flow increased again to normal and 7 of 8 mice displayed essentially normal flow rates through the injured vessel at the end of the observation period (45 min). Similar

results were obtained with GPVI-depleted mice (not shown), confirming earlier results⁸⁷.

In agreement with the reduced thrombotic activity in *Rac1*^{-/-} mice, these animals also exhibited prolonged bleeding times (Fig. 17e). Notably, bleeding times were highly variable suggesting thrombus instability as recently also described for mice lacking the α_{2A} adrenergic receptor⁸⁸.

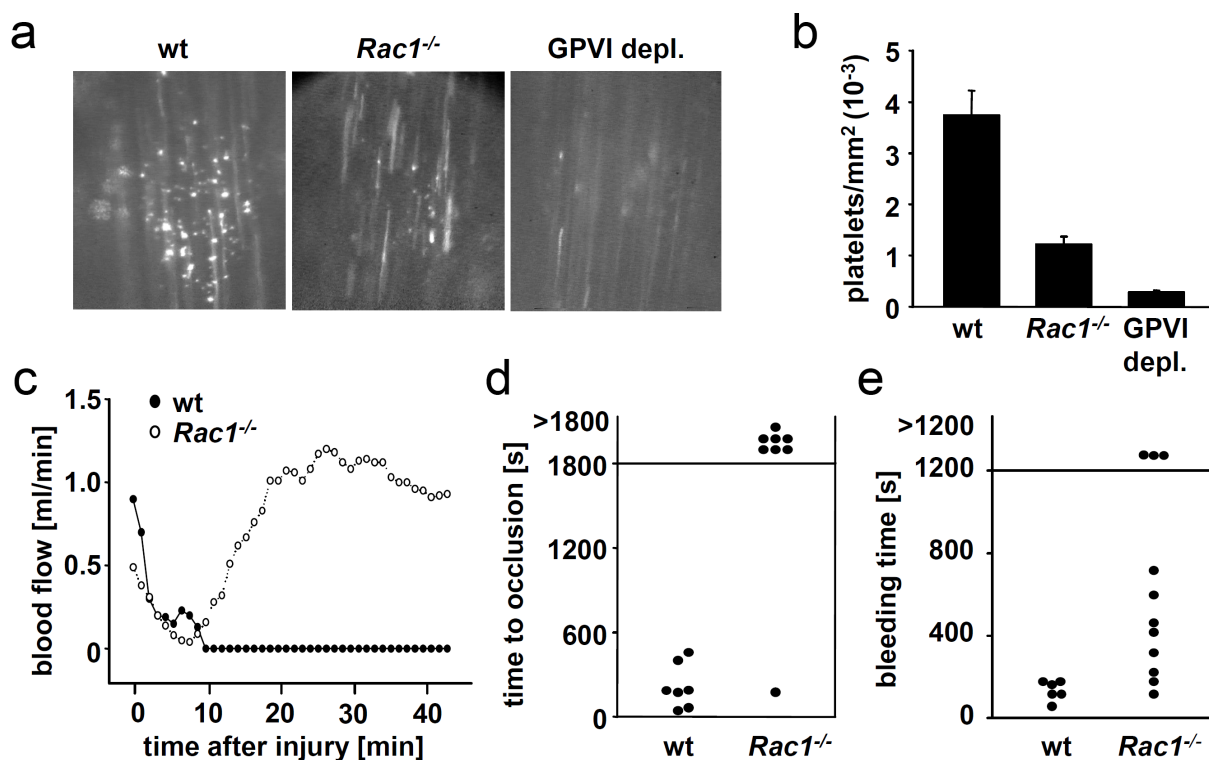


Figure 17. *Rac1*^{-/-} platelets display a severe adhesion defect *in vivo* and do not form stable thrombi. (a) Platelet adhesion to the carotid artery 5 min after injury. CFSE-labeled platelets of the same genotype were injected into anesthetized wild-type, *Rac1*^{-/-} and GPVI-depleted mice. The carotid artery was injured through ligation using a surgical filament and adhesion of platelets to the vessel wall was monitored over 10 min by fluorescence microscopy *in vivo*. (b) Statistical evaluation showing the adhesion of platelets to the vessel wall per mm² ± SD of at least three independent experiments. (c) Aorta occlusion model. Representative graph of blood flow of a wild-type and *Rac1*^{-/-} mouse after mechanical injury of the aorta [at t=0]. (d) Occlusion time after injury of the aorta. The aorta of all control mice occluded whereas in 7 out of 8 *Rac1*^{-/-} mice blood flow did not stop during the 45 min observation period. (e) Tail bleeding times in wild-type and *Rac1*^{-/-} mice. Each symbol represents one individual. (Pleines I *et al.*, *Pflugers Arch* 2009⁸⁰.)

3.2 *Cdc42*^{-/-} platelets display increased secretion but largely unaltered filopodia formation

3.2.1 *Cdc42*^{-/-} mice display mild thrombocytopenia

Constitutive deletion of the *Cdc42* gene results in embryonic lethality in mice⁴⁸. To study the function of *Cdc42* in platelets, mice carrying a *Cdc42* gene flanked by loxP sites⁷⁴ were crossed with transgenic mice expressing Cre recombinase under the control of the megakaryocyte- and platelet-specific platelet factor (PF) 4 promoter⁷⁶. In resulting *Cdc42* (fl/fl cre+) mice, gene deletion was induced intrinsically upon induction of the PF4 promoter during megakaryocyte maturation. *Cdc42* (fl/fl cre-, further referred to as wild-type) mice derived from the same litters served as controls. The absence of *Cdc42* protein in *Cdc42* (fl/fl cre+, further referred to as *Cdc42*^{-/-}) mice was confirmed by western blot analysis of platelet lysates using GPIIIa expression levels as loading control (Fig. 18a). Megakaryocyte- and platelet-specific deletion of *Cdc42* resulted in a moderate thrombocytopenia with platelet counts ranging between 50 and 80% of control animals (Fig. 18b) indicating a role for *Cdc42* in megakaryocyte differentiation and/or the formation of platelets. Platelet size was only moderately but significantly increased in *Cdc42*^{-/-} animals, as revealed by transmission electron microscopy (TEM) and determination of the platelet width (Fig. 18c,d), as well as by flow cytometric assessment of the forward scatter (FSC) signal (Table 2). Expression of major platelet surface receptors was similar to controls with exception of subunits of the GPIb/IIIb complex, where expression levels were significantly decreased by approximately 20% in *Cdc42*^{-/-} as compared to wild-type platelets (Table 2).

	wild-type	<i>Cdc42</i> ^{-/-}
mean FSC	345 ± 21	440 ± 37
GPIb	389 ± 8	306 ± 11
GPV	260 ± 4	212 ± 3
GPIX	403 ± 13	343 ± 2
CD9	1443 ± 21	1226 ± 10
GPVI	61 ± 2	52 ± 3
α2	90 ± 4	90 ± 8
β1	162 ± 10	183 ± 9
αIIbβ3	560 ± 63	513 ± 38

Table 2. Platelet glycoprotein expression in wild-type and *Cdc42*^{-/-} mice. Expression of glycoproteins on the platelet surface was determined by flow cytometry. Diluted whole blood from the indicated mice was incubated with FITC-labeled antibodies at saturating concentrations for 15 min at RT and platelets were analyzed directly by flow cytometry. Results are expressed as mean fluorescence intensity ± SD for 6 mice per group. Mean platelet size (mean FSC) was determined by FSC characteristics. (Pleines I *et al.*, in press.)

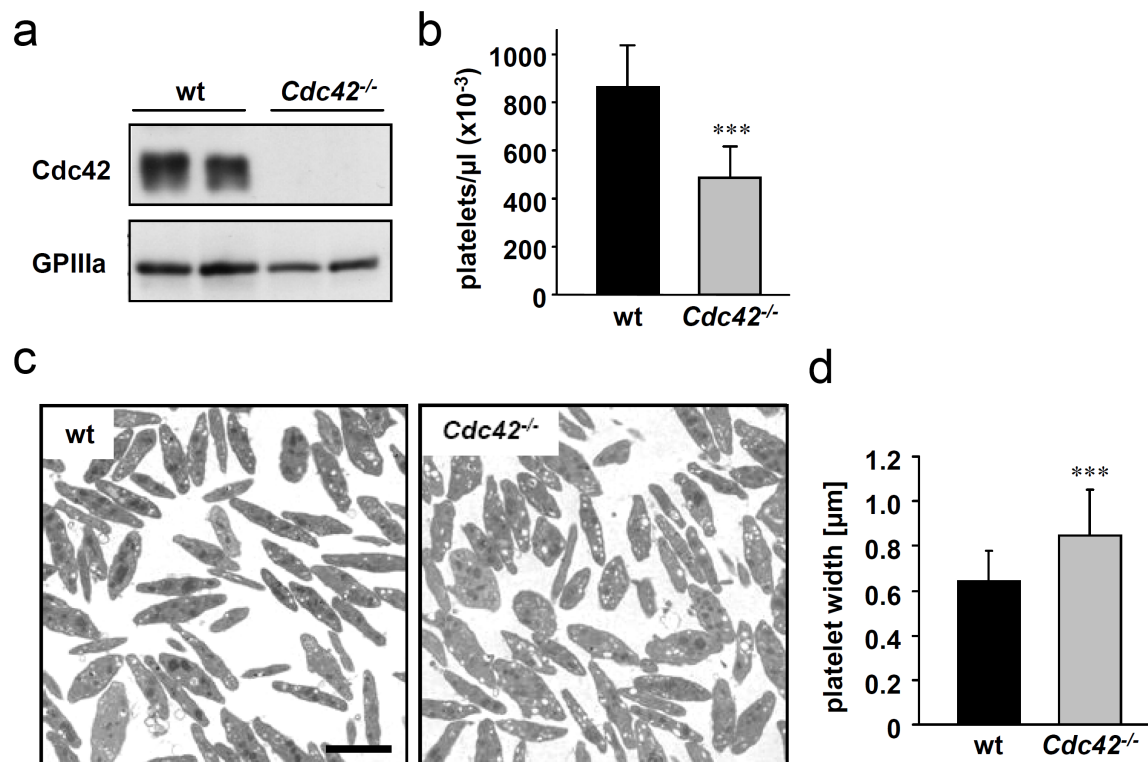


Figure 18. *Cdc42*^{-/-} mice display mild thrombocytopenia. (a) Western blot analysis of Cdc42 expression in wild-type *Cdc42*^{-/-} platelets. GPIIIa expression was used as loading control. (b) Peripheral platelet counts (n=6 per group). (c) Representative transmission electron microscopy pictures from wild-type and *Cdc42*^{-/-} platelets. Bar, 2 μm . (d) Mean platelet width of wild-type and *Cdc42*^{-/-} platelets (n=25 per group). (Pleines I *et al.*, *Blood*, in press.)

3.2.2 *Cdc42*^{-/-} platelets form filopodia and fully spread on fibrinogen

Cdc42 has been demonstrated to be crucial for filopodia formation in various cell types, and also an essential role for filopodia formation in platelets has been reported³². To test this hypothesis directly, wild-type and *Cdc42*^{-/-} platelets were allowed to spread on a fibrinogen-coated surface in the presence of thrombin (0.01 U/ml final concentration, (Fig. 19). Surprisingly, *Cdc42*^{-/-} platelets formed filopodia to a similar extent and with similar kinetics as wild-type platelets, and after 30 minutes the rate of fully spread platelets was comparable between the two groups (Fig. 19b). The filopodia formed in *Cdc42*^{-/-} platelets (Fig. 19a, lower panel) were microscopically indistinguishable from those formed in wild-type platelets (Fig. 19a, upper panel). Likewise, *Cdc42*^{-/-} and wild-type platelets exhibited similar morphology and filopodia structure upon adhesion on fibrinogen under either unstimulating conditions (Fig. 19c) or upon activation with 5 μM ADP (not shown). These data demonstrate that *Cdc42* is not required for filopodia formation and spreading of platelets on a fibrinogen matrix.

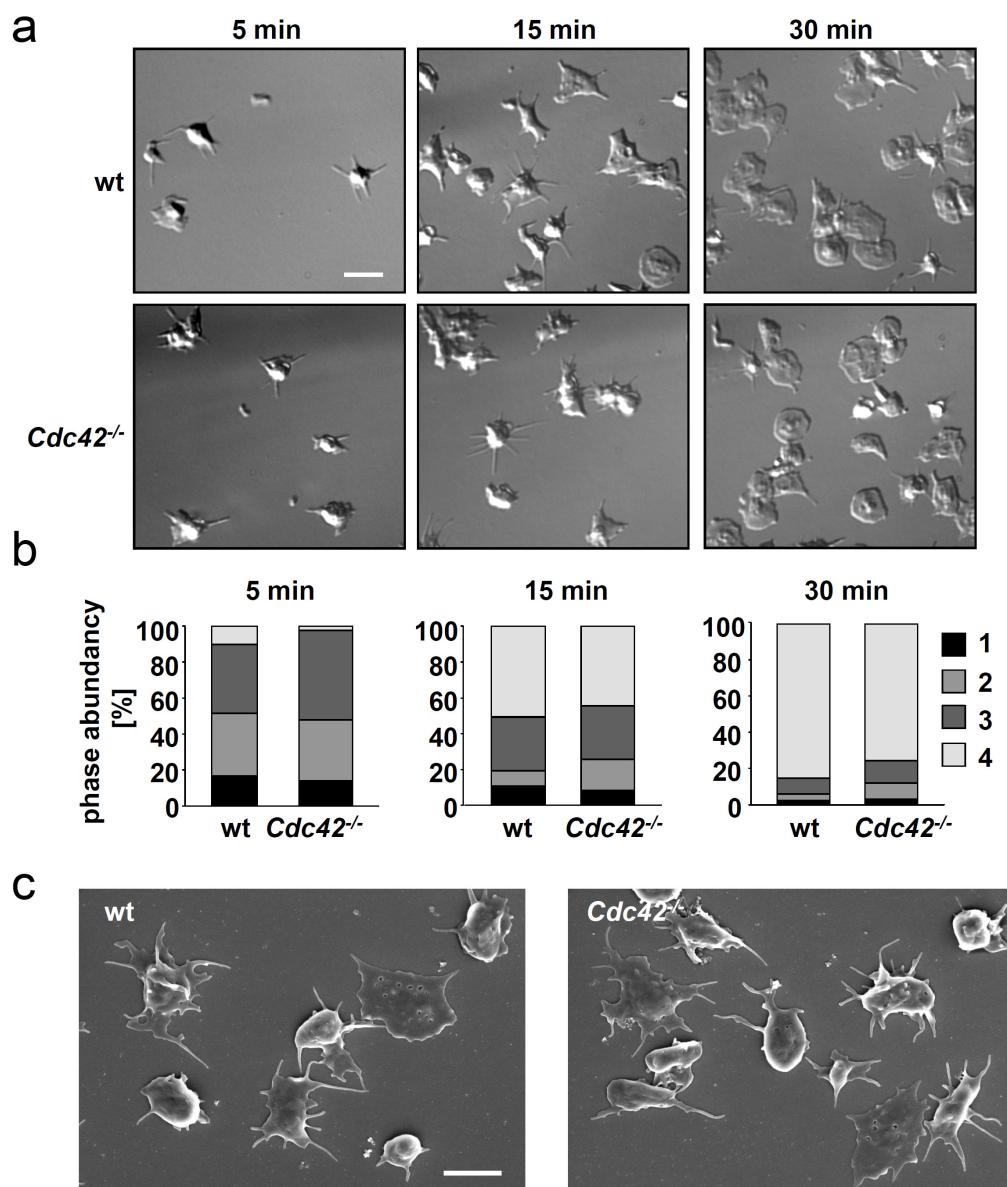


Figure 19. *Cdc42*^{-/-} platelets are able to form filopodia and to spread on fibrinogen. (a) Washed platelets from the indicated mice were allowed to adhere and spread on immobilized human fibrinogen (100 µg/ml) upon activation with thrombin (0.01 U/ml). DIC images were taken at the indicated time points (5, 15, 20 min), representative of 4 individual experiments. Bar, 5 µm. (b) Statistical analysis of the percentage of spread *Cdc42*^{-/-} and wild-type platelets observed at different spreading stages at the indicated time points. 1: roundish, no filopodia, no lamellipodia. 2: only filopodia. 3: filopodia and lamellipodia. 4: full spreading; only lamellipodia. Bar, 5 µm. (c) Scanning electron microscopy (SEM) of wild-type and *Cdc42*^{-/-} platelets upon adhesion on fibrinogen without agonist stimulation. Bar, 2.5 µm. (Pleines I *et al.*, *Blood*, in press.)

For a more detailed analysis of the cytoskeletal ultrastructure in *Cdc42*-deficient platelets, scanning electron microscopic studies were performed (Fig. 20). Apart from their increased size, no morphological differences between resting *Cdc42*^{-/-} and wild-type platelets were noted (Fig. 20a) and also thrombin-induced (30 min) filopodia were not different in length or shape between the two groups (Fig. 20b). To also study the impact of *Cdc42* deficiency on platelet shape change in suspension, washed platelets were activated with ADP or thrombin under stirring conditions for 15

seconds and visualized by scanning electron microscopy (Fig. 20c). Under these conditions, *Cdc42*^{-/-} and control platelets displayed a similar morphology including a contracted cell body and the formation of numerous filopodia (Fig. 20c, right panel).

Taken together, these results reveal normal formation and structure of filopodia and normal spreading morphology, as well as normal agonist-induced shape change in *Cdc42*^{-/-} platelets.

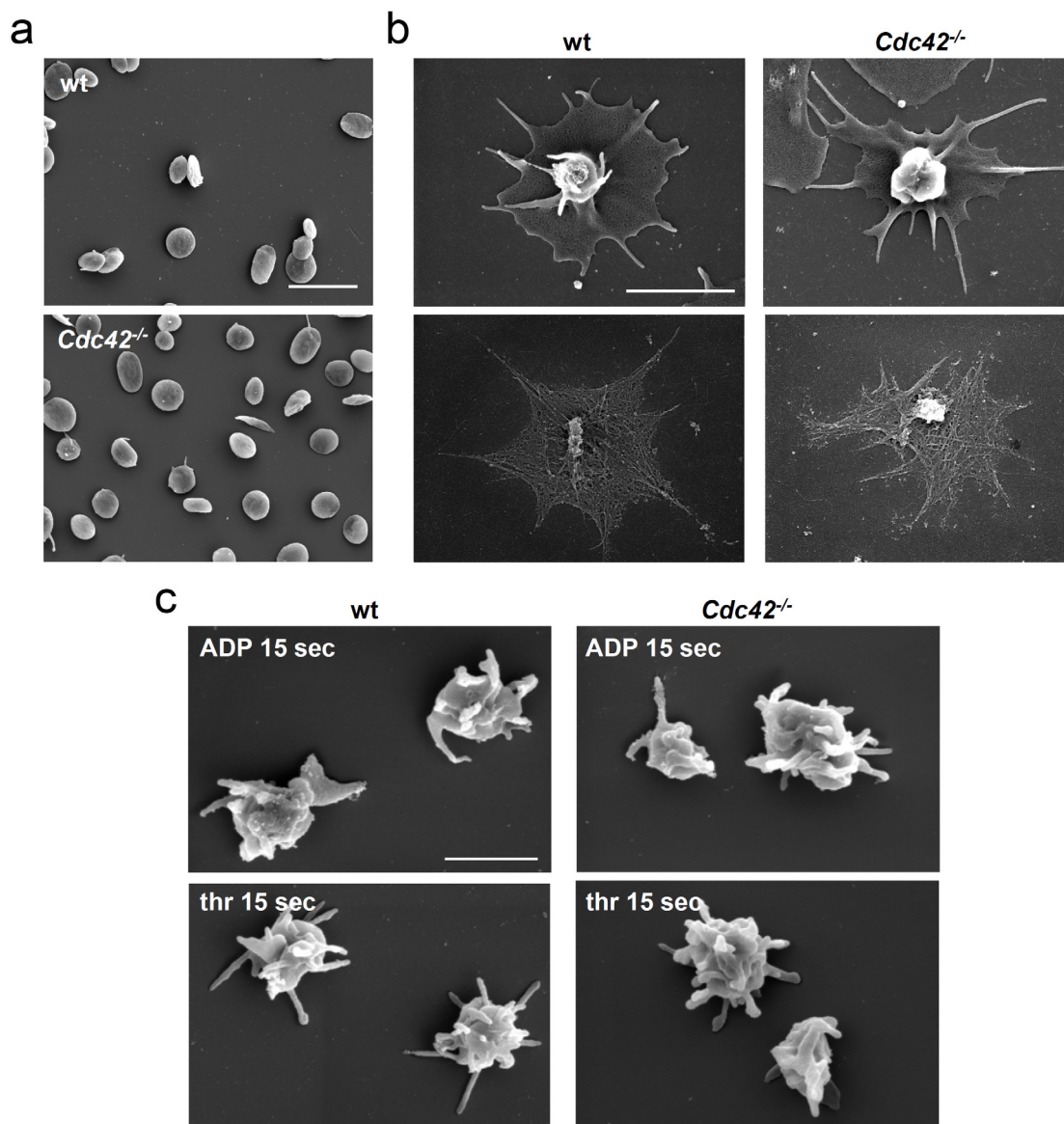


Figure 20. Normal ultrastructure of *Cdc42*^{-/-} platelets. (a–c) Scanning electron microscopy (SEM) of *Cdc42*^{-/-} and wild-type platelets. (a) resting platelets immobilized on poly-L-lysine. Bar, 5 μm. (b) Spread *Cdc42*^{-/-} and wild-type platelets upon activation with 0.01 U/ml thrombin on human fibrinogen (100 μg/ml). Upper panel: SEM of intact platelets. Lower panel: visualization of the actin cytoskeleton after denudation of the plasma membrane. Bar, 2 μm. (c) Morphology of *Cdc42*^{-/-} and wild-type platelets in suspension at 15 seconds after activation with thrombin (0.01 U/ml, upper panel) or ADP (5 μM, lower panel). Bar, 1 μm. (Pleines I *et al.*, *Blood*, in press.)

3.2.3 *Cdc42*^{-/-} platelets exhibit reduced filopodia extension following adhesion on immobilized vWF

In the next step, the platelet response upon adhesion to a mouse vWF coated surface under conditions of integrin α IIb β 3 blockade was evaluated (Fig. 21a,b). Under these conditions, a GPIb-specific signal is triggered resulting in shape change that is limited to contraction of the cell body and filopodia formation⁸⁹. In contrast to control platelets, which efficiently extended filopodia (75% showing more than 3 filopodia), *Cdc42*^{-/-} platelets exhibited a profound decrease in the ability to form filopodia with a majority displaying no (25%) or less than 4 (50%) filopodia per platelet and being unable to contract their cell body. Importantly, the observed defect in filopodia formation in *Cdc42*^{-/-} platelets was not caused by decreased GPIb expression levels of the protein since GPIb-dependent agglutination by botrocetin and human vWF was unaltered in the mutant platelets as compared to controls (Fig. 21c). Furthermore, filopodia formation upon static adhesion on collagen-related peptide (CRP), which acts via glycoprotein (GP) VI and has been proposed to induce similar signaling events as compared to GPIb, occurred to a similar extent in wild-type and *Cdc42*^{-/-} platelets (not shown). Together, these results suggest a specific role of Cdc42 in filopodia formation downstream of GPIb in a signaling pathway differing from that triggered by GPVI or G protein-coupled receptors.

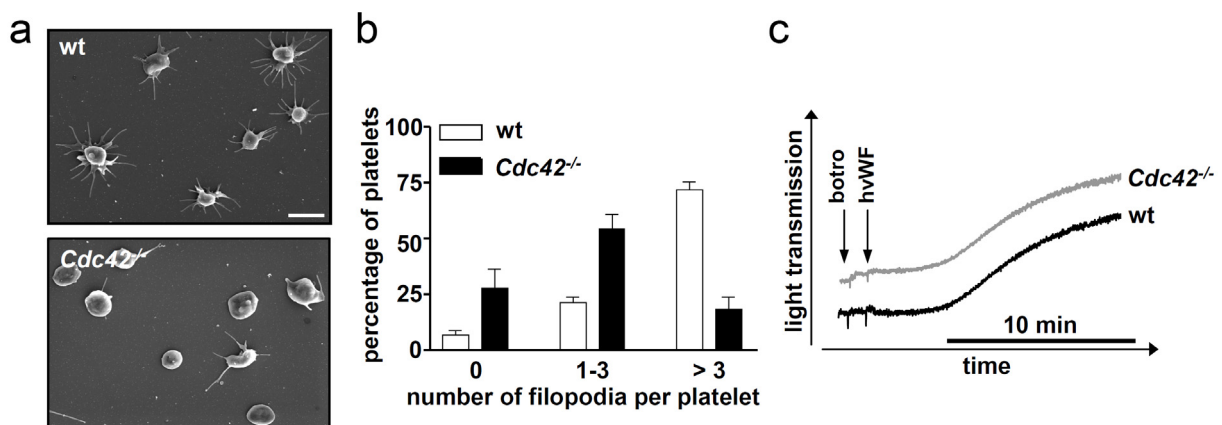


Figure 21. *Cdc42*^{-/-} platelets exhibit reduced filopodia extension on vWF. (a) Washed platelets were treated with Integrilin (40 μ g/ml) and botrocetin (2 μ g/ml) and allowed to adhere to coverslips coated with 10 μ g/ml of mouse von Willebrand factor (vWF) for 20 min at 37°C. Samples were fixed with 2.5 % glutaraldehyde and processed for SEM. Images are representative of 5 experiments (Bar, 2.5 μ m). (b) Filopodia formation was scored according to the number of extensions per platelet (0, 1 to 3, >3) in five different fields corresponding to a total surface of 9215 μ m². The results are mean values \pm SD (n=5 per group). (c) Unaltered agglutination of *Cdc42*^{-/-} platelets. Washed *Cdc42*^{-/-} and wild-type platelets were stimulated with botrocetin (5 μ g/ml) and human vWF (10 μ g/ml) in presence of 40 μ g/ml Integrilin under stirring conditions and agglutination was monitored over 15 min using an aggregometer. Curves are representative of 3 individual experiments. (Pleines I *et al.*, *Blood*, in press.)

3.2.4 Increased secretion in *Cdc42*^{-/-} platelets

Cdc42 has been demonstrated to be required for exocytotic processes in various cell types, such as mast cells, where it was shown to be crucially involved in antigen-stimulated secretion^{65,66}. To address a possible role of *Cdc42* in this process in platelets, the ability of *Cdc42*^{-/-} and wild-type platelets to release granules upon agonist activation was determined by flow cytometry (Fig. 22b). In parallel, activation of the main platelet integrin, α IIb β 3, was assessed (Fig. 22a). Surprisingly, and in contrast to studies in other cell types, it was found that P-selectin expression was not decreased but markedly increased in *Cdc42*^{-/-} as compared to wild-type platelets in response to all tested strong agonists (Fig. 22b). In contrast, integrin α IIb β 3 activation in response to strong stimuli was moderately decreased in *Cdc42*^{-/-} platelets compared to wild-type controls (Fig. 22a).

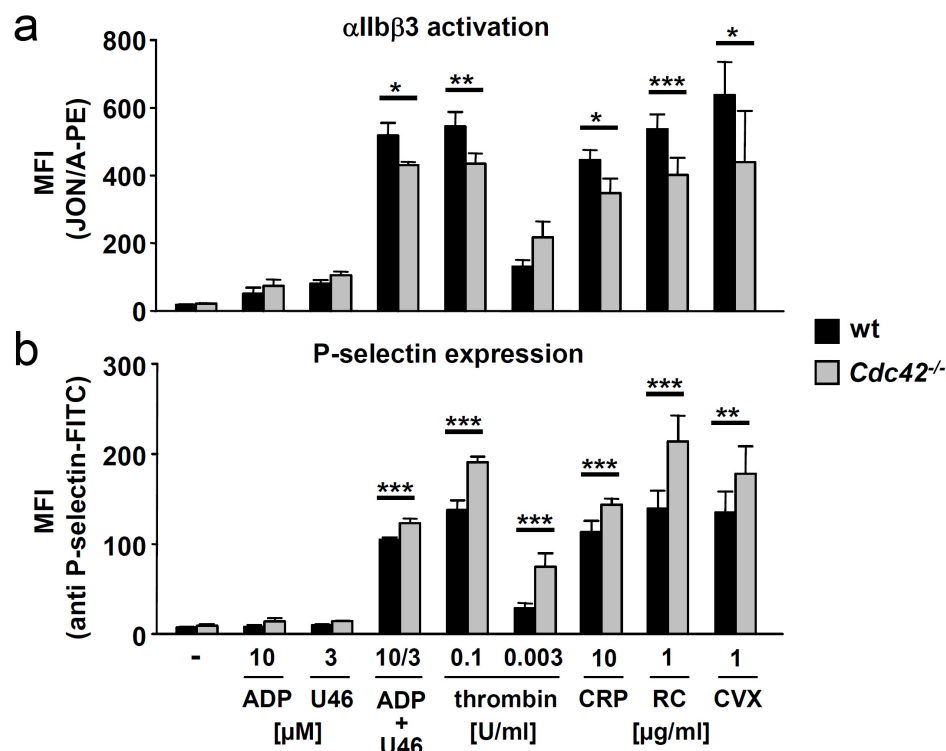


Figure 22. Increased P-selectin expression in *Cdc42*^{-/-} platelets upon activation. Flow cytometric analysis of (a) α IIb β 3 integrin activation (binding of JON/A-PE, upper panel) and (b) degranulation-dependent P-selectin exposure (lower panel) in response to the indicated agonists from control (black) or *Cdc42*^{-/-} (gray) platelets. Abbreviation: U46: U46619. Results are mean fluorescent intensities (MFI) \pm SD of 6 mice per group. (Pleines I *et al.*, *Blood*, in press.)

The increased levels of P-selectin expression in *Cdc42*^{-/-} platelets indicated enhanced release of α granules. To test whether release of dense granules was also affected, the amount of released ATP and serotonin upon agonist stimulation were measured (Fig. 23). Strongly increased ATP release in *Cdc42*^{-/-} compared to wild-

type platelets was found in response to thrombin and CRP (Fig. 23a), whereas serotonin release was not significantly different compared to the control (Fig. 23b).

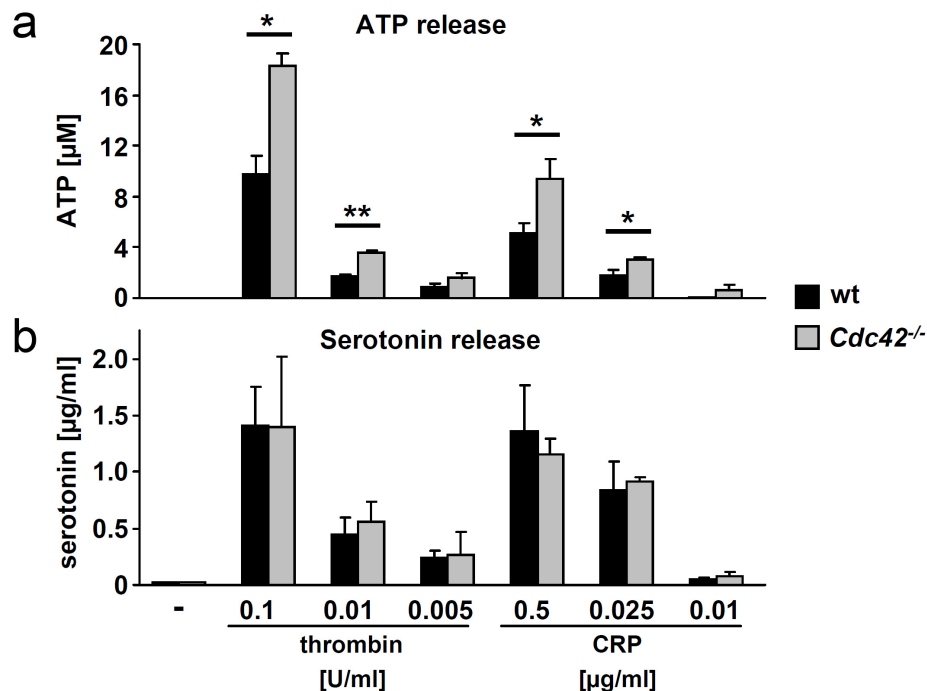


Figure 23. Increased ATP release in *Cdc42*^{-/-} platelets upon activation. Measurement of (a) released ATP and (b) serotonin in the supernatant of resting or activated wild-type (black) and *Cdc42*^{-/-} (gray) platelets. Results are given as mean ATP concentration (μM) and mean serotonin concentration (ng/3.2x10⁶ platelets) ± SD (n=4 per group). (Pleines I *et al.*, *Blood*, in press.)

Transmission electron microscopy revealed comparable numbers of α and dense granules in *Cdc42*^{-/-} and control platelets (not shown) and no significant differences between wild-type and mutant cells were found in the total amount of the representative α -granular proteins P-selectin and vWF (Fig. 24a,b). Thus, together with the results from flow cytometry, these data support the hypothesis of increased α granule-dependent secretion in *Cdc42*^{-/-} platelets.

In contrast, the content of dense granule-specific ADP and ATP was significantly increased in resting *Cdc42*^{-/-} platelets (Fig. 24c), whereas levels of serotonin were not significantly altered (Fig. 24d). The observed increased ADP/ATP content may to a certain extent be related to the increased size of *Cdc42*^{-/-} platelets compared to the control. Additionally, alterations in the process of granule packing may also contribute to the observed enhanced secretion from dense granules in *Cdc42*^{-/-} platelets.

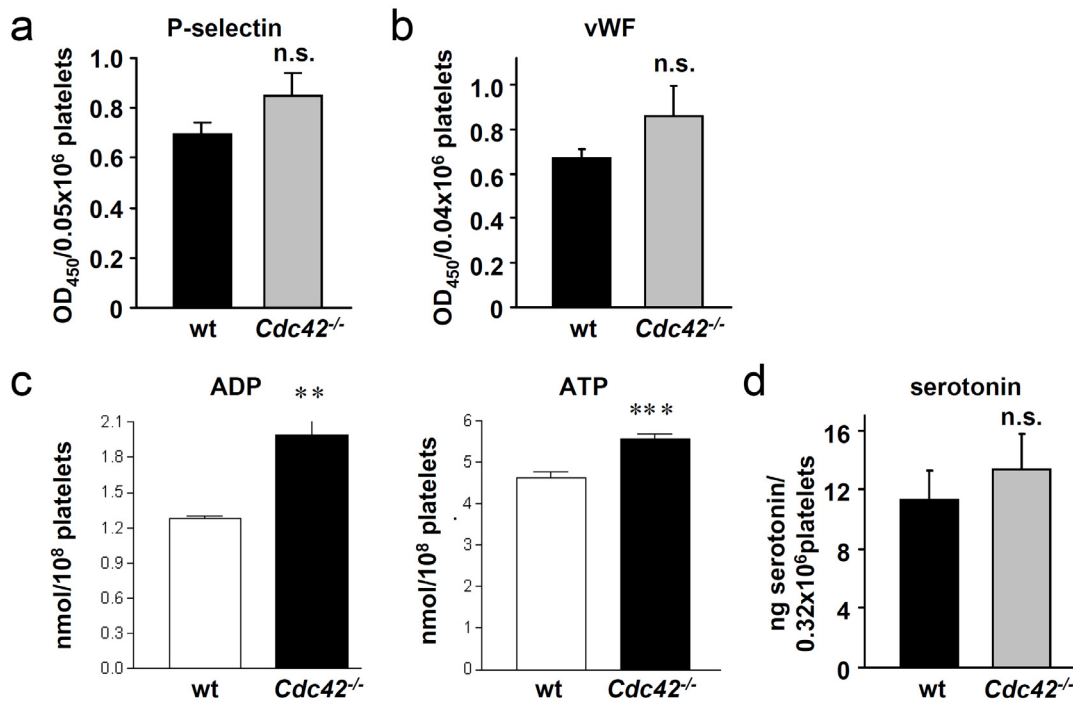


Figure 24. Partial changes in the granule content of *Cdc42*^{-/-} platelets. (a,b) No significant changes in platelet α -granular P-selectin (a) and vWF content (b) in wild-type (black) and *Cdc42*^{-/-} (white) platelets. Results are expressed as mean OD₄₅₀/0.05x10⁶ platelets and OD₄₅₀/0.04x10⁶ platelets \pm SD of 4 mice per group. (c) Increased nucleotide content in *Cdc42*^{-/-} platelets. Determination of ADP (left) and ATP (right) content in wild-type (white) and *Cdc42*^{-/-} (black) platelets by HPLC. Results are expressed as nmol/10⁸ platelets \pm SD of 6 mice per group. (d) Unaltered serotonin content in *Cdc42*^{-/-} platelets. Results are expressed as ng/3.2x10⁶ platelets \pm SD of 4 mice per group. (Pleines I *et al.*, *Blood*, in press.)

3.2.5 Enhanced aggregation of *Cdc42*^{-/-} platelets at low agonist concentrations

To study the functional consequences of the increased granule content and secretion and slightly decreased α IIb β 3 integrin activation in *Cdc42*^{-/-} platelets, aggregation studies were performed (Fig. 25). In this assay, the amount of released secondary mediators from platelet granules has a high impact on the aggregation response because of the high platelet concentrations in the suspension. Whereas the overall maximal aggregatory response to all tested agonists was similar in *Cdc42*^{-/-} and wild-type platelets (Fig. 25a-c), strongly enhanced aggregation of *Cdc42*^{-/-} platelets was seen at threshold concentrations of the thromboxane (TXA₂) analog U46619, CRP and collagen (Fig. 25b,c). The degree of aggregation in response to these agonists is known to be strongly dependent on released secondary mediators indicating that the increased secretion of *Cdc42*^{-/-} platelets accounted for this effect. Consistent with this, aggregation in response to the weak agonist ADP, which alone does not induce degranulation, was similar in *Cdc42*^{-/-} and wild-type platelets (Fig. 25a,c). No significant difference in aggregation between wild-type and mutant platelets could be detected in response to thrombin (Fig. 25a,c). Notably, *Cdc42*^{-/-} platelets did not

aggregate spontaneously upon addition of epinephrine (not shown) indicating that the mutant platelets were not *per se* in a pre-activated state under the *in vitro* conditions used here.

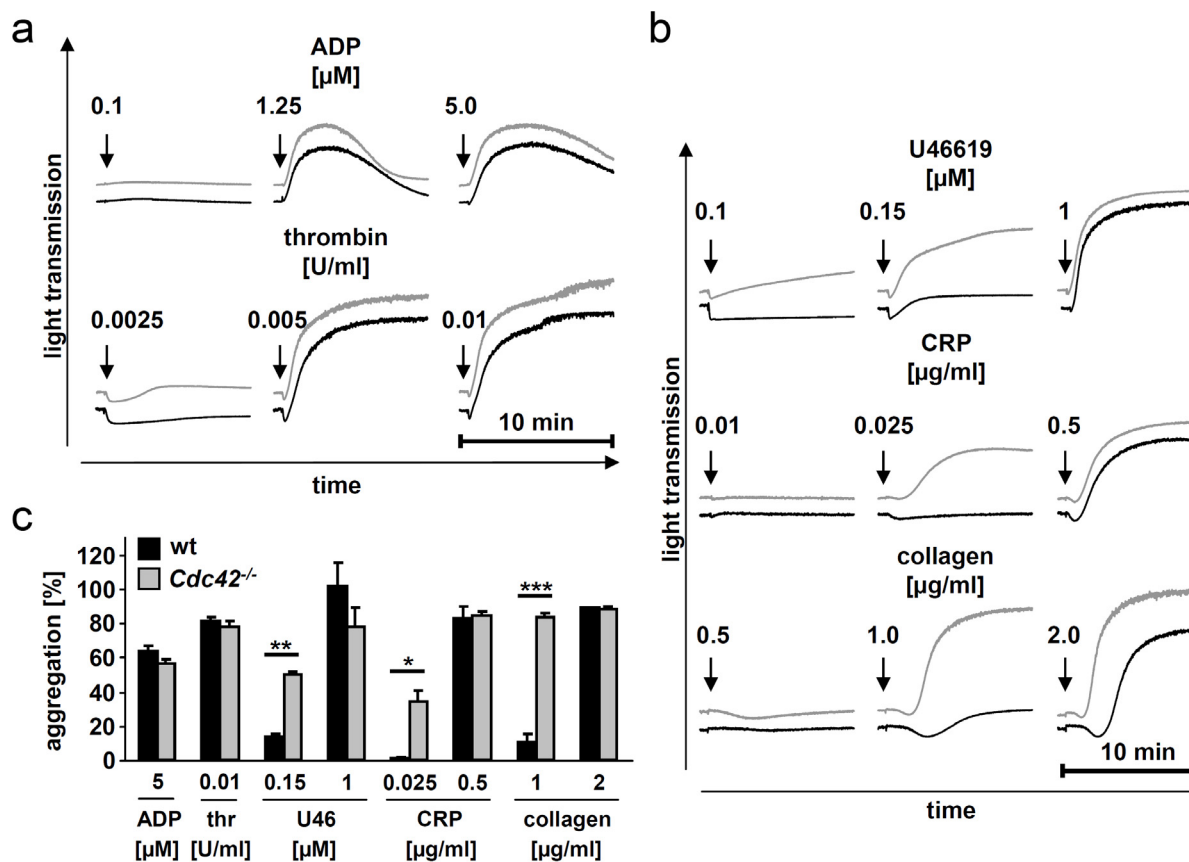


Figure 25. Enhanced aggregation of *Cdc42*^{-/-} platelets at low agonist concentrations. Washed platelets from wild-type (black) or *Cdc42*^{-/-} (gray) mice were stimulated with the indicated agonists and light transmission was recorded on a FibrinTimer 4 channel aggregometer. ADP measurements were performed using platelet-rich plasma. The results are representative of 3 individual experiments. (a,b) representative aggregation curves. (c) Bar graphs of results obtained by aggregometry. Results are given as the mean % of aggregation \pm SD. (Pleines I *et al.*, *Blood*, in press.)

3.2.6 *Cdc42*^{-/-} platelets form aggregates of increased size on collagen under flow

At sites of vessel wall injury, release of secondary mediators from activated platelets at the exposed subendothelium plays a crucial role for the recruitment and activation of further platelets to promote thrombus formation. To study the effect of enhanced secretion of *Cdc42*^{-/-} platelets on aggregate formation under flow, anti-coagulated whole blood was perfused over a collagen-coated surface at a shear rate of 1000 s⁻¹ (Fig. 26). A moderate but significant increase in aggregate size of *Cdc42*^{-/-} platelets compared to wild-type platelets was observed under these conditions (Fig. 26, right panel), whereas the surface coverage was comparable between the two groups (Fig.

26, left panel). Thus, the increased release of granule contents in *Cdc42*^{-/-} platelets translated into moderately increased aggregate formation under flow.

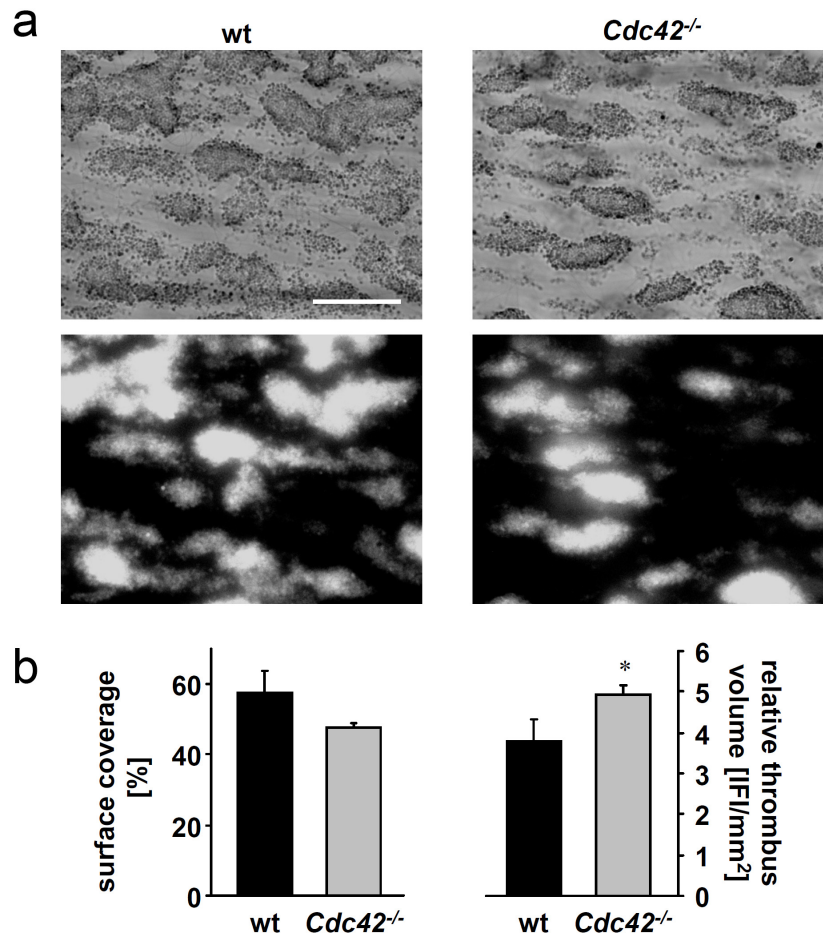


Figure 26. *Cdc42*^{-/-} platelets form stable aggregates on collagen under flow. Whole blood from wild-type or *Cdc42*^{-/-} mice was perfused over a collagen-coated surface (0.2 mg/ml). (a,b) Increased aggregate formation of *Cdc42*^{-/-} platelets at high (1000 s⁻¹) shear rates. (a) Representative phase contrast (upper panel) and fluorescence images (lower panel) of aggregate formation on collagen after 4 min perfusion time. Bar, 100 μ m. (b) Mean surface coverage (left) and relative thrombus volume expressed as integrated fluorescence intensity (IFI) per mm² (right) \pm SD of 6 mice per group. (Pleines I *et al.*, *Blood*, in press.)

3.2.7 *Cdc42*^{-/-} platelets display a decreased life span *in vivo*

Non-functional or pre-activated platelets are thought to be rapidly cleared from the circulation by the reticulo-endothelial system which may, if occurring constantly, lead to thrombocytopenia. Since *Cdc42*^{-/-} platelets displayed mild thrombocytopenia, the platelet life span in *Cdc42*^{-/-} and wild-type mice *in vivo* was determined (Fig. 27). For this, circulating platelets were labeled with a fluorescently labeled non-cytotoxic antibody derivative and the labeled platelet population was monitored over time. After 1 hour (day 0), >90% of the circulating platelets in control and *Cdc42*^{-/-} mice were labeled and this platelet population gradually decreased over 5 days in wild-type mice, which is in agreement with the approximate 5 day life span of mouse platelets.

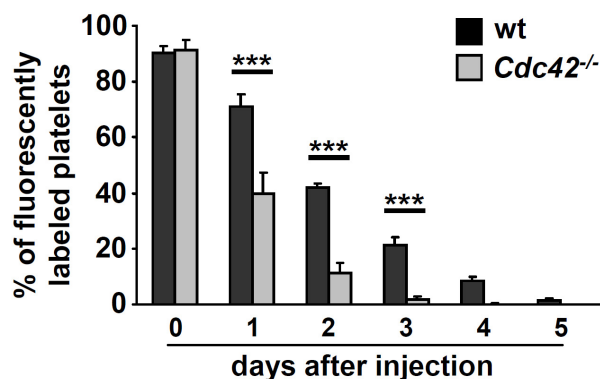


Figure 27. *Cdc42*^{-/-} platelets display a decreased life span. Determination of the percentage of fluorescently labeled platelets of wild-type (black) and *Cdc42*^{-/-} platelets (gray) for 5 days upon injection with 0.5 µg/g bodyweight anti-GPIX-Dylight 488 derivative on day 0. (Pleines I *et al.*, *Blood*, in press.)

In marked contrast, a dramatically shortened life span was seen in *Cdc42*^{-/-} mice, with a decrease to $39.8 \pm 7.6\%$ and 0% on days 1 and 3, respectively. This result clearly demonstrates that, *Cdc42* deficiency has only moderate effects on platelet function *ex vivo*, it significantly affects their homeostatic function *in vivo* resulting in a markedly increased turnover which may, at least in part, account for the moderate thrombocytopenia seen in these animals.

3.2.8 Prolonged bleeding times in *Cdc42*^{-/-} mice

To study the effect of *Cdc42* deficiency on hemostasis, tail bleeding experiments were performed (Figure 28). Very unexpectedly, a significant hemostatic defect was detectable in *Cdc42*^{-/-} mice. Whereas bleeding stopped in all control mice within 10 minutes (mean: 5.9 ± 2.2 min), bleeding times were highly variable and generally increased in *Cdc42*-deficient animals (mean: 13.5 ± 5.3 min). However, all tested animals were able to stop bleeding within the observation period of 20 minutes.

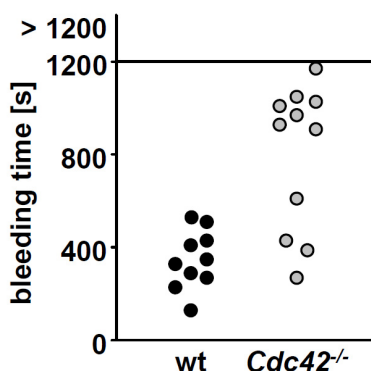


Figure 28. Prolonged bleeding in *Cdc42*^{-/-} mice. Increased tail bleeding times in *Cdc42*^{-/-} mice (gray) compared to wild-type (black) mice. Each symbol represents one individual. (Pleines I *et al.*, *Blood*, in press.)

3.2.9 Accelerated occlusive arterial thrombus formation in *Cdc42*^{-/-} mice

To investigate the effect of *Cdc42* deficiency on thrombus formation *in vivo*, platelet accumulation at sites of ferric chloride induced mesenteric arteriole injury was monitored using intravital fluorescence microscopy (Fig. 29). Remarkably, although the beginning of thrombus formation followed similar kinetics in control and *Cdc42*-deficient mice (Fig. 29a), the interval between the formation of first thrombi and complete occlusion of the respective arteriole was significantly shorter in *Cdc42*-deficient animals (Fig. 29b) as compared to wild-type controls. Within 6 minutes after appearance of the first thrombus >10 μ m, vessel occlusion occurred in 60% of the *Cdc42*-deficient animals (9/15), whereas no vessel occlusion was observed in arterioles of control mice during this time period. These results indicate that in this model of vessel wall injury, the increased secretion of *Cdc42*^{-/-} platelets plays a significant role in occlusive thrombus formation.

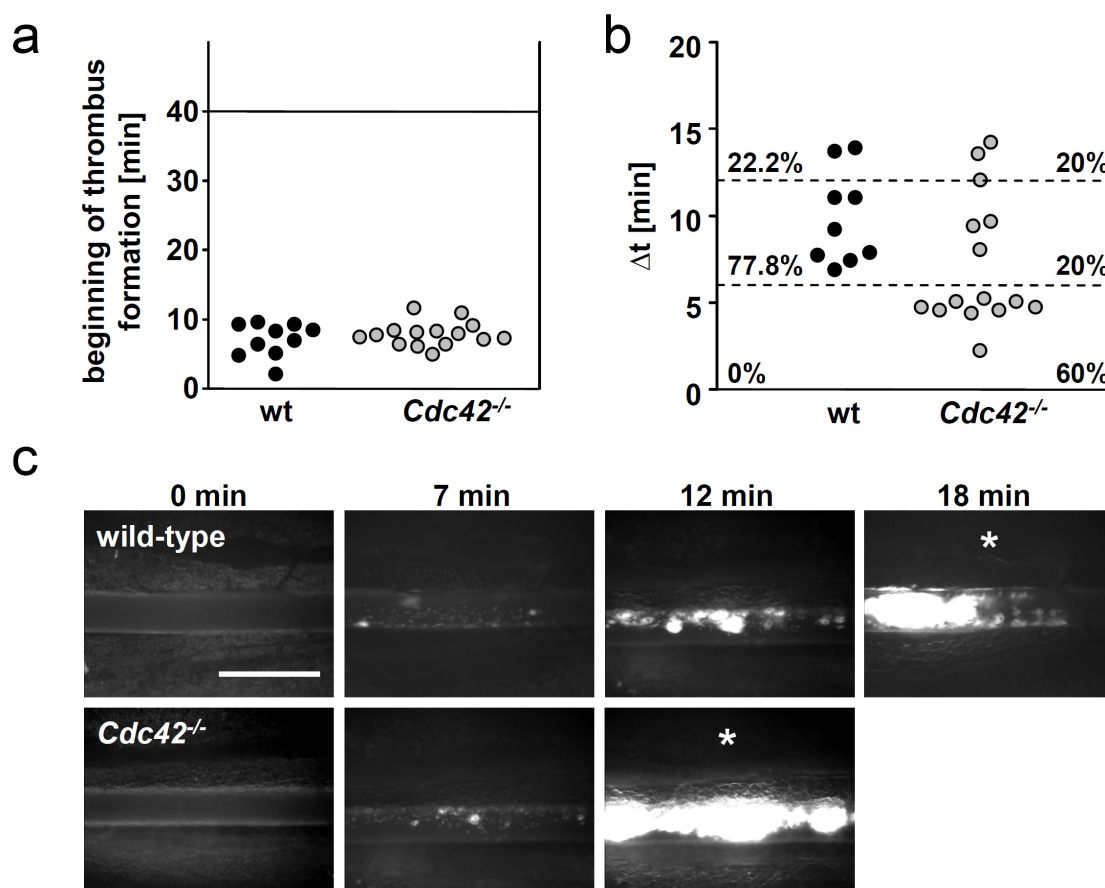


Figure 29. Accelerated thrombus formation in *Cdc42*^{-/-} mice. (a–c) Mesenteric arterioles were injured with FeCl_3 and adhesion and thrombus formation of fluorescently-labeled platelets was monitored *in vivo* by fluorescence microscopy. (a) Time to appearance of first thrombus and (b) interval between start of thrombus formation and vessel occlusion are shown. Each symbol represents one individual. (c) Representative images are depicted. Bar, 50 μ m. The asterisk indicates occlusion of the vessel. (Pleines I *et al.*, *Blood*, in press.)

3.2.10 Increased amounts of phosphorylated cofilin in *Cdc42*^{-/-} platelets

To test a possible effect of Cdc42 deficiency on agonist-induced cytoskeletal rearrangements, the Cdc42 downstream effector cofilin was examined, which is a protein known to be involved in increasing actin turnover in its active dephosphorylated form⁹⁰. Unexpectedly, and in contrast to the currently proposed function of Cdc42²⁹ (see Fig. 7), not a decrease, but a strong (approximately 3-fold) increase in the (inactive) phosphorylated cofilin form was found in resting *Cdc42*^{-/-} platelets as compared to controls (Fig. 30a,b). This finding is in accordance with a recent study showing increased cofilin phosphorylation in cortical neurons upon genetic Cdc42 deletion⁹¹. Thrombin-induced dephosphorylation of cofilin occurred to a similar extent and with similar kinetics in wild-type and *Cdc42*^{-/-} platelets, although higher levels of the inactive, phosphorylated form of the protein were consistently detected in the mutant cells under all experimental conditions (Fig. 30c).

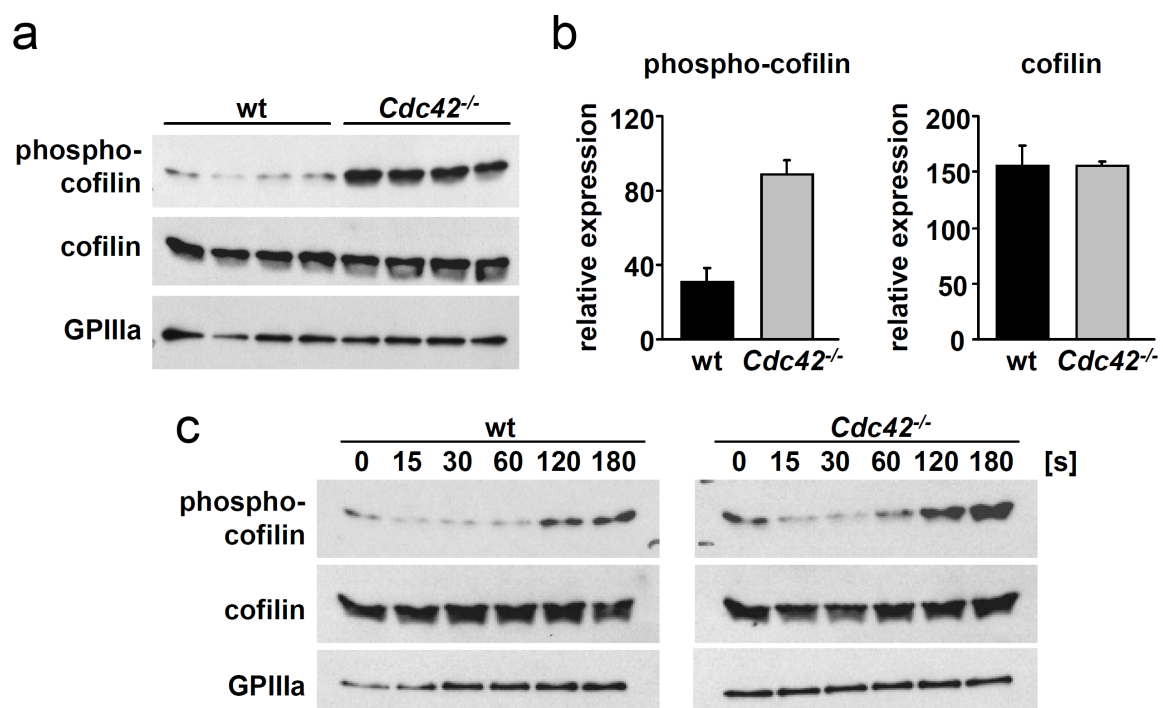


Figure 30. Increased phosphorylation of cofilin in *Cdc42*^{-/-} platelets. (a) Western blots of lysates from unstimulated wild-type (black) and *Cdc42*^{-/-} (gray) platelets using antibodies against the phosphorylated form of cofilin, cofilin and GP111a (loading control). (b) Densitometric analysis of relative expression levels of phospho-cofilin (left) and total cofilin (right) in unstimulated wild-type (black) and *Cdc42*^{-/-} (gray) platelets. (c) Washed platelets from wild-type (left) and *Cdc42*^{-/-} mice were stimulated with 0.1 U/ml thrombin and lysed at the indicated time points. Lysates were blotted and membranes were probed using antibodies against phospho-cofilin, cofilin and GP111a (loading control). (Pleines I *et al.*, *Blood*, in press.)

3.3 Double deficiency of Rac1 and Cdc42 severely affects platelet function and production

As described in Fig. 7, Rac1 and Cdc42 have been reported to share similar downstream signaling pathways and in platelets p21-activated kinase (PAK) has been shown to become activated by both GTPases⁹². Therefore, Rac1 and Cdc42 may have redundant functions in megakaryocytes and platelets. To address this question in detail by a knock-out approach, Rac1/Cdc42 (fl/fl) mice were generated by intercrossing. These mice were then crossed with either PF4-Cre or Mx-Cre transgenic mice to receive Rac1/Cdc42 (fl/fl cre+) mice.

In case of the PF4-Cre system, gene deletion occurred intrinsically during megakaryocyte maturation (see section 3.2.1). For generation of a hematopoietic Rac1/Cdc42 knock-out, the Mx-Cre system was used to induce gene deletion in adult mice as described (see section 3.1.1). For both systems, Rac1/Cdc42 (fl/fl cre-, further referred to as wild-type) mice derived from the same litters served as controls. The absence of Rac1 and Cdc42 in the respective *Rac1/Cdc42* (fl/fl cre+, further referred to as *Rac1/Cdc42*^{-/-}) mice was confirmed by western blot of platelet lysates as described (Fig. 31, see section 3.1.1).

Comparison between the two different Cre systems revealed that, while the PF4-Cre-induced knock-out was specific for megakaryocytes/platelets, the knock-out efficiency was slightly higher in the Mx-Cre system. However, due to its unspecificity, the Mx-Cre-induced double knock-out lead to death of the animals between 9 and 14 days after Cre induction. In contrast, *Rac1/Cdc42*^{-/-} mice generated using the PF4-Cre system were viable and fertile and did not show any signs of disease (not shown). Therefore, in the following studies, Mx-Cre-induced gene deletion was mainly used for platelet studies, whereas studies on megakaryocytes were performed using the PF4-Cre system.

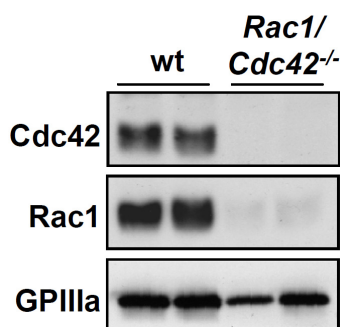


Figure 31. Absence of Rac1 and Cdc42 protein in *Rac1/Cdc42*^{-/-} platelets. Western blot analysis of Rac1 and Cdc42 expression in wild-type and *Rac1/Cdc42*^{-/-} platelets generated by the Mx-Cre/loxP system. GPIIIa expression was used as loading control.

3.3.1 Study of *Rac1/Cdc42*^{-/-} platelets

3.3.1.1 *Rac1/Cdc42* double deficiency leads to macrothrombocytopenia and formation of abnormal platelets

Interestingly, whereas *Rac1*^{-/-} mice displayed no and *Cdc42*^{-/-} mice only a moderate decrease in platelet counts, double deficiency of *Rac1* and *Cdc42* resulted in severe thrombocytopenia with platelet counts below 10% of control mice (Fig. 32b). In contrast, the size of *Rac1/Cdc42*^{-/-} platelets was dramatically increased, as demonstrated by transmission electron microscopy (TEM) and determination of the mean platelet volume (Fig. 32a,c).

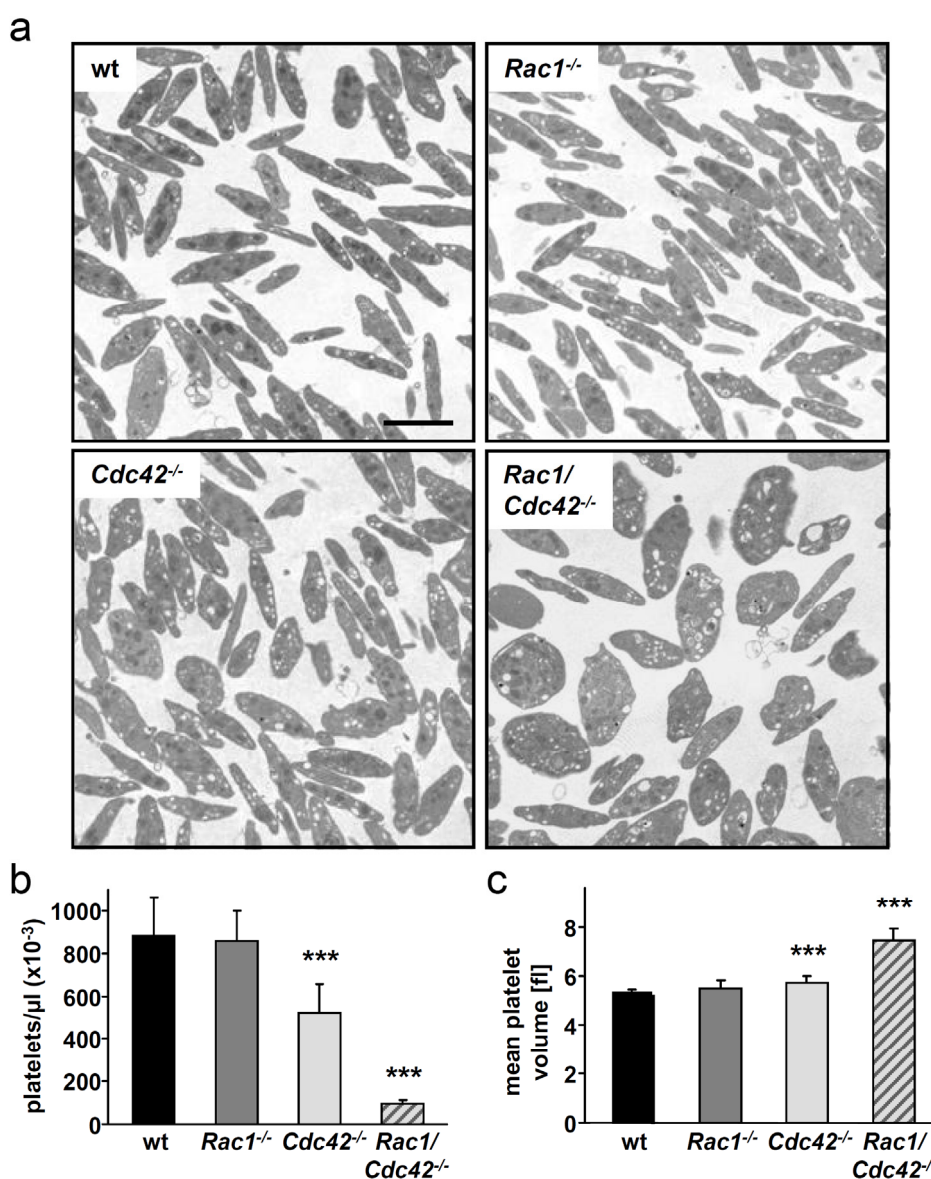


Figure 32. *Rac1/Cdc42*^{-/-} mice display severe macrothrombocytopenia. (a) Representative transmission electron microscopy pictures from wild-type and *Rac1/Cdc42*^{-/-} platelets. Bar, 2 μm . (b,c) Comparison of peripheral platelet counts (b) and mean platelet volume (c) of wild-type, *Rac1*^{-/-}, *Cdc42*^{-/-} and *Rac1/Cdc42*^{-/-} platelets (n=15 per group). Results are expressed as platelets/ μl and fl \pm SD, respectively.

Detailed analysis of platelet ultrastructure by TEM revealed dramatically altered ultrastructure in *Rac1/Cdc42*^{-/-} platelets (Fig. 33). Whereas *Rac1*^{-/-} and *Cdc42*^{-/-} platelets displayed unaltered granule number and content as compared to wild-type platelets (Fig. 33a), platelets from *Rac1/Cdc42*^{-/-} mice were partially overloaded with granules and/or vacuoles while others were found to be completely empty (Fig. 33b). Furthermore, expression levels of prominent platelet surface receptors were markedly reduced in *Rac1/Cdc42*^{-/-} platelets with exception of integrin expression which was similar to controls (Table 3).

Taken together, these results demonstrated a critical and potentially redundant function of Rac1 and Cdc42 in the processes of megakaryocyte maturation and/or platelet production.

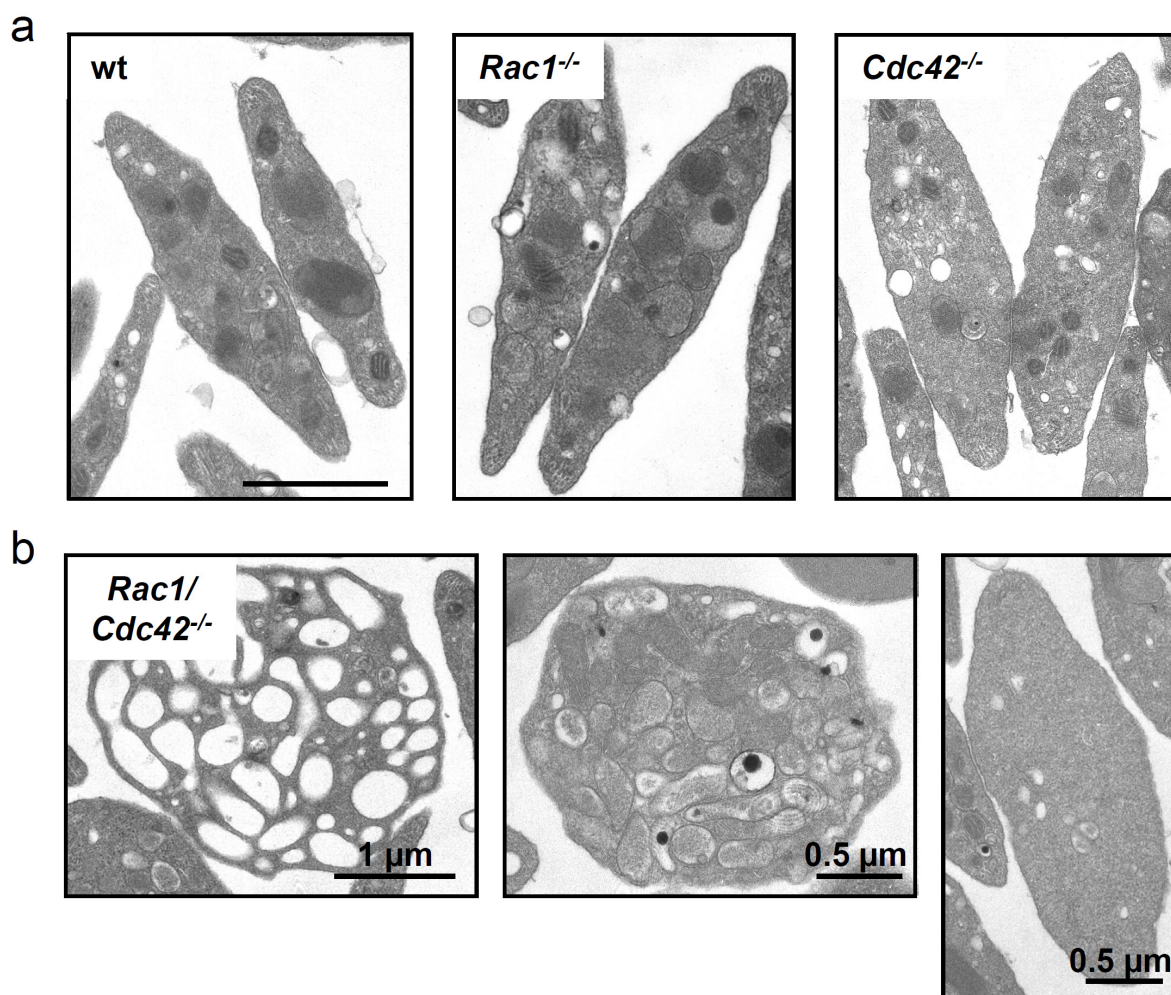


Figure 33. *Rac1/Cdc42*^{-/-} platelets show abnormal ultrastructure. Representative transmission electron microscopy pictures are depicted. (a) Normal ultrastructure of wild-type, *Rac1*^{-/-} and *Cdc42*^{-/-} platelets. Bar, 1 μm. (b) Abnormal ultrastructure of *Rac1/Cdc42*^{-/-} platelets. Bar sizes are depicted. Abbreviations: α, α granule; d, dense granule; v, vacuole.

	wild-type	<i>Rac1/Cdc42^{-/-}</i>
GPIb	452 ± 7	270 ± 23
GPV	386 ± 5	252 ± 24
GPIX	615 ± 9	416 ± 20
CD9	1210 ± 35	1113 ± 140
GPVI	44 ± 3	29 ± 1
α2	112 ± 7	107 ± 5
β1	149 ± 10	165 ± 8
αIIbβ3	813 ± 42	732 ± 27

Table 3. Platelet glycoprotein expression in wild-type and *Rac1/Cdc42^{-/-}* mice. Expression of glycoproteins on the platelet surface was determined by flow cytometry. Diluted whole blood from the indicated mice was incubated with FITC-labeled antibodies at saturating concentrations for 15 min at RT and platelets were analyzed directly. Results are expressed as mean fluorescence intensity ± SD for 5 mice per group.

3.3.1.2 *Rac1/Cdc42^{-/-}* platelets are unable to spread on fibrinogen upon activation

To test the ability of the *Rac1/Cdc42^{-/-}* platelets to undergo shape change and to rearrange the actin cytoskeleton, spreading experiments on fibrinogen (100 µg/ml) upon thrombin (0.01 U/ml) stimulation were performed. As already shown in sections 3.2.2 and 3.1.2, *Cdc42^{-/-}* platelets spread normally under these conditions, whereas *Rac1^{-/-}* platelets were unable to form lamellipodia. *Rac1/Cdc42^{-/-}* platelets were still able to tightly adhere to the fibrinogen matrix and, as expected from *Rac1* deficiency, double-deficient platelets were unable to form lamellipodia. Most adherent *Rac1/Cdc42^{-/-}* platelets contracted and partially extended long filopodia but spreading was completely abolished (Fig. 34a,b).

To determine whether the spreading defect of the double-mutant platelets was caused by defective actin assembly, F-actin contents in resting and thrombin-stimulated (1 U/ml) wild-type, *Rac1^{-/-}*, *Cdc42^{-/-}* and *Rac1/Cdc42^{-/-}* platelets were measured by flow cytometry. Interestingly, the increase in F-actin content upon thrombin stimulation was similar in all tested mouse lines, indicating that actin assembly could still take place in absence of *Rac1* and *Cdc42* (Fig. 34c). This result suggested that defective spreading in the double-deficient mice was caused by inhibited actin reorganization rather than by a general defect in F-actin assembly.

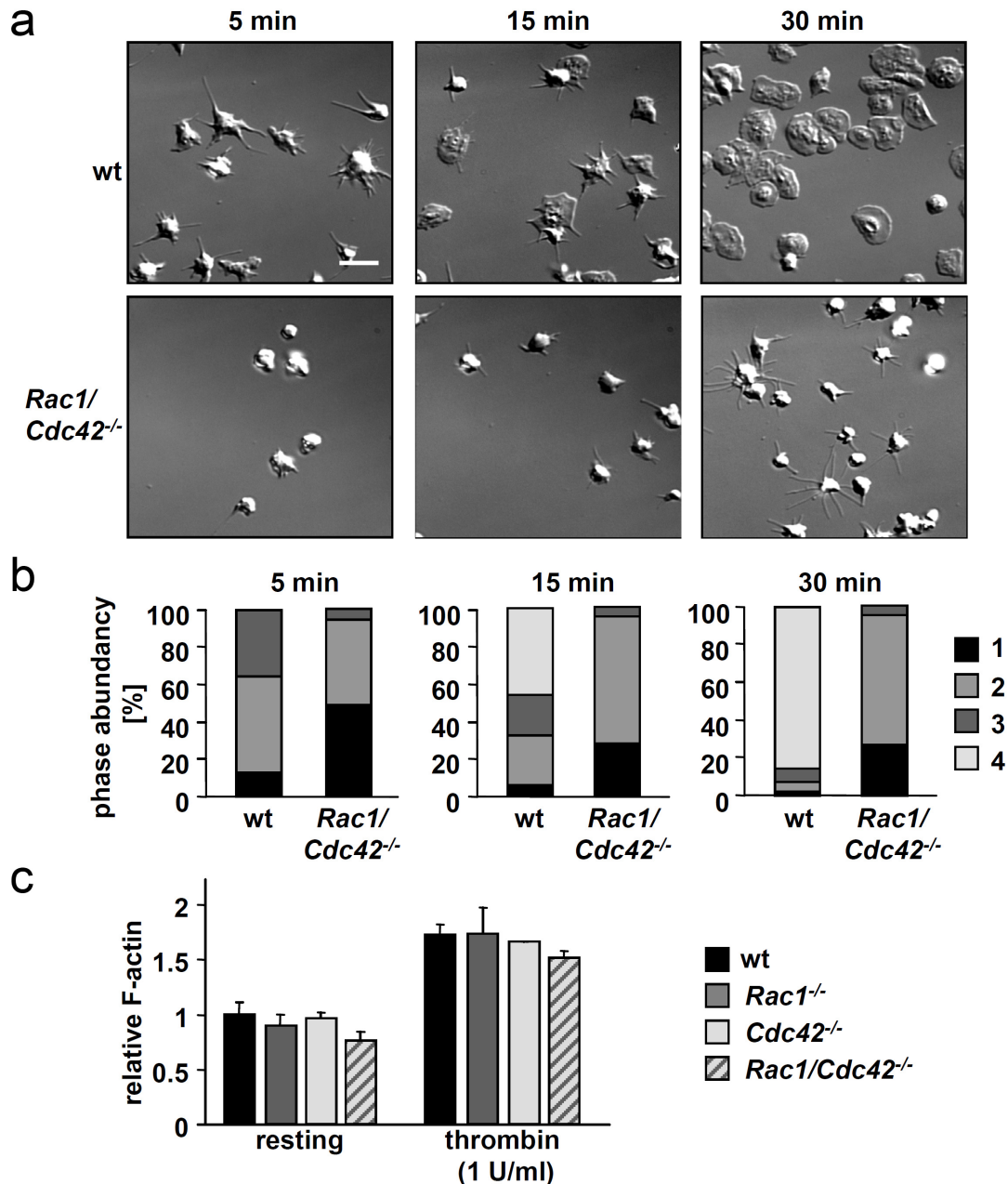


Figure 34. Defective spreading of *Rac1/Cdc42^{-/-}* platelets on fibrinogen. (a) Washed platelets from the indicated mice were allowed to adhere and spread on immobilized human fibrinogen (100 $\mu\text{g/ml}$) upon activation with thrombin (0.01 U/ml). DIC images were taken at the indicated time points (5, 15, 30 min), representative of 4 individual experiments. Bar, 5 μm . (b) Statistical analysis of the percentage of spread *Rac1/Cdc42^{-/-}* and wild-type platelets observed at different spreading stages at the indicated time points. 1: roundish, no filopodia, no lamellipodia. 2: only filopodia. 3: filopodia and lamellipodia. 4: full spreading; only lamellipodia. (c) Determination of relative F-actin contents \pm SD in resting and thrombin-activated (1 U/ml) wild-type, *Rac1^{-/-}*, *Cdc42^{-/-}* and *Rac1/Cdc42^{-/-}* platelets.

Detailed analysis of *Rac1/Cdc42^{-/-}* platelets by SEM confirmed the increased size of the cells (Fig. 35a) and revealed that spread (30 min, 0.01 U/ml thrombin) *Rac1/Cdc42^{-/-}* platelets were less contracted than *Rac1^{-/-}* platelets (see section 3.1.2) (Fig. 35b, upper and middle panel). In addition, filopodia exhibited by the mutant platelets were thinner than those formed by *Rac1^{-/-}* platelets. Visualization of the

cytoskeleton by denudation of the plasma membrane demonstrated defective actin reorganization upon activation in spread *Rac1/Cdc42*^{-/-} platelets (Fig. 35b, lower panel).

Taken together, these results showed that lack of Rac1 and Cdc42 resulted in abrogated spreading and actin rearrangement defects in double-mutant platelets.

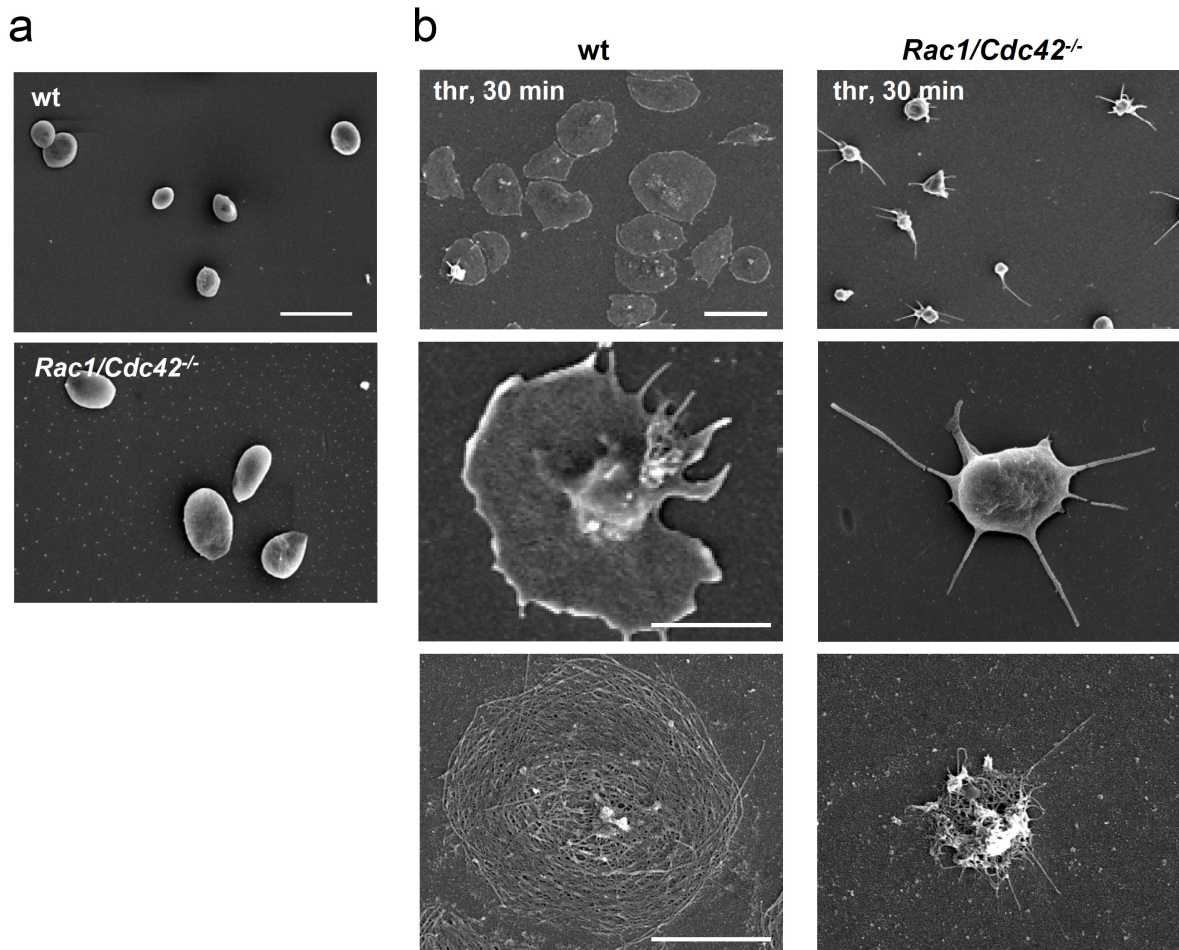


Figure 35. Scanning electron microscopical analysis of *Rac1/Cdc42*^{-/-} platelets. (a) Increased size of resting *Rac1/Cdc42*^{-/-} platelets immobilized on poly-L-lysine. Bar, 5 μ m. (b) Visualization of defective actin reorganization and spreading of *Rac1/Cdc42*^{-/-} platelets on fibrinogen (100 μ g/ml) upon activation with 0.01 U/ml thrombin (time point: 30 min). Upper panel: Overview (bar, 5 μ m). Middle and lower panel: Detail of spread wild-type and *Rac1/Cdc42*^{-/-} platelets. Middle panel: SEM of intact platelets. Bar, 2 μ m. Lower panel: visualization of the actin cytoskeleton after denudation of the plasma membrane. Bar, 2 μ m.

3.3.1.3 Defective integrin activation and degranulation in *Rac1/Cdc42*^{-/-} platelets

The results from electron microscopy and spreading studies indicated platelet function defects upon *Rac1/Cdc42* double deficiency. To investigate whether *Rac1/Cdc42*^{-/-} platelets were activatable and release granules, integrin α IIb β 3 activation and α granule-dependent P-selectin exposure upon platelet activation with

different agonists was determined by flow cytometry (Fig. 36). Whereas *Rac1*^{-/-} platelets showed a selective ITAM activation defect and P-selectin expression was enhanced in *Cdc42*^{-/-} platelets (see sections 3.1.3 and 3.2.4) *Rac1/Cdc42*^{-/-} platelets displayed markedly decreased integrin activation (Fig. 36a) and P-selectin expression (Fig. 36b) in response to all tested stimuli, including ITAM- as well as G-protein-coupled agonists.

Thus, double deficiency of *Rac1* and *Cdc42* resulted in severe activation and degranulation defects in platelets which were not restricted to specific signaling pathways.

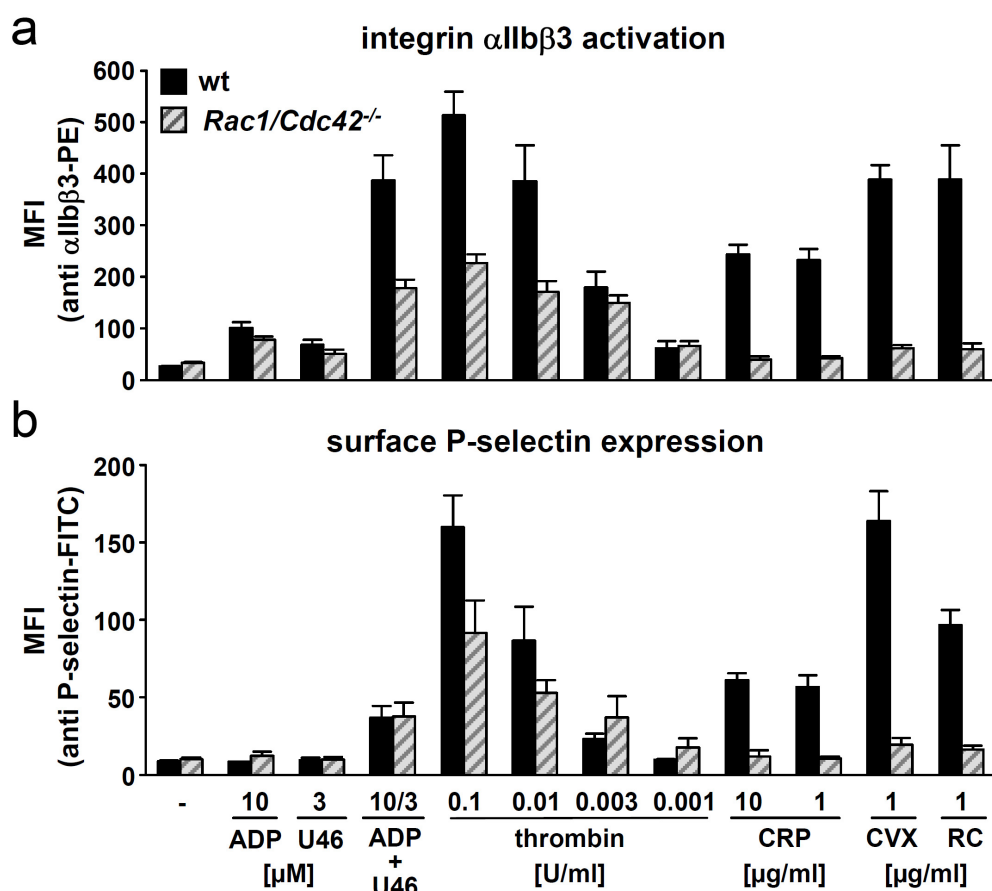


Figure 36. Decreased integrin activation and granule release in *Rac1/Cdc42*^{-/-} platelets upon activation. Flow cytometric analysis of (a) α IIb β 3 integrin activation (binding of JON/A-PE) and (b) degranulation-dependent P-selectin exposure in response to the indicated agonists from control (black) or *Rac1/Cdc42*^{-/-} (patterned) platelets. Results are mean fluorescent intensities (MFI) \pm SD of 5 mice per group.

3.3.1.4 *Rac1/Cdc42*^{-/-} platelets are rapidly cleared from the circulation

Non-functional or pre-activated platelets are constantly cleared from the circulation by the reticulo-endothelial compartment, in order to prevent spontaneous aggregation in the vascular system. To address the question whether constant removal of platelets from the circulation contributed to the macrothrombocytopenia observed in

Rac1/Cdc42^{-/-} mice, the platelet life span was determined as described in section 3.2.7. One hour after injection of a platelet-specific fluorescently labeled antibody derivative *in vivo*, 90% of wild-type, as well as *Rac1/Cdc42^{-/-}* platelets were labeled (Fig. 37a). In wild-type mice the percentage of labeled platelets gradually decreased down to 0% on day 5. In contrast, in *Rac1/Cdc42^{-/-}* mice, the population of fluorescent platelets was less than 10% already on day 2 and 0% on day 3. However, a *per-se* pre-activation of the double-deficient platelets was probably not the major cause of the decreased platelet life span, since flow cytometric measurements revealed that the weak agonist epinephrine was not able to induce integrin activation or degranulation in *Rac1/Cdc42^{-/-}* platelets *in vitro* (Fig. 37b). Thus, the rapid clearance of *Rac1/Cdc42^{-/-}* platelets was probably rather caused by intrinsic defects which is in line with the markedly altered ultrastructure observed by TEM (Fig. 33).

Taken together, these results showed that defects in production of functional *Rac1/Cdc42^{-/-}* platelets resulted in a dramatically decreased platelet span *in vivo* which may contribute to the macrothrombocytopenia observed in the double-deficient animals.

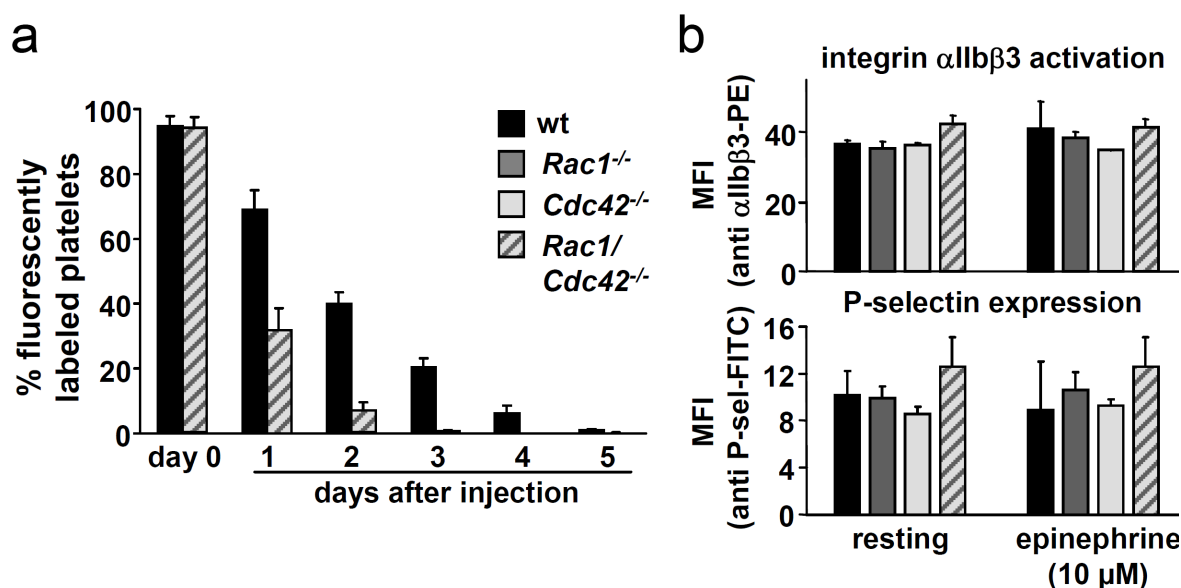


Figure 37. Decreased platelet life span in *Rac1/Cdc42^{-/-}* mice. (a) Decreased life span of *Rac1/Cdc42^{-/-}* platelets. Determination of the percentage of fluorescently labeled platelets of wild-type (black) and *Rac1/Cdc42^{-/-}* platelets (patterned) for 5 days upon injection with 0.5 μ g/g bodyweight GPIX-Dylight 488 derivate on day 0. (b) *Rac1/Cdc42^{-/-}* platelets are not *per se* pre-activated under *in vitro* conditions. Flow cytometric analysis of α IIb β 3 integrin activation (binding of JON/A-PE, upper panel) and degranulation-dependent P-selectin exposure (lower panel) in resting and epinephrine-stimulated (10 μ M) wild-type (black), *Rac1^{-/-}* (dark gray), *Cdc42^{-/-}* (light gray) and *Rac1/Cdc42^{-/-}* (patterned) platelets. Results are mean fluorescence intensities (MFI) \pm SD of 4 mice per group.

3.3.1.5 *Rac1/Cdc42*^{-/-} mice display defective hemostasis and defective thrombus formation *in vivo*

The results presented above demonstrated marked defects in the formation of functional platelets in *Rac1/Cdc42*^{-/-} mice. To investigate the relevance of GTPase double deficiency for hemostasis *in vivo*, tail bleeding times in wild-type and *Rac1/Cdc42*^{-/-} mice were determined (Fig. 38a). Whereas bleeding in wild-type animals stopped within 7 minutes, none of the double-deficient animals was able to arrest bleeding within the observation time of 20 minutes. Thus, while single deficiency in either *Rac1* or *Cdc42* resulted in variable bleeding times, lack of both GTPases lead to a severe hemostatic defect in mice.

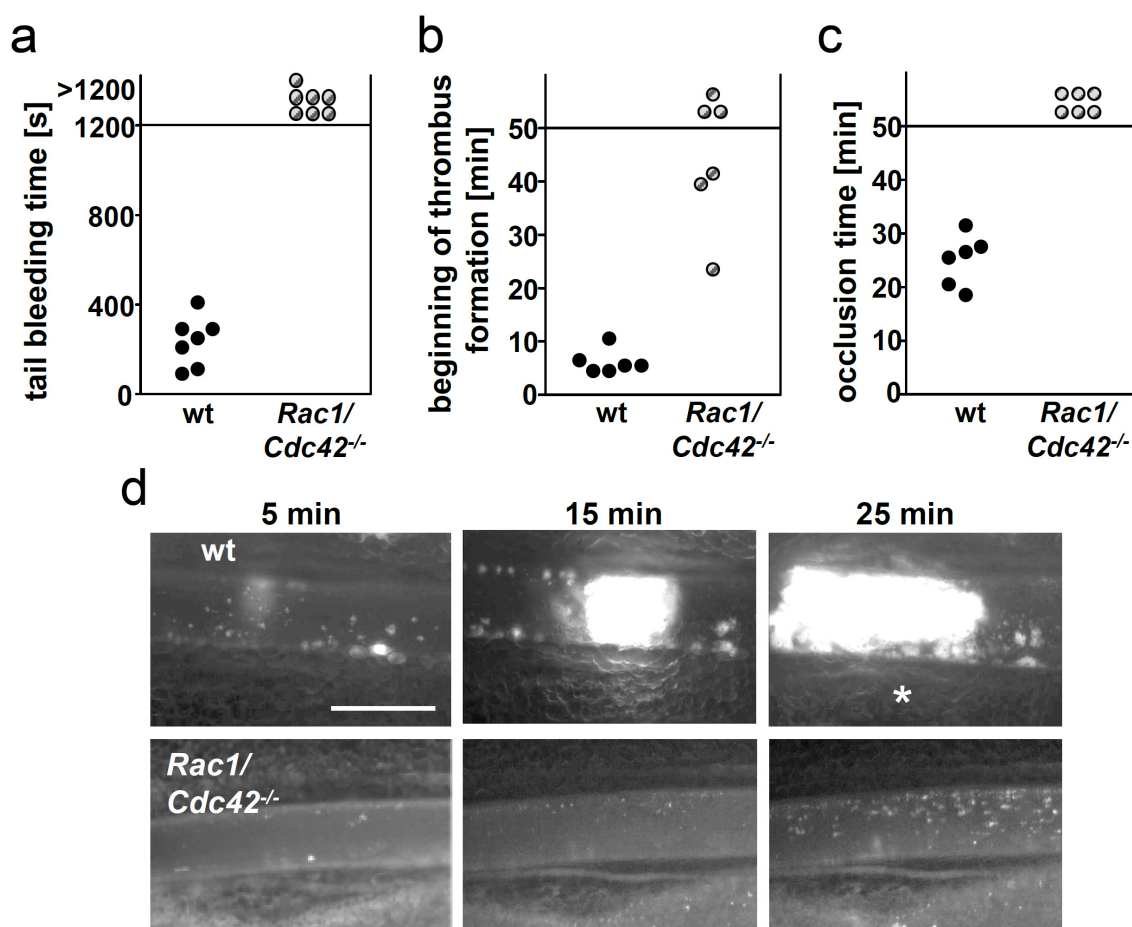


Figure 38. Defective hemostasis and thrombus formation in *Rac1/Cdc42*^{-/-} mice. (a) Infinite tail bleeding in *Rac1/Cdc42*^{-/-} mice (patterned) compared to wild-type (black) mice. Each symbol represents one individual. (b–d) Mesenteric arterioles were injured with 20% FeCl₃ and adhesion and thrombus formation of fluorescently-labeled platelets was monitored *in vivo* by fluorescence microscopy. Time to appearance of first thrombi (b) and occlusion times (c) are shown. Each symbol represents one individual. (d) Representative images are depicted. Bar, 50 μm. The asterisk indicates occlusion of the vessel.

Recent studies in mice using intravital microscopy revealed that three-dimensional thrombi can still be formed under conditions of decreased platelet counts. To test the

impact of GTPase double deficiency on arterial thrombus formation *Rac1/Cdc42*^{-/-} mice were challenged in an *in vivo* model in which oxidative injury of mesenteric arterioles is induced by application of ferric chloride (Fig. 38b-d). Under these conditions, wild-type, as well as *Rac1*^{-/-} (not shown) and *Cdc42*^{-/-} mice (see section 3.2.9) were able to form stable thrombi which occluded the injured vessels. In contrast, beginning of thrombus formation was only observed in 50% of *Rac1/Cdc42*^{-/-} mice (Fig. 38b) and the formation of three-dimensional aggregates was completely abolished. Thus, no vessel occlusion was observed in the double-deficient mice during the observation time of 50 minutes (Fig. 38c,d).

Taken together, these results demonstrated defective hemostasis and thrombus formation in *Rac1/Cdc42*^{-/-} mice.

3.3.2 Megakaryocyte studies

3.3.2.1 Megakaryocytes are present in spleen and bone marrow of *Cdc42*^{-/-} and *Rac1/Cdc42*^{-/-} mice

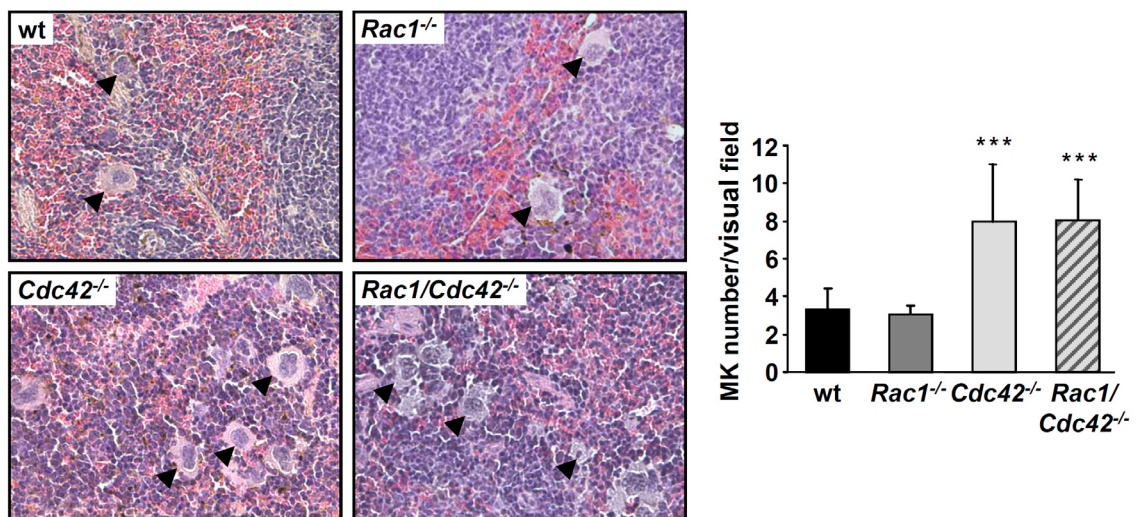
Intact megakaryocyte differentiation and maturation is critical for the formation of functional platelets. The results of the platelet studies had revealed mild thrombocytopenia in *Cdc42*^{-/-} and severe macrothrombocytopenia in *Rac1/Cdc42*^{-/-} mice. This thrombocytopenia might at least partially be caused by the constant removal of pre-activated and/or non-functional platelets as indicated by the decreased platelet life span observed in these mice. Alternatively, defects in megakaryocyte formation and/or platelet production might account for the decreased platelet counts. To compensate the low number of circulating platelets, thrombocytopenia is often associated with increased megakaryocyte production.

To address this issue, the number of megakaryocytes in spleen and bone marrow sections derived from wild-type, *Rac1*^{-/-}, *Cdc42*^{-/-} and *Rac1/Cdc42*^{-/-} mice was determined (Fig. 39). As expected from the normal platelet counts, *Rac1*^{-/-} mice displayed unaltered MK numbers as compared to wild-type mice in spleen and bone marrow.

In contrast, the number of MKs was highly increased in spleens of *Cdc42*^{-/-} and *Rac1/Cdc42*^{-/-} mice (Fig. 39a). In bone marrow, MK numbers were markedly increased in *Cdc42*^{-/-} mice whereas no alteration was detectable for *Rac1/Cdc42*^{-/-} mice as compared to wild-type animals (Fig. 39b). However, it is important to note

that the double-deficient MKs were difficult to observe in the sections due to their decreased demarcation towards surrounding cells, and therefore numbers may have been underestimated. Nevertheless, these results clearly demonstrated that MKs were present in *Cdc42*^{-/-} and *Rac1/Cdc42*^{-/-} mice, excluding a general defect in MK production as the reason for the thrombocytopenia in the animals.

a



b

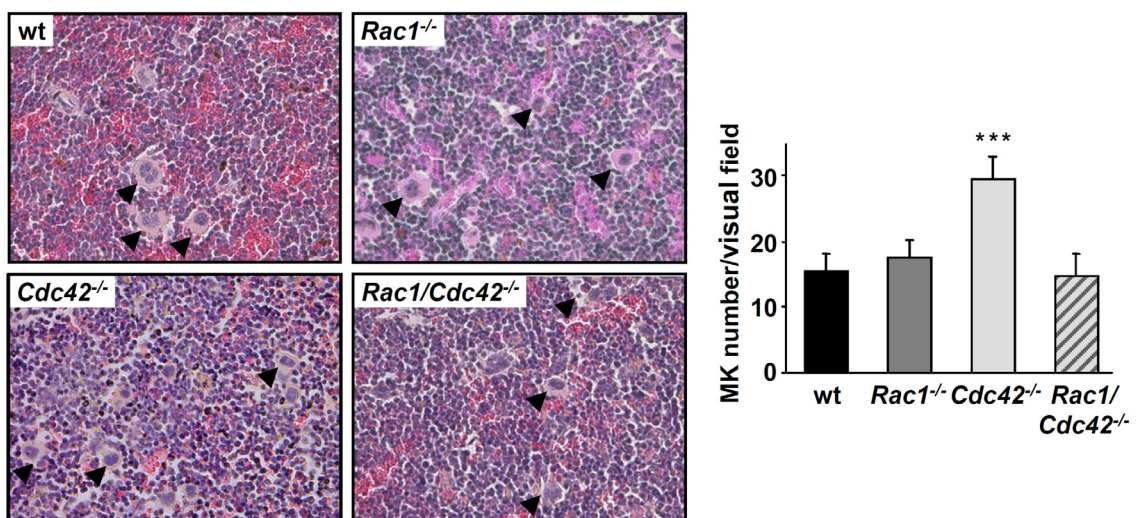


Figure 39. Megakaryocytes are present in spleen and bone marrow of *Cdc42*^{-/-} and *Rac1/Cdc42*^{-/-} mice. (a,b) Determination of MK numbers in hematoxylin-eosin-stained (a) spleen or (b) bone marrow sections from wild-type, *Rac1*^{-/-}, *Cdc42*^{-/-} and *Rac1/Cdc42*^{-/-} mice. Left: Representative images. Black arrows indicate MKs. Right: Statistical analysis of MK numbers. Results are expressed as mean MK number per visual field \pm SD of 5 mice per group.

3.3.2.2 Proplatelet formation is decreased in *Cdc42*^{-/-} MKs and nearly abrogated in *Rac1/Cdc42*^{-/-} MKs

The presence of MKs in *Cdc42*^{-/-} and *Rac1/Cdc42*^{-/-} mice indicated that a defect in platelet production might account for the thrombocytopenia in the animals. Therefore,

in the next step, the ability of MKs derived from wild-type, *Rac1*^{-/-}, *Cdc42*^{-/-} and *Rac1/Cdc42*^{-/-} mice to form proplatelets was determined. For this purpose, MKs isolated from adult bone marrow or fetal liver (E 14.5) were cultured in the presence of TPO to induce maturation and proplatelet formation *in vitro* (Fig. 40). Under these conditions, bone marrow- as well as fetal liver cell-derived *Rac1*^{-/-} MKs were able to form proplatelets to a similar extent as wild-type platelets (Fig. 40a,b). In *Cdc42*^{-/-} MKs, proplatelet formation was moderately but significantly reduced, indicating that, in case of single deficiency, Cdc42 might be of more importance for platelet production than Rac1. In marked contrast, proplatelet formation was strongly reduced in fetal liver cell-derived MKs (Fig. 40b) and nearly abrogated in bone marrow-derived MKs (Fig. 40a) from *Rac1/Cdc42*^{-/-} mice.

Thus, these results point to a redundant role of Rac1 and Cdc42 in the processes of proplatelet formation and platelet production from MKs.

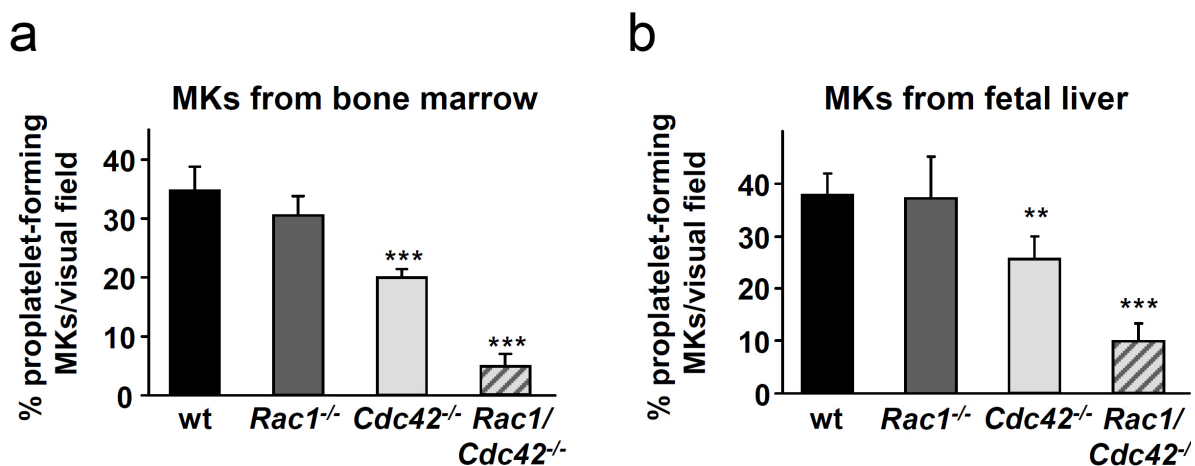


Figure 40. Decreased proplatelet formation from MKs derived from *Cdc42*^{-/-} and *Rac1/Cdc42*^{-/-} mice. (a,b) Determination of proplatelet formation from cultured MKs derived from wild-type, *Rac1*^{-/-}, *Cdc42*^{-/-} and *Rac1/Cdc42*^{-/-} mice. Results are expressed as % of proplatelet-forming MKs per visual field \pm SD from at least 5 samples per group. (a) Results from bone marrow-derived MKs (day 6 of culture). (b) Results from fetal liver-derived MKs (E 14.5, day 4 of culture).

3.3.2.3 Intact endomitosis in MKs derived from *Rac1*^{-/-}, *Cdc42*^{-/-} and *Rac1/Cdc42*^{-/-} mice

Endomitosis represents a crucial process during MK maturation, leading to a DNA content up to 64N (see section 1.3). To determine whether PF4-Cre-induced lack of Rac1 and/or Cdc42 influenced endomitotic processes in MKs, the ploidy of bone marrow- and fetal liver-derived MKs was determined by flow cytometry (Fig. 41). For this purpose, MKs from whole bone marrow of adult mice or from fetal liver cell cultures (day 3 of culture) were stained with a fluorescently-labeled anti-integrin α IIb

(GPIIb) antibody specific for MKs and platelets, as well as with propidium iodide (PI) for determination of the different DNA ploidy stages (Fig 41a). Under both conditions, the mean ploidy (counted from 8N) was similar in *Rac1*^{-/-}, *Cdc42*^{-/-} and *Rac1/Cdc42*^{-/-} MKs as compared to wild-type MKs (Fig. 41a-c). Until now, it is not clearly defined at which stage of MK differentiation the PF4-Cre-mediated gene deletion is induced. However, it is assumed that gene deletion induced by this system occurs only after termination of the endomitotic stage during MK maturation, thereby not affecting endomitosis (see Fig. 3). Alternatively, endomitosis may still take place in *Rac1* and/or *Cdc42*-deficient MKs.

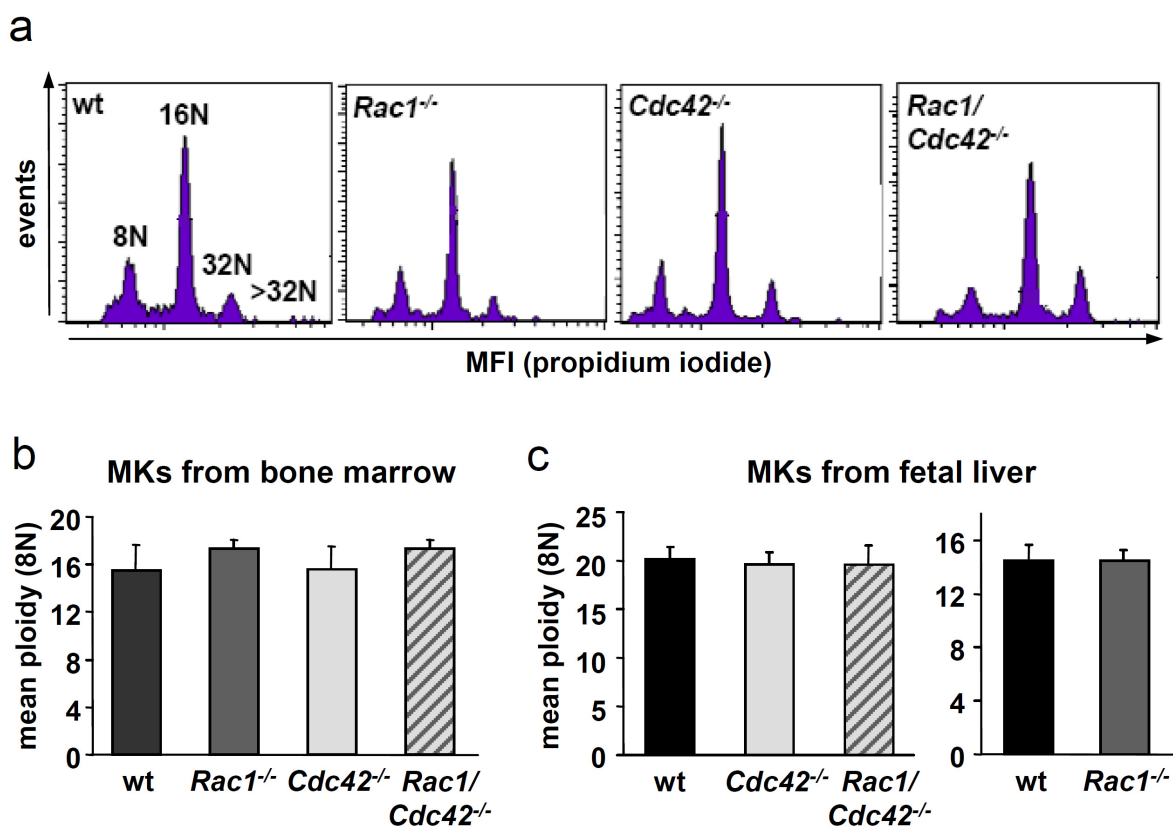


Figure 41. Normal endomitosis in MKs derived from *Rac1*^{-/-}, *Cdc42*^{-/-} and *Rac1/Cdc42*^{-/-} mice. (a-c) Determination of the ploidy status from cultured MKs derived from wild-type, *Rac1*^{-/-}, *Cdc42*^{-/-} and *Rac1/Cdc42*^{-/-} mice. (a) Representative dotplots. (b) Results from MKs derived from whole bone marrow. (c) Results from fetal liver-derived MKs (day 3 of culture). Results are expressed as mean ploidy (from 8 N) \pm SD from at least 4 samples per group.

3.3.2.4 Reduced presence of demarcation membranes in bone marrow MKs from *Cdc42*^{-/-} and *Rac1/Cdc42*^{-/-} mice

The results shown above revealed decreased proplatelet formation from cultured *Cdc42*^{-/-} and *Rac1/Cdc42*^{-/-} MKs. However, as mentioned in the Introduction (section 1.3), recent studies indicate that the characteristic proplatelet structures found in *in*

in vitro cultures do not exactly reflect the physiological situation of (pro)platelet formation. *In vivo*, membrane invaginations, called demarcation membranes (DMS), define newly formed proplatelet territories in the cytoplasm of mature MKs and proplatelets are shed into sinusoids of the marrow to allow shear-dependent platelet formation.

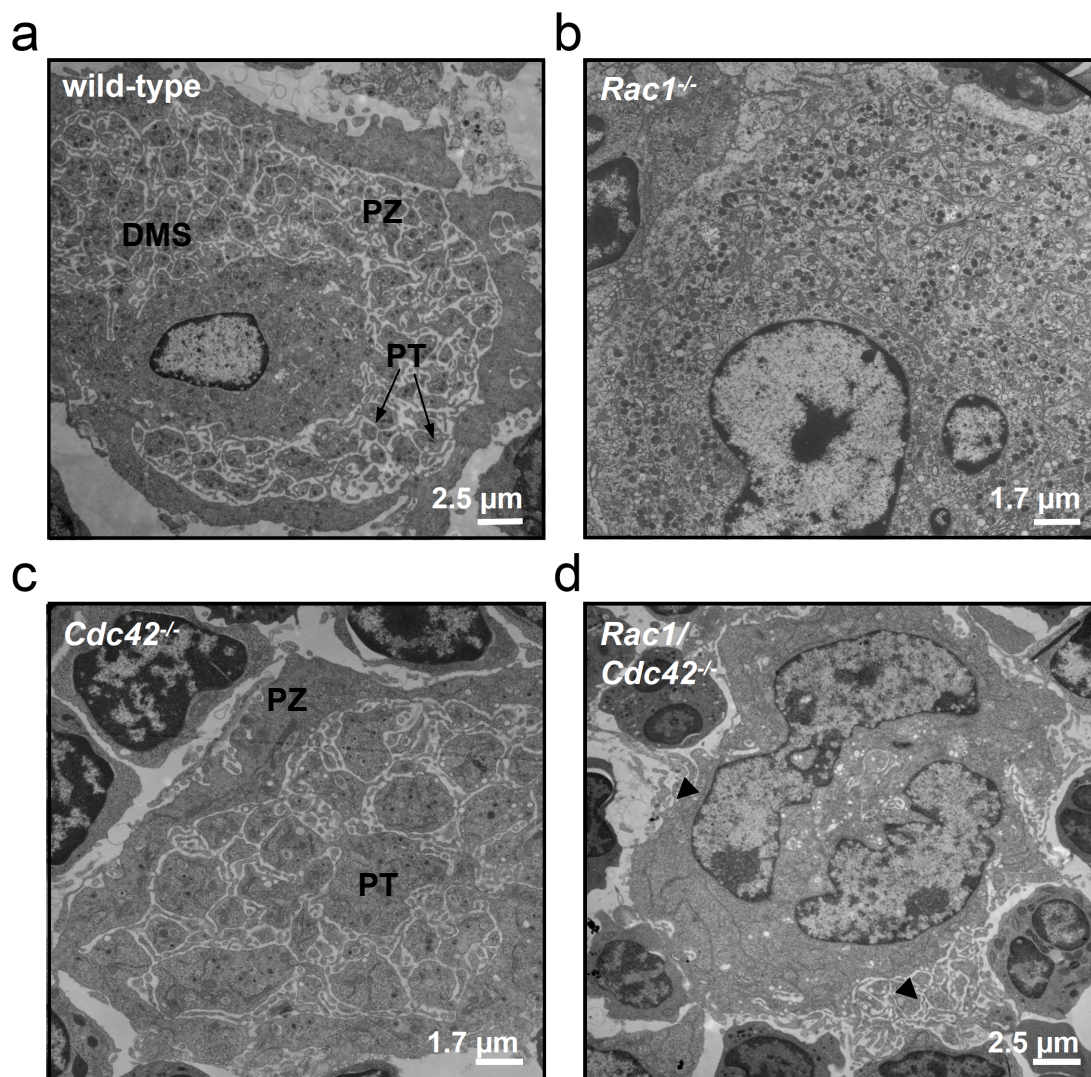


Figure 42. Altered morphology of bone marrow MKs derived from *Cdc42*^{-/-} and *Rac1/Cdc42*^{-/-} mice. (a-d) TEM of MKs in bone marrow of adult (6 week-old) mice. (a,b) Normal ultrastructure in MKs derived from (a) wild-type and (b) *Rac1*^{-/-} mice. (c,d) altered ultrastructure in MKs derived from (c) *Cdc42*^{-/-} and (d) *Rac1/Cdc42*^{-/-} mice. Note the absence of membrane invaginations and lack of the peripheral zone (PZ) in *Rac1/Cdc42*^{-/-} MKs. Abbreviations: DMS, demarcation membrane system; PT, proplatelet territory. Bar sizes are depicted.

To visualize megakaryocyte maturation in the physiological environment, bone marrow sections from wild-type, *Rac1*^{-/-}, *Cdc42*^{-/-} and *Rac1/Cdc42*^{-/-} mice were analyzed by TEM (Fig. 42/43). Mature wild-type, as well as *Rac1*^{-/-} MKs displayed demarcation membranes and proplatelet territories in the center of the cytoplasm, whereas few invaginations were found in the periphery and around the nucleus (Fig.

42/43a,b). In *Cdc42*^{-/-} MKs, membrane invaginations were still present but reduced as compared to MKs from wild-type mice, resulting in enlarged proplatelet territories and large areas without visible membrane invagination (Fig. 42/43c).

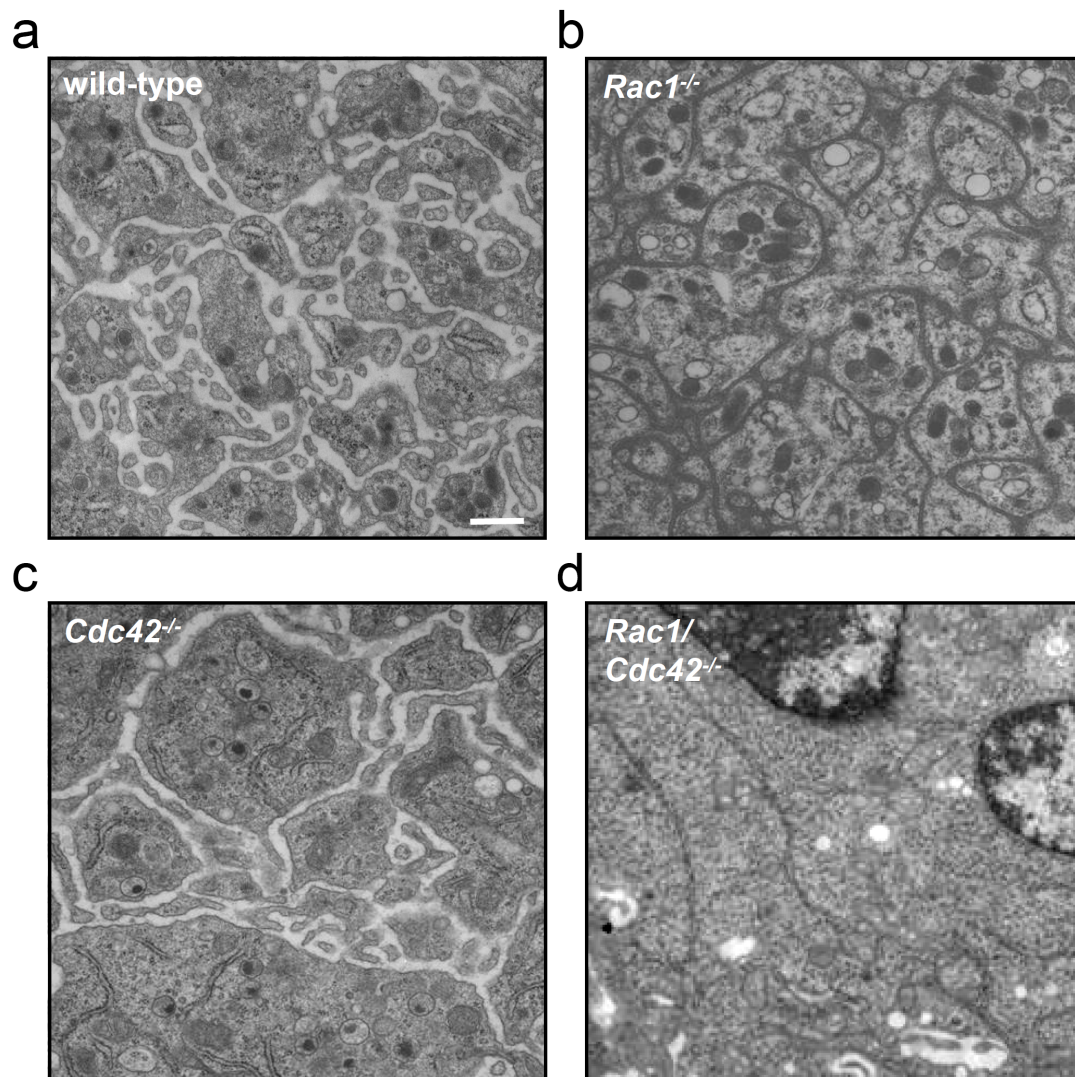


Figure 43. Reduced membrane invagination in bone marrow MKs derived from *Cdc42*^{-/-} and *Rac1/Cdc42*^{-/-} mice. (a-d) Detailed transmission electron microscopy of MKs in bone marrow of adult (6 week-old) mice. (a,b) Presence of demarcation membranes and proplatelet territories in MKs derived from (a) wild-type and (b) *Rac1*^{-/-} mice. (c) Partially reduced membrane invagination in *Cdc42*^{-/-} MKs. (d) Abrogated membrane invagination and altered granule distribution/content in *Rac1/Cdc42*^{-/-} MKs. Bar, 0.6 μ m.

By marked contrast, demarcation membranes were hardly present in MKs from *Rac1/Cdc42*^{-/-} mice or concentrated in small areas (Fig. 42/43d). Furthermore, double-deficient MKs displayed reduced numbers of granules and an incomplete peripheral zone structure, resulting in reduced delineation of the MKs to circumjacent cells (Fig. 42d). This interesting observation is in line with the reduced visibility of *Rac1/Cdc42*^{-/-} MKs in hematoxylin eosin-stained bone marrow sections (Fig 39b). Taken together, these results indicate new and redundant roles for Rac1 and Cdc42

in the regulation of MK maturation, including invagination of demarcation membranes, proplatelet territory formation and maintenance of cell integrity.

4 DISCUSSION

Platelet activation and aggregation at sites of vascular injury is essential to limit blood loss, but under pathological conditions it can lead to complete vessel occlusion resulting in myocardial infarction or stroke. Therefore, platelet signaling has become an important field of clinical research over the last decades and many widely used therapeutical drugs for prevention of cerebro- and cardiovascular diseases, such as aspirin and clopidogrel, act by inhibiting platelet function.

Platelet activation induces a massive reorganization of the actin cytoskeleton which enables adhesion and spreading on ligands immobilized on the injured vessel wall. Small GTPases of the Rho family, namely RhoA, Rac1 and Cdc42 have been shown to contribute to these processes by inducing the formation of stress fibers, lamellipodia and filopodia, respectively. Furthermore, recent reports strongly indicate that the proteins may participate in a variety of additional pathways independent of their major proposed role as regulators of the actin cytoskeleton.

A large number of studies addressing the role of Rho GTPases in various cell types, including platelets, have been performed, mainly by use of cell lines and overexpression systems. However, many of these studies yielded conflicting results which were most probably caused by unspecific side effects of the used methods and/or reagents. The recent generation of conditional knock-out mice for several GTPases has enabled the study of GTPase deficiency with a minimal risk of secondary effects.

In the current thesis, the role of the Rho GTPases Rac1 and Cdc42 for platelet function and production was investigated using conditional single- and double-deficient knock-out mice (Cre/loxP system). The results presented here reveal important and partially redundant roles for the GTPases and indicate so far unknown functions of Rac1 and Cdc42 in different platelet signaling pathways including not only regulation of actin cytoskeletal rearrangements, but also an involvement in platelet activatory and secretory events. Thus, Rho GTPases may serve as new potential targets for the development of agents in order to treat cerebro- and cardiovascular diseases.

4.1 Rac1 mediates phospholipase C- γ 2 activation in platelets independently of tyrosine phosphorylation

Binding of the major collagen platelet receptor GPVI to its ligand at sites of vascular injury is crucial for platelet activation, as well as subsequent aggregation and plug formation and involves activation of the phospholipase isoform PLC γ (see section 1.1). The results presented here using gene targeting (Mx-Cre/loxP) reveal that the small GTPase Rac1 is required for ITAM-dependent activation of PLC γ 2 in platelets. Deficiency in Rac1 resulted in defective GPVI-induced calcium mobilization and entry leading to severely defective platelet adhesion and thrombus formation on collagen *in vitro* and at the injured vessel wall *in vivo* (Fig. 16/17). In addition, it was shown that Rac1 is involved in platelet activation through CLEC-2 which employs a similar signaling pathway as GPVI involving Src family kinases, such as spleen tyrosine kinase (Syk) and PLC γ 2^{8;81} and thus represents an “ITAM-like” pathway. On the other hand, *Rac1*^{-/-} platelets showed unaltered Ca²⁺ mobilization and cellular activation in response to GPCR stimulation, suggesting that the GTPase is not involved in PLC β activation in platelets (Fig 13/14). This stands in contrast to results by Akbar *et al.* who reported a pronounced secretion defect in response to all tested agonists in Rac1-deficient mouse platelets and human platelets treated with a selective Rac1 inhibitor⁴⁴. However, in line with the results shown in this thesis, McCarty *et al.* also found unaltered secretion and aggregation of *Rac1*^{-/-} platelets in response to GPCR-coupled agonists³³. It is difficult to explain the discrepancies in the results, but they may be due to different experimental conditions.

Despite the severe defect in GPVI-induced cellular activation, no significant alterations in tyrosine phosphorylation patterns were detectable in the absence of Rac1 (Fig. 15). Importantly, also GPVI-induced PLC γ 2 phosphorylation was indistinguishable between wild-type and *Rac1*^{-/-} platelets. However, GPVI-induced IP₃ production and Ca²⁺ mobilization were severely impaired in the mutant platelets (Fig. 14/15a). This clearly shows that Rac1 acts as a co-activator of PLC γ 2 that regulates the enzyme independently of tyrosine phosphorylation events in murine platelets. Such a mechanism has recently been proposed by Piechulek *et al.* based on data obtained in heterologous cells and cell-free systems⁴⁶. They showed that PLC γ 2 activation induced by constitutively active Rac1 was independent of phosphorylation of tyrosine residues known to be modified by PLC γ 2-activating protein-tyrosine

kinases. The modality of interaction of Rac1 with PLC γ 2 and the mechanisms involved are not clear at present. Piechulek *et al.* proposed a direct interaction of activated Rac1 with one of the pleckstrin homology (PH) domains of PLC γ 2 as it was shown for PLC γ 1 where a split PH domain is known to be responsible for protein-protein interactions^{93,94}. Interestingly, a recent study from Guidetti *et al.* showed that, in human platelets, integrin $\alpha_2\beta_1$ signaling induced Rac1-mediated PLC γ 2 activation without requiring tyrosine phosphorylation of the enzyme⁹⁵. Thus, different mechanisms for PLC γ 2 activation may exist in murine and human platelets, or, alternatively, the mechanism of Rac1-mediated PLC γ 2 activation by integrin $\alpha_2\beta_1$ differs from that induced by GPVI. Clearly, further studies are required to resolve this issue.

In this work, impaired aggregation of *Rac1*^{-/-} platelets was found in response to low and intermediate concentrations of collagen and CRP, whereas largely normal responses were observed at high agonist concentrations (Fig. 11). However, these aggregometric studies had underestimated the severity of the defect in GPVI-dependent activation as flow cytometric analysis revealed a dramatic impairment of cellular activation even at very high agonist concentrations (Fig. 13a-c). Moreover, dense granule secretion, as determined by measuring released ATP, was almost abolished in *Rac1*^{-/-} platelets upon induction of GPVI signaling (Fig. 13d). It is known that in standard aggregometry robust platelet aggregation can be achieved even under conditions of very weak integrin $\alpha IIb\beta 3$ activation^{82,96}. In addition, released secondary mediators such as ADP and TXA₂ accumulate in the aggregometer cuvette and to a great extent induce/amplify the observed aggregation response. Both of these factors probably contributed to the aggregation of *Rac1*^{-/-} platelets in response to high collagen or CRP concentrations. This notion is supported by the finding that *Rac1*^{-/-} platelets were unable to aggregate in response to high concentrations of collagen or CRP under conditions excluding the contribution of ADP and TXA₂ (Fig. 12).

Similar to McCarty *et al.*, reduced adhesion of *Rac1*^{-/-} platelets to collagen and virtually abrogated thrombus formation was observed in this study (Fig. 16/17). However, McCarty *et al.* proposed this aggregate instability to be based on altered cytoskeletal regulation leading to instable aggregate formation³³. Although the defect in lamellipodia formation could also be confirmed in the current study (Fig. 10b) this

did most likely not account for the observed thrombus instability since co-infusion of ADP and U46619 to the flow system fully restored the ability of *Rac1*^{-/-} platelets to form large stable three-dimensional thrombi (Fig. 16). Furthermore, as revealed by SEM, *Rac1*^{-/-} and wild-type platelets displayed similar morphology when activated in suspension, which represents the physiological situation in the blood stream (Fig. 10c). This surprising finding demonstrates that lamellipodia formation may not be required for thrombus stability, at least under the here described experimental conditions. Rather, the data suggest that the observed defect is based on insufficient GPVI-mediated platelet activation and release of secondarily acting agonists. In fact, the adhesion and thrombus formation defect observed in *Rac1*^{-/-} mice is very similar to that previously seen in *Plcg2*^{-/-} mice⁹⁷.

GPVI has been established as an attractive antithrombotic target^{70;86} also making its downstream signaling cascade interesting for inhibition. In addition, CLEC-2 was very recently identified by our group as an important platelet-activating receptor most probably required for recruitment and activation of further platelets in a growing thrombus⁹⁸. Therefore, the pathway involving Rac1 downstream of GPVI and CLEC-2 might be an attractive target for new anti-platelet agents to prevent thrombotic events. This was confirmed by the protection of *Rac1*-deficient mice from arterial thrombosis (Fig.17). Thus, inhibitors of Rac1⁹⁹ might be effective in the prophylaxis or treatment of ischemic cerebro- or cardiovascular diseases.

4.2 A complex phenotype dominated by increased secretion in mice lacking Cdc42 in platelets

In the present study, a knock-out approach (PF4-Cre/loxP) was used to investigate the effect of *Cdc42* deficiency on platelet function *in vitro* and *in vivo*. It was found that megakaryocyte- and platelet-specific deletion of the *Cdc42* gene resulted in mild thrombocytopenia, increased platelet size and, unexpectedly, increased secretion and a shortened platelet life span in mice. On the other hand, the herein presented results did not confirm the proposed major role of *Cdc42* for filopodia formation in platelets³².

The results of this study clearly show that *Cdc42* is neither required for platelet filopodia formation and full spreading on fibrinogen upon activation with thrombin (Fig. 19a,b/20b), nor for morphological changes under non-stimulating conditions

(Fig. 19c) or upon stimulation with ADP (not shown). This indicates the involvement of proteins other than Cdc42 in filopodia formation on fibrinogen under conditions of G-protein coupled signaling. This finding is in accordance with results from Czuchra *et al.* who - also using a genetic approach - have demonstrated that Cdc42 is dispensable for filopodia formation, migration, polarization and mitosis in embryonic fibroblasts⁵⁷. Recent data suggest the existence of Cdc42-independent mechanisms of filopodia formation, mainly involving the Rho GTPase Rif and LPR1^{55;56}. Thus, one of these proteins may act in filopodia formation in *Cdc42*^{-/-} platelets. Interestingly, studies of platelet ultrastructure revealed no differences in filopodia morphology between *Cdc42*^{-/-} and wild-type platelets (Fig. 20b,c), whereas filopodia induced by Rif and LPR1 were shown to have a longer and more hairy appearance than those induced by Cdc42. Clearly, further studies are required to investigate the signaling pathways that lead to agonist-induced filopodia formation in platelets.

Notably, *Cdc42*^{-/-} platelets displayed a clear defect in GPIb signaling-dependent filopodia formation induced by adhesion on vWF (Fig. 21a,b) which was most likely not caused by decreased GPIb expression levels since agglutination induced by botrocetin and human vWF was unaltered in the mutant cells (Figure 21c). This finding is intriguing since it establishes Cdc42 as a GPIb-specific downstream signaling molecule. A role of Cdc42 in platelet filopodia formation has been previously proposed downstream of the human platelet integrin $\alpha 6\beta 1$ using secramine A as a Cdc42 specific inhibitor³². It was found that secramine A also prevented the GPIb-dependent response (Nieswandt and Gachet, personal communication) but non-specific effects of this compound were suggested by its ability to induce shape change in resting platelets. The signaling pathway downstream of GPIb leading to filopodia formation remains to be fully characterized. Under the assay condition used in this study, which prevents signal amplification by the $\alpha IIb\beta 3$ integrin, ADP or TXA₂, the signaling response evoked by GPIb involves calcium mobilization from intracellular stores downstream of a Src kinase and PLC $\gamma 2$ ¹⁰⁰ (see also Fig. 2). These effectors are not restricted to GPIb signaling but also take part in GPVI and Fc receptor/ITAM-dependent activation, as demonstrated in this thesis (see chapter 3.1). An increased rather than decreased response of *Cdc42*^{-/-} platelets to CRP and collagen observed here reinforces the notion of a GPIb-restricted role of Cdc42 and indicates existence of a separate pathway unrelated to those induced by ITAM-coupled receptors. This hypothesis is consistent with reports

showing biochemical and functional interaction of Cdc42 with two known GPIb partners, filamin and 14-3-3^{101;102}.

Unexpectedly, *Cdc42*^{-/-} platelets displayed increased secretion in response to agonist stimulation, whereas integrin α IIb β 3 activation was slightly decreased (Figure 22/23). A significant increase in P-selectin expression despite unaltered protein content strongly indicates enhanced secretion of α granules in *Cdc42*^{-/-} platelets (Fig. 22/24a). In contrast, the observed strong increase of dense granule-dependent ATP release coincided with a significantly increased ADP/ATP content in the mutant platelets that may only partially be explained by their increased size since content and release of the dense granular mediator serotonin was not significantly altered (Fig. 23/24c,d). Thus, the increase in ADP/ATP content might contribute to the hyper-reactivity observed in aggregometry where released mediators accumulate and to a great extent reinforce platelet activation and secretion. However, Cdc42 may also have a direct function in the degranulation machinery as increased P-selectin exposure was observed also in flow cytometric studies (Fig. 22), where highly diluted platelet samples are analyzed under conditions that minimize the influence of released mediators on the activation state of the cells⁸².

The results of this study stand in contrast to a report by Pula *et al.*, who found that platelets treated with the Cdc42 inhibitor securamine A show a selective aggregation and adhesion defect in response to collagen¹⁰³. This discrepancy is difficult to explain at present but it might be related to limited specificity of the inhibitor. The observed increased secretion in *Cdc42*^{-/-} platelets stands in clear contrast to observations made in other cell types showing decreased exocytosis upon inhibition of Cdc42, including endothelial cells and mast cells^{63;65;66}. This indicates that Cdc42 might be able to fulfil multiple functions that may differ between cell types, however, methodological differences may as well account for the discrepant results. For the studies presented in this thesis, a direct genetic approach was used to delete Cdc42 expression/function *in vivo*, whereas all other here mentioned studies used cell culture systems and transfection models. Notably, Czuchra *et al.* showed that expression of dominant-negative Cdc42 in Cdc42-null cells most likely resulted in the inhibition of other Rho GTPases, thereby significantly influencing the observed phenotype⁵⁷. This finding would be in accordance with the observation by Hong-Geller *et al.* who indeed observed an unexplained decrease in exocytosis when overexpressing wild-type Cdc42 in RBL mast cells⁶⁵.

Cdc42^{-/-} platelets formed larger aggregates on collagen under flow *in vitro* (Fig. 26). Although this effect was significant it was surprisingly moderate suggesting that the amount of released granule content may not be the only determinant of thrombus growth under these conditions. In line with this observation, the recent analysis of mice lacking functional CLEC-2 revealed that this receptor plays a fundamental role in the activation of platelets in a growing aggregate/thrombus under flow⁹⁸ (see also section 3.1). Very similar to the results obtained by flow adhesion studies *in vitro*, thrombus formation in *Cdc42*^{-/-} mice was found to be significantly accelerated in an arterial injury model *in vivo* (Fig. 29). Considering the increased secretion observed in *Cdc42*^{-/-} platelets *in vitro* one might speculate that this effect was caused by the increased presence of platelet released thrombogenic factors at the site of injury. This notion would be in line with studies from other groups demonstrating the significance of degranulation-dependent release of platelet agonists, such as ADP and ATP, for thrombus formation under physiological conditions^{104;105}. Furthermore, the here presented results clearly show that effective thrombus formation can still take place under conditions of decreased circulating platelets numbers¹⁰⁶. In contrast to these observations, *Cdc42*-deficient mice displayed variable, but significantly prolonged bleeding times, clearly indicating impaired platelet plug formation (Fig. 28). Possibly, the impaired GPIb-dependent signaling observed in *Cdc42*^{-/-} platelets (Fig. 21a,b) contributed to this effect. Furthermore, decreased GPIb expression levels and decreased integrin α IIb β 3 activation in *Cdc42*^{-/-} platelets may also influence their function in this assay¹⁰⁷.

Cdc42^{-/-} platelets displayed a markedly decreased life span (Fig. 27). It is hypothesized that this effect was at least in part caused by increased clearing of the platelets, which would suggest a non-functional or pre-activated state of the cells under physiological conditions *in vivo*. In line with this hypothesis, the constant removal of such pre-activated *Cdc42*^{-/-} platelets might contribute to the thrombocytopenia in *Cdc42*-deficient animals. Furthermore, as shown by megakaryocyte studies, decreased proplatelet formation from *Cdc42*^{-/-} MKs also contributed to the decreased platelet counts in *Cdc42*^{-/-} animals.

The results presented here indicate a new regulatory role for *Cdc42* in platelet activatory/secretory events *in vitro* and *in vivo*. Importantly, the increased secretion of *Cdc42*^{-/-} platelets was not restricted to a specific agonist but occurred in response to G protein-, as well as ITAM-coupled agonists, indicating a general function of the

Cdc42 protein in platelet granule content organization and secretion. In line with this, the increased ADP/ATP content suggests that Cdc42 may be required for proper granule formation/packing during platelet production. Moreover, our results indicate that Cdc42 deficiency directly leads to enhanced secretion of α granules in platelets.

Currently, the exact role of the regulation of actin cytoskeleton in exocytotic events in platelets is controversial. Several studies using actin-disrupting agents supported a model in which the cytoskeleton in resting platelets may act as a barrier for granule release and that platelet activation leads to (partial) disrapture of actin filaments, thereby enabling degranulation¹⁰⁸. However, this model is questioned because of the risk of artefacts caused by actin-disrupting agents. To test a possible effect of Cdc42 deficiency on agonist-induced cytoskeletal rearrangements, the Cdc42 downstream effector cofilin was examined, a protein known to be involved in increasing actin turnover in its active dephosphorylated form⁹⁰. Unexpectedly, and in contrast to the currently proposed function of Cdc42¹⁰⁹, not a decrease, but a strong (approximately 2-fold) increase in the (inactive) phosphorylated cofilin form was found in resting *Cdc42*^{-/-} platelets as compared to controls (Fig. 30a,b). This finding is in accordance with a recent study showing increased cofilin phosphorylation in cortical neurons upon genetic Cdc42 deletion⁹¹. Thrombin- and CRP-induced dephosphorylation of cofilin occurred to a similar extent and with similar kinetics in wild-type and *Cdc42*^{-/-} platelets, although higher levels of the inactive, phosphorylated form of the protein were consistently detected in the mutant cells under all experimental conditions (Fig. 30c). Furthermore, similar levels of F-actin in resting and thrombin-activated *Cdc42*^{-/-} and wild-type platelets were observed (Fig. 37b), indicating that a reorganization rather than a disassembly of actin might be responsible for the cytoskeletal effects evoked by Cdc42 deficiency. Further studies are ongoing to determine the role of Cdc42 in actin turnover regulation during platelet degranulation.

In addition to actin remodeling, Cdc42 could also participate directly or indirectly in the exocytotic processes in platelets. Recently, it became evident that platelets possess a secretory machinery similar to that of other cell types^{110;111;112}. Thus, Cdc42 may be involved in signaling events during platelet exocytosis which may be of importance for rapid but controlled platelet degranulation upon activation.

Taken together, the results from this study have revealed multiple and novel roles for Cdc42 during platelet activation and granule organization/exocytosis, whereas its

proposed essential role for filopodia formation in the cells could not be confirmed, except under conditions of selective GPIb dependent activation. These findings point to Cdc42 and/or its downstream effector molecules as potential targets for the development of novel drugs for the regulation of intravascular platelet activation.

4.3 Rac1 and Cdc42 play redundant roles in megakaryocyte maturation and platelet formation

The results presented in the first two parts of this thesis focused on the effect of either Rac1 or Cdc42 deficiency on platelet function *in vitro* and *in vivo*. In the following, it was of interest to investigate the effect of deletion of both GTPases for platelet function. Furthermore, the impact of GTPase deficiency on platelet production from MKs was assessed.

As already mentioned, very little is known about the role of Rho GTPases and the actin cytoskeleton in MK maturation and platelet formation. Since Rac1 and Cdc42 have been shown to both induce activation of p21-activated kinase (PAK) isoforms and thus might share similar downstream signaling pathways^{92;113}, it was of interest to study a putative redundant role of the GTPases in platelet function and production. To study this, double-deficient mice were generated using the PF4-Cre/loxP system for MK studies and the Mx-Cre/loxP system for platelet studies. In parallel, the single-deficient animals generated by the PF4-Cre/loxP approach were also analyzed.

MK numbers were normal in spleen and bone marrow of *Rac1*^{-/-} mice (Fig 39). Furthermore, *Rac1*^{-/-} bone marrow MKs displayed no changes in ultrastructure and *in vitro* proplatelet formation from the mutant MKs was unaltered as compared to wild-type MKs (Fig. 40) resulting in normal platelet counts with unaltered life span in *Rac1*^{-/-} mice (Fig. 9c). These results confirm our and other studies^{33;44} that Rac1 is dispensable for MK maturation and platelet production.

So far, the role of Cdc42 during MK maturation and platelet production has not been directly addressed, although the GTPase was recently speculated to positively regulate proplatelet formation during late MK maturation²⁶. Indeed, in this study, a significant reduction in proplatelet formation from *Cdc42*^{-/-} MKs *in vitro* was observed (Fig. 40). *In situ* analysis of *Cdc42*^{-/-} MKs in bone marrow revealed partially reduced invagination of demarcation membranes and enlargement of proplatelet territories (Fig. 42/43). As a compensatory mechanism for decreased platelet production from

Cdc42^{-/-} MKs and the shortened life span of *Cdc42*^{-/-} platelets (Fig 27), MK numbers were highly increased in spleen and bone marrow of the mutant mice (Fig. 39). Thus, the results presented in this thesis clearly demonstrate a role for Cdc42 in late MK maturation, thereby significantly affecting platelet production and function as demonstrated by the study of *Cdc42*^{-/-} platelets.

Interestingly, the phenotype observed in *Cdc42*^{-/-} MKs was in many respects similar to MKs lacking the GPIIb β subunit of the GPIIb/IIIa complex¹¹⁴. Like *Cdc42*^{-/-} MKs, *GpiIb* β ^{-/-} MKs displayed normal ploidy and maturation, but less development of demarcation membranes and reduced proplatelet formation. Although GPIIb β deficiency had a more severe impact on platelet production and function one might speculate that Cdc42 may act as a downstream effector of GPIIb during megakaryocyte maturation and (pro)platelet formation. This hypothesis is supported by our observation that Cdc42 is involved in GPIIb signaling also in platelets (Fig. 21). Further studies are ongoing to resolve the signaling processes involved in Cdc42 activation and downstream signaling during MK maturation.

This study showed that already Cdc42 deficiency alone affected MK maturation and platelet production, although the resulting phenotype was relatively mild. On the other hand, Rac1 was dispensable for platelet production. In contrast, combined deletion of both GTPases resulted in normal MK ploidy but strongly reduced proplatelet formation *in vitro* (Fig. 41/40). Bone marrow MKs from *Rac1/Cdc42*^{-/-} mice exhibited dramatically reduced demarcation membrane invagination and proplatelet territory formation, indicating an important role of the GTPases in morphological rearrangements necessary for these processes (Fig. 42/43). Furthermore, Rac1 and Cdc42 seemed to be required for efficient granule synthesis and for the structural integrity of mature MKs as revealed by the partial absence of peripheral zones and loss of demarcation of *Rac1/Cdc42*^{-/-} MKs to surrounding cells *in situ*. A similar MK phenotype has been described recently using mice with MK- and platelet-restricted myosin IIA deficiency²⁷ confirming an important role of cytoskeletal rearrangements for proper MK maturation. Preliminary studies from our group on actin/tubulin dynamics in *Rac1/Cdc42*^{-/-} furthermore indicate increased presence of tubulin coils in the periphery and in proplatelets of double-mutant MKs, suggesting a role of the GTPases in microtubule organization during proplatelet formation. This hypothesis is in line with results from studies in fibroblasts and neurons^{28;115}. Abnormal tubulin

organisation was also observed by Strassel *et al.* in MKs lacking GPIIb/IIIa, further emphasizing a potential role of GTPase signaling downstream of GPIIb in MKs¹¹⁴.

As a result from defective (pro)platelet formation, *Rac1/Cdc42*^{-/-} animals displayed marked thrombocytopenia which was probably predominantly caused by decreased platelet production from *Rac1/Cdc42*^{-/-} MKs and by the constant clearing of non-functional platelets from the vascular system. Circulating *Rac1/Cdc42*^{-/-} platelets showed severely altered morphology and displayed multiple activation and functional defects resulting in defective hemostasis and *in vivo* thrombus formation (Fig. 32-38).

Taken together, the results presented here demonstrate that, whereas lack of either Rac1 or Cdc42 alone resulted in no or relatively mild effects on megakaryocyte maturation, platelet production and function, double deficiency of Rac1 and Cdc42 abrogated the maturation of MKs and thus the production of functional platelets. This demonstrates for the first time a functional redundancy of Rac1 and Cdc42 in the positive regulation of these processes. Together with the recently described role of RhoA as a negative regulator, these findings emphasize that differential signaling from Rho GTPases is significantly involved in MK maturation and platelet formation in mice.

4.4 Concluding remarks and outlook

The work presented here provides new insights into the role of the Rho GTPases Rac1 and Cdc42 for platelet function and their production from megakaryocytes using genetically modified mice.

In humans, mutations and/or deficiencies of Rho GTPases have not been described, most probably because such alterations would be associated with early lethality during embryogenesis. Importantly, this study points out that the mouse system bears several advantages for analysis of GTPase function. By the use of conditional knock-out mice an otherwise lethal phenotype is circumvented and gene deletion can be restricted to the desired cell type. Furthermore, side effects often occurring when using cellular overexpression systems or inhibitors for study of GTPase function are avoided by this method.

Further studies are planned in our laboratory to investigate the function of Rho GTPases not only in platelets and megakaryocytes, but also in cells of the immune

system. This includes the study of Rac1-deficient macrophages, as well as deeper analysis of the exact function of Cdc42 in megakaryocytes and platelets, focusing on its role in GPIb signaling. Together with the analysis of recently generated megakaryocyte- and platelet-specific RhoA knock-out mice, these studies will shed new light on the impact of GTPase signaling for cellular function.

5 REFERENCES

1. Savage, B., F. mus-Jacobs, and Z. M. Ruggeri. Specific synergy of multiple substrate-receptor interactions in platelet thrombus formation under flow. *Cell* 1998; 94:657-666.
2. Nieswandt, B., C. Brakebusch, W. Bergmeier, V. Schulte, D. Bouvard, R. Mokhtari-Nejad, T. Lindhout, J. W. Heemskerk, H. Zirngibl, and R. Fassler. Glycoprotein VI but not alpha2beta1 integrin is essential for platelet interaction with collagen. *EMBO J.* 2001;20:2120-2130.
3. Furie, B. C. and B. Furie. Tissue factor pathway vs. collagen pathway for in vivo platelet activation. *Blood Cells Mol.Dis.* 2006;36:135-138.
4. Offermanns, S. Activation of platelet function through G protein-coupled receptors. *Circ.Res.* 2006;99:1293-1304.
5. Varga-Szabo, D., I. Pleines, and B. Nieswandt. Cell adhesion mechanisms in platelets. *Arterioscler.Thromb.Vasc.Biol.* 2008;28:403-412.
6. Offermanns, S., C. F. Toombs, Y. H. Hu, and M. I. Simon. Defective platelet activation in G alpha(q)-deficient mice. *Nature* 1997;389:183-186.
7. Nieswandt, B. and S. P. Watson. Platelet-collagen interaction: is GPVI the central receptor? *Blood* 2003;102:449-461.
8. Suzuki-Inoue, K., G. L. Fuller, A. Garcia, J. A. Eble, S. Pohlmann, O. Inoue, T. K. Gartner, S. C. Hughan, A. C. Pearce, G. D. Laing, R. D. Theakston, E. Schweighoffer, N. Zitzmann, T. Morita, V. L. Tybulewicz, Y. Ozaki, and S. P. Watson. A novel Syk-dependent mechanism of platelet activation by the C-type lectin receptor CLEC-2. *Blood* 2006;107:542-549.
9. Watson, S. P., N. Asazuma, B. Atkinson, O. Berlanga, D. Best, R. Bobe, G. Jarvis, S. Marshall, D. Snell, M. Stafford, D. Tulasne, J. Wilde, P. Wonerow, and J. Frampton. The role of ITAM- and ITAM-coupled receptors in platelet activation by collagen. *Thromb.Haemost.* 2001;86:276-288.
10. Berridge, M. J., M. D. Bootman, and H. L. Roderick. Calcium signalling: dynamics, homeostasis and remodelling. *Nat.Rev.Mol.Cell Biol.* 2003;4:517-529.
11. Bird, G. S., O. Aziz, J. P. Lievremont, B. J. Wedel, M. Trebak, G. Vazquez, and J. W. Putney, Jr. Mechanisms of phospholipase C-regulated calcium entry. *Curr.Mol.Med.* 2004;4:291-301.
12. Ren, Q., S. Ye, and S. W. Whiteheart. The platelet release reaction: just when you thought platelet secretion was simple. *Curr.Opin.Hematol.* 2008;15:537-541.
13. White, J. G. and W. Krivit. Fine structural localization of adenosine triphosphatase in human platelets and other blood cells. *Blood* 1965;26:554-568.
14. White, J. G. and S. M. Burris. Morphometry of platelet internal contraction. *Am.J.Pathol.* 1984;115:412-417.
15. Pang, L., M. J. Weiss, and M. Poncz. Megakaryocyte biology and related disorders. *J.Clin.Invest* 2005;115:3332-3338.

16. Ogawa, M. Differentiation and proliferation of hematopoietic stem cells. *Blood* 1993;81:2844-2853.
17. Kaushansky, K. The molecular mechanisms that control thrombopoiesis. *J.Clin.Invest* 115:3339-3347.
18. Schulze, H. and R. A. Shivdasani. 2005. Mechanisms of thrombopoiesis. *J.Thromb.Haemost.* 2005;3:1717-1724.
19. Chang, Y., D. Bluteau, N. Debili, and W. Vainchenker. From hematopoietic stem cells to platelets. *J.Thromb.Haemost.* 2007;1:318-327.
20. Schulze, H., M. Korpál, J. Hurov, S. W. Kim, J. Zhang, L. C. Cantley, T. Graf, and R. A. Shivdasani. Characterization of the megakaryocyte demarcation membrane system and its role in thrombopoiesis. *Blood* 2006;107:3868-3875.
21. Italiano, J. E., Jr., S. Patel-Hett, and J. H. Hartwig. Mechanics of proplatelet elaboration. *J.Thromb.Haemost.* 2007;1:18-23.
22. Junt, T., H. Schulze, Z. Chen, S. Massberg, T. Goerge, A. Krueger, D. D. Wagner, T. Graf, J. E. Italiano, Jr., R. A. Shivdasani, and U. H. von Andrian. Dynamic visualization of thrombopoiesis within bone marrow. *Science* 2007;317:1767-1770.
23. Patel, S. R., J. L. Richardson, H. Schulze, E. Kahle, N. Galjart, K. Drabek, R. A. Shivdasani, J. H. Hartwig, and J. E. Italiano, Jr. Differential roles of microtubule assembly and sliding in proplatelet formation by megakaryocytes. *Blood* 2005.;106:4076-4085.
24. Richardson, J. L., R. A. Shivdasani, C. Boers, J. H. Hartwig, and J. E. Italiano, Jr. Mechanisms of organelle transport and capture along proplatelets during platelet production. *Blood* 2005;106:4066-4075.
25. Patel, S. R., J. H. Hartwig, and J. E. Italiano, Jr. The biogenesis of platelets from megakaryocyte proplatelets. *J.Clin.Invest* 2005;115:3348-3354.
26. Bluteau, D., L. Lordier, S. A. Di, Y. Chang, H. Raslova, N. Debili, and W. Vainchenker. Regulation of megakaryocyte maturation and platelet formation. *J.Thromb.Haemost.* 2009;1:227-234.
27. Eckly, A., C. Strassel, M. Freund, J. P. Cazenave, F. Lanza, C. Gachet, and C. Leon. Abnormal megakaryocyte morphology and proplatelet formation in mice with megakaryocyte-restricted MYH9 inactivation. *Blood* 2009;113:3182-3189.
28. Jaffe, A. B. and A. Hall. Rho GTPases: biochemistry and biology. *Annu.Rev.Cell Dev.Biol.* 2005;21:247-269.
29. Heasman, S. J. and A. J. Ridley. Mammalian Rho GTPases: new insights into their functions from in vivo studies. *Nat.Rev.Mol.Cell Biol.* 2008;9:690-701.
30. Moers, A., N. Wettschureck, S. Gruner, B. Nieswandt, and S. Offermanns. Unresponsiveness of platelets lacking both Galpha(q) and Galpha(13). Implications for collagen-induced platelet activation. *J.Biol.Chem.* 2004;279:45354-45359.
31. Huang, J. S., L. Dong, T. Kozasa, and G. C. Le Breton. Signaling through G(alpha)13 switch region I is essential for protease-activated receptor 1-mediated human platelet shape change, aggregation, and secretion. *J.Biol.Chem.* 2007;282:10210-10222.

32. Chang, J. C., H. H. Chang, C. T. Lin, and S. J. Lo. The integrin alpha6beta1 modulation of PI3K and Cdc42 activities induces dynamic filopodium formation in human platelets. *J.Biomed.Sci.* 2005;12:881-898.
33. McCarty, O. J., M. K. Larson, J. M. Auger, N. Kalia, B. T. Atkinson, A. C. Pearce, S. Ruf, R. B. Henderson, V. L. Tybulewicz, L. M. Machesky, and S. P. Watson. Rac1 is essential for platelet lamellipodia formation and aggregate stability under flow. *J.Biol.Chem.* 2005;280:39474-39484.
34. Sugihara, K., N. Nakatsuji, K. Nakamura, K. Nakao, R. Hashimoto, H. Otani, H. Sakagami, H. Kondo, S. Nozawa, A. Aiba, and M. Katsuki. Rac1 is required for the formation of three germ layers during gastrulation. *Oncogene* 1998;17:3427-3433.
35. Cancelas, J. A., A. W. Lee, R. Prabhakar, K. F. Stringer, Y. Zheng, and D. A. Williams. Rac GTPases differentially integrate signals regulating hematopoietic stem cell localization. *Nat.Med.* 2005;11:886-891.
36. Walmsley, M. J., S. K. Ooi, L. F. Reynolds, S. H. Smith, S. Ruf, A. Mathiot, L. Vanes, D. A. Williams, M. P. Cancro, and V. L. Tybulewicz. Critical roles for Rac1 and Rac2 GTPases in B cell development and signaling. *Science* 2003;302:459-462.
37. Guo, F., J. A. Cancelas, D. Hildeman, D. A. Williams, and Y. Zheng. Rac GTPase isoforms Rac1 and Rac2 play a redundant and crucial role in T-cell development. *Blood* 2008;112:1767-1775.
38. Dumont, C., A. Corsoni-Tadrzak, S. Ruf, B. J. de, A. Williams, M. Turner, D. Kioussis, and V. L. Tybulewicz. Rac GTPases play critical roles in early T-cell development. *Blood* 2009;113:3990-3998.
39. Azim, A. C., K. Barkalow, J. Chou, and J. H. Hartwig. Activation of the small GTPases, rac and cdc42, after ligation of the platelet PAR-1 receptor. *Blood* 2000;95:959-964.
40. Gratacap, M. P., B. Payrastre, B. Nieswandt, and S. Offermanns. Differential regulation of Rho and Rac through heterotrimeric G-proteins and cyclic nucleotides. *J.Biol.Chem.* 2001;276:47906-47913.
41. Hartwig, J. H., G. M. Bokoch, C. L. Carpenter, P. A. Janmey, L. A. Taylor, A. Toker, and T. P. Stossel. Thrombin receptor ligation and activated Rac uncap actin filament barbed ends through phosphoinositide synthesis in permeabilized human platelets. *Cell* 1995;82:643-653.
42. Soulet, C., S. Gendreau, K. Missy, V. Benard, M. Plantavid, and B. Payrastre. Characterisation of Rac activation in thrombin- and collagen-stimulated human blood platelets. *FEBS Lett.* 2001;507:253-258.
43. Miranti, C. K., L. Leng, P. Maschberger, J. S. Brugge, and S. J. Shattil. Identification of a novel integrin signaling pathway involving the kinase Syk and the guanine nucleotide exchange factor Vav1. *Curr.Biol.* 1998;8:1289-1299.
44. Akbar, H., J. Kim, K. Funk, J. A. Cancelas, X. Shang, L. Chen, J. F. Johnson, D. A. Williams, and Y. Zheng. Genetic and pharmacologic evidence that Rac1 GTPase is involved in regulation of platelet secretion and aggregation. *J.Thromb.Haemost.* 2007;5:1747-1755.
45. Suzuki-Inoue, K., Y. Yatomi, N. Asazuma, M. Kainoh, T. Tanaka, K. Satoh, and Y. Ozaki. Rac, a small guanosine triphosphate-binding protein, and p21-activated kinase

- are activated during platelet spreading on collagen-coated surfaces: roles of integrin alpha(2)beta(1). *Blood* 2001;98:3708-3716.
46. Piechulek, T., T. Rehlen, C. Walliser, P. Vatter, B. Moepps, and P. Gierschik. Isozyme-specific stimulation of phospholipase C-gamma2 by Rac GTPases. *J.Biol.Chem.* 2005;280:38923-38931.
 47. Etienne-Manneville, S. and A. Hall. Rho GTPases in cell biology. *Nature* 2002;420:629-635.
 48. Chen, F., L. Ma, M. C. Parrini, X. Mao, M. Lopez, C. Wu, P. W. Marks, L. Davidson, D. J. Kwiatkowski, T. Kirchhausen, S. H. Orkin, F. S. Rosen, B. J. Mayer, M. W. Kirschner, and F. W. Alt. Cdc42 is required for PIP(2)-induced actin polymerization and early development but not for cell viability. *Curr.Biol.* 2000;10:758-765.
 49. Yang, L., L. Wang, T. A. Kalfa, J. A. Cancelas, X. Shang, S. Pushkaran, J. Mo, D. A. Williams, and Y. Zheng. Cdc42 critically regulates the balance between myelopoiesis and erythropoiesis. *Blood* 2007;110:3853-3861.
 50. Guo, F., C. S. Velu, H. L. Grimes, and Y. Zheng. Rho GTPase Cdc42 is essential for B-lymphocyte development and activation. *Blood* 2009;114:2909-2916.
 51. Szczur, K., Y. Zheng, and M. D. Filippi. The small Rho GTPase Cdc42 regulates neutrophil polarity via CD11b integrin signaling. *Blood.* 2009;114:4527-37
 52. Allen, W. E., D. Zicha, A. J. Ridley, and G. E. Jones. A role for Cdc42 in macrophage chemotaxis. *J.Cell Biol.* 1998;141:1147-1157.
 53. Park, H. and D. Cox. Cdc42 regulates Fc gamma receptor-mediated phagocytosis through the activation and phosphorylation of Wiskott-Aldrich syndrome protein (WASP) and neural-WASP. *Mol.Biol.Cell* 2009;20:4500-4508.
 54. Weber, K. S., L. B. Klickstein, P. C. Weber, and C. Weber. Chemokine-induced monocyte transmigration requires cdc42-mediated cytoskeletal changes. *Eur.J.Immunol.* 1998;28:2245-2251.
 55. Pellegrin, S. and H. Mellor. The Rho family GTPase Rif induces filopodia through mDia2. *Curr.Biol.* 2005;15:129-133.
 56. Sigal, Y. J., O. A. Quintero, R. E. Cheney, and A. J. Morris. Cdc42 and ARP2/3-independent regulation of filopodia by an integral membrane lipid-phosphatase-related protein. *J.Cell Sci.* 2007;120:340-352.
 57. Czuchra, A., X. Wu, H. Meyer, H. J. van, T. Schroeder, R. Geffers, K. Rottner, and C. Brakebusch. Cdc42 is not essential for filopodium formation, directed migration, cell polarization, and mitosis in fibroblastoid cells. *Mol.Biol.Cell* 2005;16:4473-4484.
 58. Malacombe, M., M. Ceridono, V. Calco, S. Chasserot-Golaz, P. S. McPherson, M. F. Bader, and S. Gasman. Intersectin-1L nucleotide exchange factor regulates secretory granule exocytosis by activating Cdc42. *EMBO J.* 2006;25:3494-3503.
 59. Momboisse, F., S. Ory, V. Calco, M. Malacombe, M. F. Bader, and S. Gasman. Calcium-regulated exocytosis in neuroendocrine cells: intersectin-1L stimulates actin polymerization and exocytosis by activating Cdc42. *Ann.N.Y.Acad.Sci.* 2009;1152:209-214.

60. Nevins, A. K. and D. C. Thurmond. Glucose regulates the cortical actin network through modulation of Cdc42 cycling to stimulate insulin secretion. *Am.J.Physiol Cell Physiol* 2003;285:C698-C710.
61. Nevins, A. K. and D. C. Thurmond. A direct interaction between Cdc42 and vesicle-associated membrane protein 2 regulates SNARE-dependent insulin exocytosis. *J.Biol.Chem.* 2005;280:1944-1952.
62. Wang, Z., E. Oh, and D. C. Thurmond. Glucose-stimulated Cdc42 signaling is essential for the second phase of insulin secretion. *J.Biol.Chem.* 2007;282:9536-9546.
63. Klarenbach, S. W., A. Chipiuk, R. C. Nelson, M. D. Hollenberg, and A. G. Murray. Differential actions of PAR2 and PAR1 in stimulating human endothelial cell exocytosis and permeability: the role of Rho-GTPases. *Circ.Res.* 2003;92:272-278.
64. Hobert, M. E., K. A. Sands, R. J. Mrsny, and J. L. Madara. Cdc42 and Rac1 regulate late events in *Salmonella typhimurium*-induced interleukin-8 secretion from polarized epithelial cells. *J.Biol.Chem.* 2002;277:51025-51032.
65. Hong-Geller, E. and R. A. Cerione. Cdc42 and Rac stimulate exocytosis of secretory granules by activating the IP(3)/calcium pathway in RBL-2H3 mast cells. *J.Cell Biol.* 2000;148:481-494.
66. Hong-Geller, E., D. Holowka, R. P. Siraganian, B. Baird, and R. A. Cerione. Activated Cdc42/Rac reconstitutes Fcepsilon RI-mediated Ca²⁺ mobilization and degranulation in mutant RBL mast cells. *Proc.Natl.Acad.Sci.U.S.A* 2001;98:1154-1159.
67. Tiwari, S., J. E. Italiano, Jr., D. C. Barral, E. H. Mules, E. K. Novak, R. T. Swank, M. C. Seabra, and R. A. Shivdasani. A role for Rab27b in NF-E2-dependent pathways of platelet formation. *Blood* 2003;102:3970-3979.
68. Chang, Y., F. Aurade, F. Larbret, Y. Zhang, J. P. Le Couedic, L. Momeux, J. Larghero, J. Bertoglio, F. Louache, E. Cramer, W. Vainchenker, and N. Debili. Proplatelet formation is regulated by the Rho/ROCK pathway. *Blood* 2007;109:4229-4236.
69. Chen, Z., O. Naveiras, A. Balduini, A. Mammoto, M. A. Conti, R. S. Adelstein, D. Ingber, G. Q. Daley, and R. A. Shivdasani. The May-Hegglin anomaly gene MYH9 is a negative regulator of platelet biogenesis modulated by the Rho-ROCK pathway. *Blood* 2007;110:171-179.
70. Nieswandt, B., V. Schulte, W. Bergmeier, R. Mokhtari-Nejad, K. Rackebrandt, J. P. Cazenave, P. Ohlmann, C. Gachet, and H. Zirngibl. Long-term antithrombotic protection by in vivo depletion of platelet glycoprotein VI in mice. *J.Exp.Med.* 2001;193:459-469.
71. Nieswandt, B., W. Bergmeier, K. Rackebrandt, J. E. Gessner, and H. Zirngibl. Identification of critical antigen-specific mechanisms in the development of immune thrombocytopenic purpura in mice. *Blood* 2000;96:2520-2527.
72. Bergmeier, W., V. Schulte, G. Brockhoff, U. Bier, H. Zirngibl, and B. Nieswandt. Flow cytometric detection of activated mouse integrin alphaIIb beta3 with a novel monoclonal antibody. *Cytometry* 2002;48:80-86.

73. Chrostek, A., X. Wu, F. Quondamatteo, R. Hu, A. Sanecka, C. Niemann, L. Langbein, I. Haase, and C. Brakebusch. Rac1 is crucial for hair follicle integrity but is not essential for maintenance of the epidermis. *Mol. Cell Biol.* 2006;26:6957-6970.
74. Wu, X., F. Quondamatteo, T. Lefever, A. Czuchra, H. Meyer, A. Chrostek, R. Paus, L. Langbein, and C. Brakebusch. Cdc42 controls progenitor cell differentiation and beta-catenin turnover in skin. *Genes Dev.* 2006;20:571-585.
75. Kuhn, R., F. Schwenk, M. Aguet, and K. Rajewsky. Inducible gene targeting in mice. *Science* 1995;269:1427-1429.
76. Tiedt, R., T. Schomber, H. Hao-Shen, and R. C. Skoda. Pf4-Cre transgenic mice allow the generation of lineage-restricted gene knockouts for studying megakaryocyte and platelet function in vivo. *Blood* 2007;109:1503-1506.
77. Shivdasani, R. A. and H. Schulze. Culture, expansion, and differentiation of murine megakaryocytes. *Curr. Protoc. Immunol.* 2005;Chapter 22:Unit.
78. Gajewski, A. and G. Krohne. Subcellular distribution of the Xenopus p58/lamin B receptor in oocytes and eggs. *J. Cell Sci.* 1999;112 (Pt 15):2583-2596.
79. Nieswandt, B., M. Moser, I. Pleines, D. Varga-Szabo, S. Monkley, D. Critchley, and R. Fassler. Loss of talin1 in platelets abrogates integrin activation, platelet aggregation, and thrombus formation in vitro and in vivo. *J. Exp. Med.* 2007;204:3113-3118.
80. Pleines, I., M. Elvers, A. Strehl, M. Pozgajova, D. Varga-Szabo, F. May, A. Chrostek-Grashoff, C. Brakebusch, and B. Nieswandt. Rac1 is essential for phospholipase C-gamma2 activation in platelets. *Pflugers Arch.* 2009;457:1173-1185.
81. Fuller, G. L., J. A. Williams, M. G. Tomlinson, J. A. Eble, S. L. Hanna, S. Pohlmann, K. Suzuki-Inoue, Y. Ozaki, S. P. Watson, and A. C. Pearce. The C-type lectin receptors CLEC-2 and Dectin-1, but not DC-SIGN, signal via a novel YXXL-dependent signaling cascade. *J. Biol. Chem.* 2007;282:12397-12409.
82. Nieswandt, B., V. Schulte, A. Zywietz, M. P. Gratacap, and S. Offermanns. Costimulation of Gi- and G12/G13-mediated signaling pathways induces integrin alpha IIb beta 3 activation in platelets. *J. Biol. Chem.* 2002;277:39493-39498.
83. Moers, A., B. Nieswandt, S. Massberg, N. Wettschureck, S. Gruner, I. Konrad, V. Schulte, B. Aktas, M. P. Gratacap, M. I. Simon, M. Gawaz, and S. Offermanns. G13 is an essential mediator of platelet activation in hemostasis and thrombosis. *Nat. Med.* 2003;9:1418-1422.
84. Heemskerk, J. W., W. M. Vuist, M. A. Feijge, C. P. Reutelingsperger, and T. Lindhout. Collagen but not fibrinogen surfaces induce bleb formation, exposure of phosphatidylserine, and procoagulant activity of adherent platelets: evidence for regulation by protein tyrosine kinase-dependent Ca²⁺ responses. *Blood* 1997;90:2615-2625.
85. Gruner, S., M. Prostredna, B. Aktas, A. Moers, V. Schulte, T. Krieg, S. Offermanns, B. Eckes, and B. Nieswandt. Anti-glycoprotein VI treatment severely compromises hemostasis in mice with reduced alpha2beta1 levels or concomitant aspirin therapy. *Circulation* 2004;110:2946-2951.
86. Massberg, S., M. Gawaz, S. Gruner, V. Schulte, I. Konrad, D. Zohlnhofer, U. Heinzmann, and B. Nieswandt. A crucial role of glycoprotein VI for platelet recruitment to the injured arterial wall in vivo. *J. Exp. Med.* 2003;197:41-49.

87. Gruner, S., M. Prostredna, M. Koch, Y. Miura, V. Schulte, S. M. Jung, M. Moroi, and B. Nieswandt. Relative antithrombotic effect of soluble GPVI dimer compared with anti-GPVI antibodies in mice. *Blood* 2005;105:1492-1499.
88. Pozgajova, M., U. J. Sachs, L. Hein, and B. Nieswandt. Reduced thrombus stability in mice lacking the alpha2A-adrenergic receptor. *Blood* 2006;108:510-514.
89. Yuan, Y., S. Kulkarni, P. Ulsemer, S. L. Cranmer, C. L. Yap, W. S. Nesbitt, I. Harper, N. Mistry, S. M. Dopheide, S. C. Hughan, D. Williamson, S. C. de la, H. H. Salem, F. Lanza, and S. P. Jackson. The von Willebrand factor-glycoprotein Ib/V/IX interaction induces actin polymerization and cytoskeletal reorganization in rolling platelets and glycoprotein Ib/V/IX-transfected cells. *J.Biol.Chem.* 1999;274:36241-36251.
90. Bamburg, J. R. Proteins of the ADF/cofilin family: essential regulators of actin dynamics. *Annu.Rev.Cell Dev.Biol.* 1999;15:185-230.
91. Garvalov, B. K., K. C. Flynn, D. Neukirchen, L. Meyn, N. Teusch, X. Wu, C. Brakebusch, J. R. Bamburg, and F. Bradke. Cdc42 regulates cofilin during the establishment of neuronal polarity. *J.Neurosci.* 2007;27:13117-13129.
92. Vidal, C., B. Geny, J. Melle, M. Jandrot-Perrus, and M. Fontenay-Roupie. Cdc42/Rac1-dependent activation of the p21-activated kinase (PAK) regulates human platelet lamellipodia spreading: implication of the cortical-actin binding protein cortactin. *Blood* 2002;100:4462-4469.
93. Thodeti, C. K., R. Massoumi, L. Bindslev, and A. Sjolander. Leukotriene D4 induces association of active RhoA with phospholipase C-gamma1 in intestinal epithelial cells. *Biochem.J.* 2002;365:157-163.
94. Chang, J. S., H. Seok, T. K. Kwon, D. S. Min, B. H. Ahn, Y. H. Lee, J. W. Suh, J. W. Kim, S. Iwashita, A. Omori, S. Ichinose, O. Numata, J. K. Seo, Y. S. Oh, and P. G. Suh. Interaction of elongation factor-1alpha and pleckstrin homology domain of phospholipase C-gamma 1 with activating its activity. *J.Biol.Chem.* 2002;277:19697-19702.
95. Guidetti, G. F., B. Bernardi, A. Consonni, P. Rizzo, C. Gruppi, C. Balduini, and M. Torti. Integrin alpha2beta1 induces phosphorylation-dependent and phosphorylation-independent activation of phospholipase Cgamma2 in platelets: role of Src kinase and Rac GTPase. *J.Thromb.Haemost.* 2009;7:1200-1206.
96. Kauffenstein, G., W. Bergmeier, A. Eckly, P. Ohlmann, C. Leon, J. P. Cazenave, B. Nieswandt, and C. Gachet. The P2Y(12) receptor induces platelet aggregation through weak activation of the alpha(IIb)beta(3) integrin--a phosphoinositide 3-kinase-dependent mechanism. *FEBS Lett.* 2001;505:281-290.
97. Nonne, C., N. Lenain, B. Hechler, P. Mangin, J. P. Cazenave, C. Gachet, and F. Lanza. Importance of platelet phospholipase Cgamma2 signaling in arterial thrombosis as a function of lesion severity. *Arterioscler.Thromb.Vasc.Biol.* 2005;25:1293-1298.
98. May, F., I. Hagedorn, I. Pleines, M. Bender, T. Vogtle, J. Eble, M. Elvers, and B. Nieswandt. CLEC-2 is an essential platelet-activating receptor in hemostasis and thrombosis. *Blood* 2009;114:3464-3472.
99. Nassar, N., J. Cancelas, J. Zheng, D. A. Williams, and Y. Zheng. Structure-function based design of small molecule inhibitors targeting Rho family GTPases. *Curr.Top.Med.Chem.* 2006;6:1109-1116.

100. Mangin, P., Y. Yuan, I. Goncalves, A. Eckly, M. Freund, J. P. Cazenave, C. Gachet, S. P. Jackson, and F. Lanza. Signaling role for phospholipase C gamma 2 in platelet glycoprotein Ib alpha calcium flux and cytoskeletal reorganization. Involvement of a pathway distinct from FcR gamma chain and Fc gamma RIIA. *J.Biol.Chem.* 2003;278:32880-32891.
101. Ohta, Y., N. Suzuki, S. Nakamura, J. H. Hartwig, and T. P. Stossel. The small GTPase RalA targets filamin to induce filopodia. *Proc.Natl.Acad.Sci.U.S.A* 1999;96:2122-2128.
102. Bialkowska, K., Y. Zaffran, S. C. Meyer, and J. E. Fox. 14-3-3 zeta mediates integrin-induced activation of Cdc42 and Rac. Platelet glycoprotein Ib-IX regulates integrin-induced signaling by sequestering 14-3-3 zeta. *J.Biol.Chem.* 2003;278:33342-33350.
103. Pula, G. and A. W. Poole. Critical roles for the actin cytoskeleton and cdc42 in regulating platelet integrin alpha2beta1. *Platelets.* 2008;19:199-210.
104. Remijn, J. A., Y. P. Wu, E. H. Jeninga, M. J. IJsseldijk, W. G. van, P. G. de Groot, J. J. Sixma, A. T. Nurden, and P. Nurden. Role of ADP receptor P2Y(12) in platelet adhesion and thrombus formation in flowing blood. *Arterioscler.Thromb.Vasc.Biol.* 2002;22:686-691.
105. Konopatskaya, O., K. Gilio, M. T. Harper, Y. Zhao, J. M. Cosemans, Z. A. Karim, S. W. Whiteheart, J. D. Molkenkin, P. Verkade, S. P. Watson, J. W. Heemskerk, and A. W. Poole. PKCalpha regulates platelet granule secretion and thrombus formation in mice. *J.Clin.Invest* 2009;119:399-407.
106. Grosse, J., A. Braun, D. Varga-Szabo, N. Beyersdorf, B. Schneider, L. Zeitlmann, P. Hanke, P. Schropp, S. Muhlstedt, C. Zorn, M. Huber, C. Schmittwolf, W. Jagla, P. Yu, T. Kerkau, H. Schulze, M. Nehls, and B. Nieswandt. An EF hand mutation in Stim1 causes premature platelet activation and bleeding in mice. *J.Clin.Invest* 2007;117:3540-3550.
107. Scarborough, R. M., N. S. Kleiman, and D. R. Phillips. Platelet glycoprotein IIb/IIIa antagonists. What are the relevant issues concerning their pharmacology and clinical use? *Circulation* 1999;100:437-444.
108. Flaumenhaft, R., J. R. Dilks, N. Rozenvayn, R. A. Monahan-Earley, D. Feng, and A. M. Dvorak. The actin cytoskeleton differentially regulates platelet alpha-granule and dense-granule secretion. *Blood* 2005;105:3879-3887.
109. Wang, W., R. Eddy, and J. Condeelis. The cofilin pathway in breast cancer invasion and metastasis. *Nat.Rev.Cancer* 2007;7:429-440.
110. Flaumenhaft, R., B. Furie, and B. C. Furie. Alpha-granule secretion from alpha-toxin permeabilized, MgATP-exposed platelets is induced independently by H⁺ and Ca²⁺. *J.Cell Physiol* 1999;179:1-10.
111. Reed, G. L., M. L. Fitzgerald, and J. Polgar. Molecular mechanisms of platelet exocytosis: insights into the "secrete" life of thrombocytes. *Blood* 2000;96:3334-3342.
112. Polgar, J., S. H. Chung, and G. L. Reed. Vesicle-associated membrane protein 3 (VAMP-3) and VAMP-8 are present in human platelets and are required for granule secretion. *Blood* 2002;100:1081-1083.

113. Edwards, D. C., L. C. Sanders, G. M. Bokoch, and G. N. Gill. Activation of LIM-kinase by Pak1 couples Rac/Cdc42 GTPase signalling to actin cytoskeletal dynamics. *Nat. Cell Biol.* 1999;1:253-259.
114. Strassel, C., A. Eckly, C. Leon, C. Petitjean, M. Freund, J. P. Cazenave, C. Gachet, and F. Lanza. Intrinsic impaired proplatelet formation and microtubule coil assembly of megakaryocytes in a mouse model of Bernard-Soulier syndrome. *Haematologica* 2009;94:800-810.
115. Georges, P. C., N. M. Hadzimichalis, E. S. Sweet, and B. L. Firestein. The yin-yang of dendrite morphology: unity of actin and microtubules. *Mol. Neurobiol.* 2008;38:270-284.

6 APPENDIX

Abbreviations

aa	amino acid
AC	adenylate cyclase
ADP	adenosine diphosphate
APS	ammonium peroxodisulphat
ARP	actin-related protein
ATP	adenosine triphosphate
BFU	burst-forming units
BSA	bovine serum albumin
°C	degree Celsius
CFSE	carboxyfluorescein succinimidyl ester
CFU	colony-forming units
CLEC-2	C-type lectin-like receptor 2
$[Ca^{2+}]_i$	intracellular calcium concentration
cm ²	square centimetre
CRP	collagen-related peptide
CVX	convulxin
DAG	diacylglycerol
ddH ₂ O	double-distilled water
DIC	differential interference contrast
DMEM	Dulbecco/Vogt Modified Eagle's Minimal Essential Medium
DMS	demarcation membrane system
E	embryonic day
ECL	enhanced Chemiluminescence
ECM	extracellular matrix
EDTA	ethylenediaminetetraacetic acid
ELISA	enzyme-linked immuno absorbance assay
<i>et al.</i>	<i>et alteri</i>
F-actin	filamentous actin
f.c.	final concentration
Fc	Fragment crystallisable
FcR	Fc receptor
FCS	fetal calf (bovine) serum
Fg	fibrinogen
Fig.	figure
FITC	fluorescein isothiocyanate
FSC	foreward scatter
g	gramme
GAP	GTPase-activating protein
GATA	globin transcription factor
GAP	GTPase-activating protein
GDP	guanosine diphosphate
GEF	guanine nucleotide exchange factor
GM-SCF	granulocyte macrophage colony-stimulating factor
GP	glycoprotein

GPCR	G protein-coupled receptor
GTP	guanosine triphosphate
h	hour(s)
HCl	hydrogen chloride
HPLC	high- performance liquid chromatography
HRP	horseradish peroxidase
HSC	hematopoietic stem cell
H ₂ O	water
IFI	integrated fluorescence intensity
Ig	immunoglobulin
IL	interleukin
IMDM	Iscove's Modified Dulbecco's Medium
IP	immunoprecipitation
IP ₃	inositol 1,4,5-trisphosphate
IRSp53	insulin-receptor substrate p53
ITAM	immunoreceptor tyrosine-based activation motif
kb	kilo base pair
kDa	kilo Dalton
l	litre
LAT	linker for activation of T-cells
LIMK	LIM kinase
LPR1	lipid-phosphatase-related protein-1
M	molar
MFI	mean fluorescence intensity
min	minute(s)
MK	megakaryocyte
ml	millilitre
MLC	myosin light chain
mm	millimetre
μ	micro
NaCl	sodium chloride
NaOH	sodium hydroxide
NF-E2	nuclear factor (erythroid-derived 2)
OD	optical density
o/n	overnight
PAA	polyacrylamide
PAK	Ser/Thr p21-activated kinase
PBS	phosphate buffered saline
PCR	polymerase chain reaction
PE	phycoerythrin
PF4	platelet factor 4
PH	pleckstrin homology
PI	propidium iodide
PIP ₂	phosphatidyinositol-4,5-bisphosphate
PI-3-K	phosphoinositide-3-kinase
PKC	proteinkinase C
PL (C)	phospholipase (C)
PMA	phorbol 12 myristate 13 acetate
PPF	proplatelet formation
pI-pC	polyinosinic-polycytidylic acid
PCR	polymerase chain reaction

prp	platelet-rich plasma
PT	proplatelet territory
PVDF	polyvinylidene difluoride
PZ	peripheral zone
RC	rhodocytin
Rif	Rho in filopodia
rpm	rounds per minute
RT	room temperature
s	second(s)
SD	standard deviation
SDF	stromal cell-derived factor
SDS	sodium dodecyl sulfate
SDS-PAGE	sodium dodecyl sulfate polyacrylamide gel electrophoresis
SEM	scanning electron microscopy
SLP-76	Src-homology 2 domain-containing leukocyte-specific phospho-protein of 76 kDa
SOCE	store-operated Ca ²⁺ entry
SSC	sideward scatter
Syk	spleen tyrosine kinase
TAE	TRIS acetate EDTA buffer
TE	TRIS EDTA buffer
TEM	transmission electron microscopy
TF	tissue factor
TPO	thrombopoietin
TRIS	trishydroxymethylaminomethane
TxA ₂	thromboxane A ₂
U	units
vWF	von Willebrand factor
WASP	Wiscott-Aldrich syndrome protein
WAVE	WASP family verprolin-honologous protein
wt	wild-type
x g	acceleration of gravity (9.81 m/ s ²)

Curriculum Vitae

Name	Irina Pleines
Date of birth	
Place of birth	
Nationality	German

School education

1985-1998	primary, secondary and high school, Witzenhausen
1998	German high school diploma

University education

1998-2004	Faculty of Biology, University of Würzburg, Faculty of Biology, University of Barcelona, and Faculty of Medicine, University of Freiburg i. Brsg.
2004 (graduation)	Diploma in biology (Dipl. Biol.) at the University of Würzburg

Postgraduate education

2006-now	PhD student in the group of Prof. Dr. Bernhard Nieswandt, Chair of Vascular Medicine and Rudolf-Virchow-Center for Experimental Biomedicine (Julius-Maximilians Universität Würzburg)
----------	---

Würzburg,

Acknowledgements

The work presented here was accomplished at the Chair of Vascular Medicine and the Rudolf Virchow Center, DFG Research Center for Experimental Biomedicine, University of Würzburg, in the group of Prof. Bernhard Nieswandt.

During the period of my PhD project (January 2006 - December 2009), many people helped and supported me. Therefore I would like to thank:

- My supervisor, Prof. Bernhard Nieswandt, for giving me the opportunity to work in his laboratory and for his great ideas and support. Especially I would like to thank him for introducing me to the scientific community and for allowing me to present my work at various international conferences, which enabled me to gain important experience for my future career.
- Prof. Georg Krohne, for the pleasant and fruitful collaboration during my PhD and for reviewing my thesis.
- Prof. Ulrich Walter, for helpful discussions and for reviewing my thesis.
- My colleagues and friends Alejandro Berna Erro, Frauke May and Ina Hagedorn for their support and for carefully reading my thesis.
- My sister Thekla for carefully reading my thesis.
- Margitta Elvers for supporting me in the good and the bad times of the projects.
- Sylvia Hengst for her kind help in resolving technical problems.
- All external collaboration partners for introducing me into new techniques and for important advice.
- All other members of the Nieswandt Lab, who have not been mentioned by name, for their support, the helpful discussions, and for the good atmosphere in the group.
- Finally, and most importantly, I would like to thank my family and Martin for their everlasting encouragement and support.

Publications

Articles

Pleines I, Eckly A, Elvers M, Hagedorn I, Eliautou S, Bender M, Wu X, Lanza F, Gachet G, Brakebusch C, Nieswandt B. A complex phenotype dominated by increased secretion in mice lacking Cdc42 in platelets. *Blood*. 2010. In press.

Pleines I, Elvers M, Strehl A, Pozgajova M, Varga-Szabo D, May F, Chrostek-Grashoff A, Brakebusch C, Nieswandt B. Rac1 is essential for phospholipase C-gamma2 activation in platelets. *Pflugers Arch*. 2009;457(5):1173-85.

Elvers M, Pozgaj R, **Pleines I**, May F, Kuijpers M J E, Heemskerk J, Yu P, Nieswandt B. Platelet hyperreactivity and a prothrombotic phenotype in mice with a gain-of-function mutation in phospholipase C γ 2. *J Thromb Haemost*. In revision.

May F, Hagedorn I, **Pleines I**, Bender M, Vögtle T, Eble J, Elvers M, Nieswandt B. CLEC-2 is an essential platelet-activating receptor in hemostasis and thrombosis. *Blood*. 2009;114(16):3464-72.

Schröder J, Lüllmann-Rauch R, Himmerkus N, **Pleines I**, Nieswandt B, Orinska Z, Koch-Nolte F, Schröder B, Bleich M, Saftig P. Deficiency of the tetraspanin CD63 is associated with kidney pathology but normal lysosomal function. *Mol Cell Biol*. 2009;29(4):1083-94.

Braun A, Varga-Szabo D, Kleinschnitz C, **Pleines I**, Bender M, Austinat M, Bösl M, Stoll G, Nieswandt B. Orai1 (CRACM) is the platelet SOC channel and essential for pathological thrombus formation. *Blood*. 2009;113(9):2056-63.

Varga-Szabo D, Braun A, Kleineschnitz C, Bender M, **Pleines I**, Pham M, Renné T, Stoll G, Nieswandt B. The calcium sensor STIM1 is an essential mediator of arterial thrombosis and ischemic brain infarction. *J Exp Med*. 2008;205(7):1583-91.

Nieswandt B, Moser M, **Pleines I**, Varga-Szabo D, Monkley , Critchley D, Fässler R. Loss of talin1 in platelets abrogates integrin activation, platelet aggregation, and thrombus formation in vitro and in vivo. *J Exp Med*. 2007; 204(13):3113-8.

Review

Varga-Szabo D, **Pleines I**, Nieswandt B. Cell adhesion mechanisms in platelets. *Arterioscler Thromb Vasc Biol*. 2008;28(3):403-12.

Oral Presentations

Double deficiency of Rac1 and Cdc42 severely affects platelet function and production. XXIst Congress of the International Society on Thrombosis and Hemostasis, July 2007, Geneva (Switzerland).

Winner of the **Young Investigator's Award** (prize money: 1,000 CHF).

Defective activation of platelet integrins in Talin1-deficient mice. XXIInd European Platelet Meeting, October 2007, Lutherstadt Wittenberg (Germany).

Animal models of platelet dysfunction. Congrès 2009 de la Société Française d'Hématologie, May 2009, Paris (France).

Megakaryocyte-specific deletion of Rac1 and Cdc42 abrogates proplatelet formation in vitro and in vivo. XXIInd Congress of the International Society on Thrombosis and Hemostasis, July 2009, Boston (MA, USA).

Winner of the **Young Investigator's Award** (prize money: 500 US\$).

Poster

Function of Rho GTPases in platelets and megakaryocytes. GPCR Dimer Symposium, October 2009, Würzburg (Germany).

Affidavit

I hereby declare that my thesis entitled “The role of the Rho GTPases Rac1 and Cdc42 for platelet function and formation” is the result of my own work. I did not receive any help or support from commercial consultants. All sources and / or materials are listed and specified in the thesis.

Furthermore, I verify that this thesis has not yet been submitted as part of another examination process neither in identical nor in similar form.

Würzburg,